THE SOLID-PHASE SPECIATION OF ARSENIC IN ROASTED AND WEATHERED SULFIDES AT THE GIANT GOLD MINE, YELLOWKNIFE, NWT

Application of Synchrotron microXANES and microXRD at the Grain Scale

By

Stephen Richard Walker

A thesis submitted to the Department of Geological Sciences and Geological Engineering

In conformity with the requirements for

the degree Doctor of Philosophy

Queen's University

Kingston, Ontario, Canada

September, 2006

Your file Votre référence
ISBN: 978-0-494-18559-9
Our file Notre référence
ISBN: 978-0-494-18559-9

Abstract

Understanding the solid-phase speciation of arsenic (As) in soils and sediments is important for determining potential As mobility and bioavailability in the environment. This is especially true in mine-influenced environments, where arsenic commonly is present at concentrations two and three orders of magnitude above quality criteria for soils and sediments. Arsenic-bearing particulates dispersed through hydraulic transport or aerosol emissions can represent a persistent source of contamination in sediments and soils adjacent to past mining and metallurgical operations. The stability and mobility of As associated with these phases depends on the chemical form and oxidation state of the As and the interaction with post-depositional geochemical conditions.

The Giant mine in Yellowknife, NWT roasted As-bearing gold ore from 1949 to 1999. The roasting process decomposed As-bearing sulfides (pyrite and arsenopyrite) to produce a calcine containing fine (generally < 50 μm) As-bearing Fe oxides. Synchrotron As K-edge micro-X-ray Absorption Near Edge Structure (μXANES) and μXRD were applied as part of a grain-by-grain mineralogical approach for the direct determination of As host mineralogy and oxidation state of As in these roaster-derived Fe oxides. The grain scale approach has resolved potential ambiguities that would have existed had only bulk XANES and XRD methods been applied. Using combined optical microscopy, electron microprobe and μXRD, we have determined that the roaster Fe oxides are nanocrystalline grains of maghemite containing < 0.5 wt.% to 7 wt.% As. Some of these As-bearing nanocrystalline grains are a mixture of maghemite and hematite. All roaster Fe oxides including those present in 50-year old tailings contain mixtures of As^{V} and As^{III}. The persistence of As^{III} in roaster-derived maghemite in shallow subaerial (oxidized) shoreline tailings for over 50 years suggests that the As is relatively stable under these conditions,

even though As^{III} is a reduced form of arsenic, and maghemite is normally considered a metastable phase.

The mixed oxidation state of As in the roaster-derived wastes appears to be established by reactions occurring at the time of roasting and this mixed oxidation state persists in the environment. In unweathered calcines, it can be seen that roaster-derived iron oxide grains with relic sulfide cores contain the highest As^{III}/As^{V} ratios.

In addition, sulfides deposited in unsaturated conditions (subaerial Yellowknife Bay tailings and Townsite waste-rock) have weathered, leaving a replacement rim of As-bearing Fe oxyhydroxide or in the case of arsenopyrite a Ca-Fe arsenate. Sequential selective extraction (SSE) fractions for Fe oxides and sulfides, in Townsite waste rock samples, were in good qualitative agreement with petrographic observations of the degree of sulfide weathering in these samples. Samples with higher percentages of As extracted in the Fe oxide fraction showed typically thicker Fe oxyhydroxide weathering rims and less sulfide. The reverse was true for samples with greater amounts of As extracted in the sulfide fraction of the SSE. Arsenic-bearing Fe oxyhydroxide on pyrrhotite in waste-rock has been determined by μXRD to be finely to nanocrystalline goethite.

Acknowledgements

First, I would like to thank my supervisor, Dr. Heather Jamieson, for her support, encouragement and patience. Heather's enthusiastic approach to science and her willingness to take on a thirty-something graduate student speak highly of her commitment to academia. Her helpful advice extended beyond the thesis to maintaining a balance between raising a family and coping with the rigors of research. Above all, Heather's keen interest in science constantly guided me forward.

There are also many others in the department who have helped me along the way. I would especially like to thank Dr. Gema Olivo for the generous use of her microscope and some critical support in the early days of my re-acquaintance with the petrographic microscope and Dr. Ron Peterson who lent an ear and fleshed out some important ideas about arsenic and maghemite. I would also like to thank Al Grant and Dave Kempson for their technical support and analytical assistance and Chris Munro and Anna Markiw for their assistance in the two excursions to Yellowknife. Roger Innes was always available when needed to help out with sample handling and preparation. Mark Badham brought the resources of the Miller Museum and collection to my aid on several occasions and undertook tedious grain-by-grain separation of important minerals for this research without hesitation.

Dr. Tony Lanzirotti, at beamline X26A, NSLS, has provided constant and invaluable support along the way as synchrotron methods became ever more integral and important for this work. Those that have helped out in one or more trips to the synchrotron include: Anna Markiw, Andrew Rollo, Dr. Barbara Sherriff, Madeleine Corriveau, Claudio Andrade, Dr. Ron Peterson and if I have missed anyone from the numerous trips over many years, I thank them as well. The

exchange of ideas and assistance with data and data collection while at the beamline has been very much appreciated.

I would especially like to thank Claudio Andrade for the sharing of ideas on the Giant mine and arsenic in Yellowknife, and his specific efforts developing the technique for lifting thin-sections from glass slides. Skya Fawcett also deserves special mention for picking up where Claudio left off on those Yellowknife discussions and jumping in without hesitation to help out in the darker final days of pulling this all together.

Lastly, but most importantly, I thank my family; whose commitment, understanding and support seldom waivered, and never failed. To my parents Len and Lois Walker, I cannot thank you enough for the countless hours of support including helping out with the children. I'm proud to have you both here to share in the culmination of this rewarding endeavor. To my mother-in-law, Bev McLellan, I likewise cannot adequately express my appreciation for all you have done for the children and us. I thank my son Josh for stepping up to the plate and helping out often at a moments notice and for having an understanding way in advance of his years. To my daughters, Rachael and Lauren, who are probably confused to no end by the fact that their father has been in school for their entire lives, I thank you for keeping me grounded on what matters most. To my patient wife Cathy, there are no words to adequately acknowledge your sacrifice and support. Without you this would not have been possible.

Co-authorship

This thesis includes three manuscripts for journal publication incorporated as Chapters 2, 3 and 4. Chapter 2 is a published manuscript (Walker *et al.* 2005) entitled "The Speciation Of Arsenic In Iron Oxides In Mine Wastes From The Giant Gold Mine, N.W.T.: Application Of Synchrotron Micro-XRD And Micro-XANES At The Grain Scale". Coauthors are Heather Jamieson, Queen's University; Antonio Lanzirotti, University of Chicago; Claudio Andrade, formerly of Queen's University now with Klohn Crippen Berger; and Gwendy Hall, Geological Survey of Canada. H. Jamieson acted in a supervisory and review capacity, A. Lanzirotti provided technical guidance on synchrotron methods and review, G. Hall provided review and the initial recommendation to become involved in the NRCan Synchrotron program, and C. Andrade developed the removable thin section technique based on ideas and guidance provided by H. Jamieson and myself.

Chapter 3 is a manuscript in preparation to be submitted for journal publication. Coauthors are Heather Jamieson, Antonio Lanzirotti, and Gwendy Hall. H. Jamieson provided supervision and review, A. Lanzirotti provided guidance on synchrotron methods and G. Hall provided the sequential selective extraction results (samples run at Chemex Labs of Vancouver).

Chapter 4 is a manuscript in preparation to be submitted for journal publication. Coauthor is Heather Jamieson who acted in a supervisory and review capacity.

Table of Contents

LIST OF TABLES

LIST OF FIGURES

List of Abbreviations

Al	aluminium
As	arsenic
Aspy	arsenopyrite
Ca	calcium
CCME	Canadian Council of Ministers of the Environment
Cu	copper
EPMA	electron probe micro-analyses
ESP	electrostatic precipitator
Fe	iron
INAC	Indian and Northern Affairs Canada
mg/kg	milligram per kilogram
Mg	magnesium
mhCal	monohydrocalcite
mm	millimetre
Mn	managanese
Musc	muscovite
Na	sodium
Ni	nickel
NSLS	National Synchrotron Light Source, Brookhaven National Lab, Upton N.Y.
P	phosphorus
Pb	lead
Po	pyrrhotite
Py	pyrite

Qtz	quartz
S	sulfur
Sb	antimony
SO_4^{2-}	sulfate
μm	micron
μXANES	micro-X-ray absorption near edge structure
μXRD	micro-X-ray diffraction
μXRF	micro-X-ray fluorescence
XAS	X-ray absorption spectroscopy
Zn	zinc

Chapter 1 - Introduction

Metal and metalloid contamination due to mining and metallurgical processing is well documented in many mining areas (Berube *et al.* 1974, Amasa 1975, Hocking *et al.* 1978, Ragaini *et al.* 1977, Mok & Wai 1990, Moore & Luoma 1990, Mitchell & Barr 1995, Henderson *et al.* 1998, Reimann *et al.* 2000). A recent study for the Rio Tinto area of Spain even suggests that watershed scale contamination from mining may have occurred as much as 4,500 years ago (Leblanc *et al.* 2000). Primitive copper smelting of arsenical ores developed as early as the 4th millenium B.C. (Wertime 1973) and undoubtedly metalworkers of the day were exposed to As fumes. It has been suggested that the Greek God Hephaestus (Vulcan in Roman Mythology) is evidence that As poisoning was the first occupational disease recognized by mankind (Azcue & Nriagu 1994, and Charles 1980 cited in Azcue & Nriagu 1994). Hephaestus was the only metalworker mentioned by Homer and he was described as being physically imperfect and lame. The 5300 year old "Man in Ice" discovered in the Alps in the early 1990s had an arsenical-copper axe in his possession and high As concentrations in his hair (Gossler, *et al. 1995*). Arsenic trioxide obtained by smelting copper and iron ores has been used as a medicine and poison since 2000 BC (Frost 1967). All of this is evidence that rather than being wholly a problem of the 19th and 20th century, parts of the human population have been living with incidental exposure to As due to metallurgy from before the Bronze age. However, in the 19th century and especially since 1930 the cumulative global anthropogenic As production and dissipation into the environment has been enormous (Han *et al.* 2003) and, as of 2000, has been estimated at 4.53 million tonnes. Han *et al.* (2003) estimate that between 1900 and 2000 the potential As inputs to civilization-useable land surface went from 6.1 to 190 kg As km^{-2}. If the values presented by Han *et al.* withstand scrutiny this would indicate that the As trioxide stored underground at the Giant mine constitutes 3% of all anthropogenic As ever produced.

1.1 BACKGROUND

Gold mining has been integral with the foundation, growth and prosperity of Yellowknife since the staking of the claims that would become the Giant mine in July 1935, and the subsequent staking rush that began in the fall of that year (Moir *et al.* 2005). The Consolidated Mining and Smelting Co. began production from the Con mine in 1938 on claims they staked in 1935. Production at Giant began in 1948 and roasting of the ore concentrate began in January 1949 (Grogan 1953). The Giant mine is located 5 km to the north of Yellowknife and Con mine (which today includes Rycon and Negus mines) is located on the outskirts of the present day City (Figure 1-1). A summary of former mining and milling operations around Yellowknife is provided in Table 1-1. There was a three year interruption in mining and milling at Con during WW II, but otherwise Con and Giant remained in near continuous operation until 2003 and 2004 respectively. Both mines saw disruptions in the 1990s due to labour strikes including the bitter strike at Giant in 1992, when nine replacement workers tragically lost their lives.

Milling (and roasting) of ore ceased at Giant in 1999 with the bankruptcy of Royal Oak Mines. However, an agreement was reached for Miramar Mining to assume production of Giant ore and processing at the Con Mine mill (2000 to 2004). Indian and Northern Affairs Canada assumed liability for all existing environmental conditions at the Giant Mine property. The Giant Mine produced over 7.0 million ounces of gold and the Con mine over 5.8 million ounces. The 66 years of mining activity in Yellowknife have left a legacy of As-related concerns at both mine sites and surrounding area.

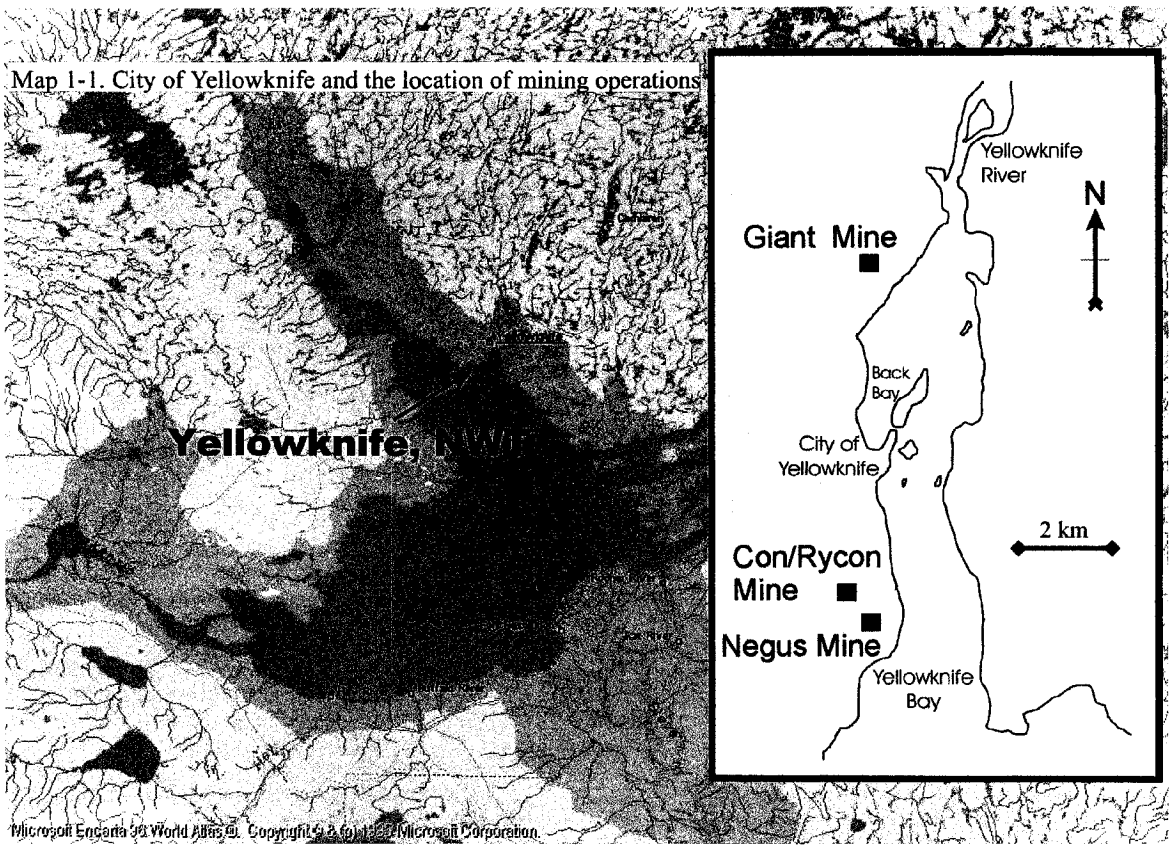

Figure 1-1. Site location showing Yellowknife and mine sites. (Modified from ESG & Queen's 2001)

Arsenic contamination of terrestrial environments, surface water and groundwater poses a risk to human and ecological health in Canada and around the world. This contamination can result from both natural and anthropogenic sources, and the mobility of As in the environment is complex and depends on how (in what form) it occurs (Bhumbla & Keefer 1994) and the environment in which it is deposited (Inskeep *et al.* 2002, Smedley & Kinniburgh 2002). Arsenic may be dissolved in the aqueous phase, weakly or strongly sorbed to a mineral surface, or bound within a mineral structure (Smith & Huyck 1998). Thus, toxicity to humans and the environment is determined not by the total As content of a medium, but by the accessibility of biota to that medium and the specific form of the As present.

Table 1-1 Mining and Milling in Yellowknife
(Lord 1951, Tait 1961, More & Pawson 1978, Egli & MacPhail 1978, Martin 1990, Silke 1999)

Mill	Year	Capacity (tons/day)	Method[a]	Mine (Mill Feed)	Years
Con Closed 2004	1938 1939	100 175	FM-Cyn	Con	1938-1943 1946-2003
	1942*	300	H-Rst-FC	Rycon	1939-1943 1946-1958
	1955**	465	H-Rst-FC		
	1970	470	FM-Cyn	Vol	1964-1967
	1978	650	FM-Cyn		
	1992	1200	(1)FM-Cyn (2)Autoclave	Giant	2000-2004
Negus Closed 1952	1939 1947	50-70 170	FM-Cyn H-Rst-FC	Negus	1939-1944 1945-1952
Giant Closed 1999‡	1948†	225	H-Rst-FC	Giant (includes Lolor and Supercrest)	1948-1999
	1952	850	(1)H-Rst-FC (2)FS-Rst-FC		
	1958	1000	FS-Rst-FC		
	1958	1000	FS-Rst-FC		

[a] FM-Cyn=Free milling with cyanide extraction. H-Rst-FC=Hearth Roasting of Flotation Concentrate and cyanide extraction. FS-Rst-FC=Fluosolids Roasting of Flotation Concentrate and cyanide extraction. (1) & (2) indicate concurrent processing by two methods. All three mills used Hg amalgamation to recover free gold in the early days of milling. Giant and Con discontinued amalgamation in 1958 and 1968 respectively.
* Roaster operated from April to Nov. 1942 mill continued with out roaster until 1943 and then closed temporarily due to wartime restrictions. Mill including roaster restarted in 1946. Gas treatment by wet scrubber began in 1949 and roasting was discontinued in 1970.
** Between 1950 and 1970 capacity varied reaching a maximum of 500 tons per day in 1956.
† Mining and milling began at Giant in May 1948, but roasting did not commence until Jan. 1949. Cold electrostatic precipitator (ESP) for gas treatment commenced in Oct. 1951 replaced by a more effective hot ESP and baghouse system in 1958.
‡ Mill and Roaster closed in 1999. Giant 'C' Shaft complex operated by Miramar Mining from 2000 to 2004 supplying ore to the Con Mill.

Dissolved As in groundwater is a world-wide issue of growing concern (Nordstrom 2002) which can have a natural or anthropogenic source. Natural As in groundwater has placed an estimated 36 million people at risk in the region of the Bengal Delta (Bangladesh and West Bengal). This region and others with similar elevated natural As concentrations in groundwater are typified by low As in sediments, similar to world average concentrations, and an elusive solid phase source of the As. The conditions responsible for high As concentrations in such aquifers generally

involve geologically young (Quaternary) deposits with strongly reducing or oxidizing high-pH (>8.5) conditions (Nordstrom 2002, Smedley & Kinniburgh 2002).

In many areas contaminated by As with an anthropogenic origin, the concentrations of solid phase As are both elevated and exposed in near surface environments (soils and sediments) at concentrations well above world average concentrations and local back-ground (often in the 1000 ppm to 1 wt% range or more). In these areas the soils and sediments themselves pose a potential risk to human health and the environment in addition to local groundwater resources if they exist.

In the case of Yellowknife, the As impacts resulting from mining and metallurgical processing of the arsenopyrite-rich ore have resulted in As concentrations in both soils and sediments that can be two to three orders of magnitude above soil and sediment quality guidelines. From a human health stand point, there is little (if any) potable groundwater use in the area of Yellowknife (or much of the NWT) so health concerns related to As in the region are primarily related to the inadvertent ingestion of soil. More localized issues of concern may also include ingestion of locally grown foods (if As were shown to accumulate in edible portions), inhalation of fugitive dusts and contact with contaminated sediments through recreational activities. In the past both air quality (due to roaster emissions) and drinking water quality (from surface water sources) were concerns (CPHA 1977). However, most of these major issues date back to at least the 1970s (or earlier). The potable water source for the City of Yellowknife has, since 1969, been the Yellowknife River up flow from the mines. Potable water at the mines is also provided from the Yellowknife River and has been since the 1970s and any remaining air quality concerns were largely eliminated with the closure of the Giant Mill and roaster in 1999.

Though the concentrations of As in environmental media are elevated in Yellowknife and other areas throughout the world, it is often difficult to establish definitive links between the metal and metalloid contamination and adverse health effects (Thornton 1996). This may be especially true in isolated and mining communities whose population can be transitory, and occupational exposures are likely to be important in those employed at the mine. Human health risk assessments for soil ingestion, including the recent risk assessment for Yellowknife, (Risklogic 2002) probably overestimate risk, since they typically assume As in the solids is 100% bioavailable, or present in a soluble form which is generally not the case (Valberg *et al.* 1997).

Assessing and managing the contamination in mining communities from both a human health and ecological risk perspective is further complicated by the potential presence of naturally elevated concentrations in the environment from geological processes. For Yellowknife, this includes the inferred deposition (and any subsequent reworking) of As-rich glacial debris scoured from the As-bearing shear zones in the region. While it can be beneficial to understand natural background concentrations in the environment, from a human health perspective it is ultimately the form, concentration and resulting bioavailability of the As that matters. It is also important to realize that natural cycling of As has been interrupted and unbalanced by anthropogenic influences of mining and ore processing (Mitchell & Barr 1995) and As may be subject to volatilization, dissolution, adsorption, precipitation, oxidation, reduction and methylation in soils and sediments. Environmental mobility, availability and bioavailability of As in solids need to be understood in terms of the form of the As (eg. As oxidation state, mineralogy, grain size, surface area and morphological properties such as encapsulation or rinding of grains), their physical location and the geochemical environment in which they exist (Bhumbla and Keefer 1994, Ruby *et al.* 1999). The form of the As, the geochemical and biogeochemical conditions,

and reactions occurring on a relevant time scale determine whether it is accessible and bioavailable, and whether it will become more or less available in the future.

1.2 Arsenic in the Environment

Arsenic abundance among the elements in the earths crust is low and less abundant than many of the rare earth elements (Nordstrom 2002, Wedepohl 1995). However, it is one of several mobile or volatile elements that are especially accumulated in the sedimentary cover of the upper crust (Wedepohl 1995). Arsenic is a metalloid and its chemical behaviour leads to a range of polyhedral coordination relationships in chemical compounds and minerals (Greenwood & Earnshaw 1998, Baur & Onishi 1969). It is the main constituent of more than 200 mineral species of which 60% are arsenates, 20% sulfides and sulfosalts and the remaining 20% include arsenides, arsenites, oxides, silicates and elemental As (Baur & Onishi 1969). A search by element (for As) on two web databases (Webmineral 2006, Pierre Perroud 2006) returned over 500 mineral names in each (including many solid solutions). This represents ~12% of all minerals entered in the Webmineral database at that date. The breakdown by arsenates, sulfides/sulfosalts etc. was similar to that reported by Baur & Onishi (1969).

Arsenic is released to the atmosphere through natural processes (wind blown mineral dust, biological processes, and volcanic activity) and anthropogenic inputs, mostly from ore roasting and smelting operations, and coal combustion (Han *et al.* 2003, Cullen & Reimer 1989). In the past, arsenical pesticides were significant anthropogenic sources of As in the environment (NRCC 1978). Arsenical pesticides for agriculture and wood preservation continue to decline in use with the recent decision to discontinue production of most treated wood products containing chromated copper arsenate (Health Canada 2003, US EPA 2003). Chromated copper arsenate-treated wood is still used in some commercial applications.

Understanding As behaviour in the environment is complicated by the fact that it readily changes chemical form (oxidation state and species) and not all forms of As are toxic. A number of oxidation states are possible resulting in a range of thermodynamically stable solid and aqueous phases that vary with pH and Eh. In addition to the generally recognized (formal) oxidation states of -3, 0, +3, and +5, As also forms covalently bonded solid species with nominal oxidation states (oxidation numbers) that include –2, -1, and +2. Only the +3 and +5 states are common as aqueous species although in very reduced systems dissolved arsine and organic arsine gases (As^{III}) may exist. Arsenic forms largely ionic bonds when coordinated with oxygen and largely covalent bonds when coordinated with Fe, S, C and itself (Greenwood & Earnshaw 1998). Thermodynamic data for As has been recently reviewed (Nordstrom & Archer 2003).

The large number of minerals with diversity in form (ionic and covalent bonded solids, and reduced and oxidized species), the range of dissolved pH and redox sensitive species, sorption of many dissolved species to a range of solid phases (Fe, Mn and Al oxides, clay minerals, and organic material) and the presence of gaseous forms all testify to the wide ranging and complex behaviour of As in the environment.

1.2.1 Aqueous Arsenic Species

Arsenic occurs in the aqueous phase as a variety of inorganic and organic species (Table 1-2). The most common species in natural waters are inorganic As^{V} (eg. $H_2AsO_4^-$, $HAsO_4^{2-}$) and As^{III} ($H_3AsO_3^0$). Equilibrium thermodynamics predict arsenate as the dominant form in oxidizing environments. However, arsenite often co-exists in natural waters at concentrations well in excess of thermodynamic predicted concentrations, suggesting that this redox couple is often not in equilibrium or that oxidation is kinetically very slow in natural waters (Inskeep *et al.* 2002). Similarly, in more reduced environments, arsenate can coexist with arsenite at concentrations well above those predicted. In natural waters organic As species (Table 1-2) are generally present

in low proportions to the inorganic forms (< 10%) (Le 2002).

It is generally recognized that aqueous species other than arsenite and arsenate are likely present in some reduced environments, but at present they remain poorly understood (eg. thioarsenites and arsines, Table 1-2). The volatile methylarsines (eg. trimethylarsine) which are very common products of microbial activity (Cullen & Reimer 1989) could be important in certain reducing environments, particularly those low in sulfur (Frankenberger & Arshad 2002). All of the arsines are volatile, posing unique difficulties for sampling, storage and preservation which makes them particularly susceptible to loses and transformations prior to and during analysis. The potential presence of arsenocarbonate and thioarsenite species (Kim *et al.* 2000, Tossell 2000, Lee & Nriagu 2003, Table 1-2) is important not only since their presence would increase the number of dissolved complexes and potential reactions, but because they could lead to misleading results in some analytical speciation methods. For methods that rely on anion exchange to separate the uncharged arsenite species from arsenate anions (eg. Le *et al.* 2000), additional anionic As complexes (eg. arsenocarbonates and thiosarsenites) would be retained along with any arsenate (As+5) due to their negative charge. This would suggest a larger arsenate presence than really existed.

1.2.2 Arsenic Mobility and Solid Phases

Arsenic solid phases include a variety of mineral forms (Table 1-3) ranging from the more oxidized forms (arsenates and arsenites) to more reduced forms including sulfosalts, elemental As, sulfides and arsenides. Activities of arsenate and arsenite in solution are unlikely to be controlled by precipitation of arsenate or arsenite salts (Inskeep *et al.* 2002), rather they are commonly controlled by sorption reactions. Both arsenate and arsenite have a strong affinity for Fe (hydro)oxides. Arsenate can also sorb strongly to clay minerals and (hydro)oxides of Mn and Al. Biologically mediated reduction of arsenate to arsenite and oxidation of arsenite to arsenate is

Table 1-2 - Dissolved Arsenic Complexes

Dissolved Phase		Species	As Oxidation State
norganic	**Arsenates**	H_3AsO_4 **$H_2AsO_4^-$** **$HAsO_4^{2-}$** AsO_4^{3-}	+5
	Arsenites	**$H_3AsO_3^0$** $H_2AsO_3^-$ $HAsO_3^{2-}$	+3
	Thioarsenites	*$AsS(OH)_2^-$* * *$AsS(SH)(OH)^-$* * *$AsS(SH)_2^-$* * *AsS_2^-* † *AsS_3^{2-}* ‡	+3
	Arseno-carbonate complexes	*$As(CO_3)_2^-$* ** *$As(CO_3)OH_2^-$* ** *$As(CO_3)_2OH^2$* ** *$AsCO_3^+$* **	+3
	Arsine	H_3As	-3
Organic	Monomethylarsonic acid ($MMAA^V$)	$CH_3AsO(OH)_2$ **$CH_3AsO(OH)O^-$**	+5
	Monomethylarsonous acid ($MMAA^{III}$)	$CH_3As(OH)_2$	+3
	Dimethylarsenic acid ($DMAA^V$)	$(CH_3)_2AsO(OH)$ **$(CH_3)_2AsO(O)^-$**	+5
	Dimethylarsinous acid ($DMAA^{III}$)	$(CH_3)_2As(OH)$	+3
	Trimethylarsine oxide (TMAO)	$(CH_3)_3AsO$	+5
	Trimethylarsine (TMA)	$(CH_3)_3As$	+3
	Tetramethylarsine ion ?	*$(CH_3)_4As^+$*	+5

Bold type - indicates common species in natural waters.
Italics - indicate possible species that remain speculative.
* Tossell 2000. † Wilkin 2001. ‡ Cullen & Reimer 1989 ** Kim *et al.* 2000.

well established, as is abiotic oxidation of arsenite to arsenate by Mn oxides (Hering and Kneebone 2002 and references therein). There also remains some evidence that that precipitation of hydrous Ca and Mg arsenates may be important solubility controls at neutral to alkaline pH (Raposo *et al.* 2004).

Under reducing conditions, arsenite may precipitate as an authigenic sulfide (eg. orpiment or arsenopyrite phase) although the concentration of dissolved As in such systems may not be particularly low (Hering & Kneebone 2002). It has recently been shown that under reducing conditions in the laboratory, As can form an arsenopyrite-like surface precipitate on Fe sulfides (Bostick & Fendorf 2003).

Arsenic can be released from solids to the aqueous phase by reductive dissolution of As-bearing Fe (hydro)oxides or, conversely, oxidative dissolution of As-bearing sulfides. In oxic conditions, sorbed As phases (eg. arsenate and arsenite) can also be destabilized by changing environmental conditions (eg. pH, ionic strength or concentration of competing anions) (Smedley & Kinniburgh 2005, Smedley & Kinniburgh 2002, Hering & Kneebone 2002).

1.3 The Con and Giant Mines, Yellowknife

The work in this thesis largely investigated As in soil, tailings and mine waste-rock at the Giant mine. However, the Giant and Con mine deposits are closely linked geologically so, both are discussed in a general fashion to provide a holistic picture rather than just a part. In addition, one objective set early on in this thesis (see objectives below) was to develop a broad understanding of the influences on As origin and cycling in the Yellowknife area in general since it is complicated and rarely considered from this view. Therefore information on the Giant and Con mines in terms of similarities and differences is summarized in the following sections. More

Table 1-3 - Selected Arsenic Minerals

Group	Examples	Formula
Arsenates	Scorodite	$FeAsO_4 \cdot 2H_2O$
	Angellelite	$Fe_4(AsO4)_2O_3$
	Arseniosiderite	$Ca_2Fe_3(AsO_4)_3O_2.3H_2O$
	Yukonite	$Ca_2Fe_3(AsO_4)_3(OH)_4.4H_2O$*
Arsenate/Arsenite†	Synadelphite	$(Mn,Mg,Ca,Pb)_9(As^{III}O_3)(As^{V}O_4)_2(OH)_9 \cdot 2H_2O$ (?)
Oxides	Arsenolite	As_2O_3
	Claudetite	As_2O_3
Arsenites	Schneiderhohnite	$Fe^{II}Fe^{III}{}_3As^{III}{}_5O_{13}$
Sulfosalts	Tetrahedrite-Tennantite	$(Cu, Fe)_{12}Sb_4S_{13}$)-$(Cu,Fe)_{12}As_4S_{13}$)
Elements	Arsenic	As
	Arsenolamprite	As
Sulfides	Orpiment	As_2S_3
	Realgar	AsS
	Arsenopyrite	FeAsS
	Arsenical pyrite	FeS_2 (up to 5 wt.% substitution of As for S)‡
Arsenides	Loelingite	$FeAs_2$
	Westerveldite	(Fe,Ni,Co)As

* As proposed by Nishikawa *et al.* (2006).
† The mixed oxidation state phase (not mineral) $Fe_2(As^{III}(As^{V}O_4)_3$ has recently been identified in As calciner dumps in south west England (van Elteren *et al.* 2006).
‡ National Research Council 1977.

detailed information on Giant ore processing and As-related issues follows this general discussion.

1.3.1 Geology

The Con and Giant Mine ore-bodies are hosted within a major brittle-ductile shear system that transects the Kam Group of the Archean Yellowknife Greenstone Belt (Hubbard 2005). The shear system consists of hydrothermally altered and deformed sericite- or chlorite-rich rocks with or without apparent schistosity (Siddorn 2005). Mineralization at the Giant and Con mines occurs as disseminated sulfides (and sometimes sulfosalts) in broad silicified zones or quartz carbonate veins bounded by sericite or chlorite schist (Boyle 1960, Ellis & Hearn 1990). The original deposits exploited at the Con and Negus mines were hosted in mineralized sub-parallel westward dipping shear zones (Con system and Rycon/Negus system) while the Giant shear system displays complex folded geometries (Siddorn 2005). The Giant and Con Mine deposits

have been interpreted to be part of a single shear zone system that has since been dismembered by recent faults. The classic reconstruction of displacement on the main regional fault (West Bay fault) by Campbell (1947) was instrumental in discovery of the major ore-bearing deeper Campbell shear at the Con mine. Based on his work, the Giant deposit was believed to be the faulted extension of the Campbell shear. However, recent work has suggested that the Giant Deposit may actually be the faulted off-set of the shallower Con Shear (Siddorn *et al.* 2005) with the intriguing implication that the Campbell shear at the Giant Mine remains in unexplored ground.

Though the deposits share much similarity beyond the structural differences, there is also significant mineralogical inhomogeneity between the Con and Giant deposits and also within each (Armstrong 1997, Canam 2005, Hubbard 2005, Siddorn 2005). Ore shoots typically contain less than 10% sulfide content and more often less than 5%, though up to 15% sulfide has been reported (Coleman 1957). According to Lewis (1985), the principal sulfide and sulfosalt mineralogy at the Giant Mine includes (in decreasing order of abundance): pyrite, arsenopyrite, sphalerite, chalcopyrite, sulfosalts (jamesonite, berthierite, bournonite and tetrahedrite), pyrrhotite, and galena. However, the actual abundance is variable within individual ore shoots and different regions of the mine (Coleman 1957, Canam 2005 and Hubbard 2005). A study of flotation concentrate in 1990 (originating from stopes being mined at the time) indicated that pyrite and arsenopyrite combined account for 95% of the sulfides and that marcasite, chalcopyrite, sphalerite, acanthite, boulangerite, tetrahedrite, berthierite, gudmundite, stibnite were present in trace amounts (Chryssoulis 1990). Gold at Giant is often refractory being mostly incorporated submicroscopically within arsenopyrite making it unavailable to conventional cyanide extraction (Halverson 1990, Stefanski & Halverson 1992). However, free gold is sometimes present (Hubbard 2005) and certain regions exploited early in mining contained

significant free milling ore (Tait 1961). The Sb content within ore zones in the mine is also heterogeneous, but Canam (2005) notes a generally increasing Sb content from south to north and shallow to deep in the mine. The Sb content in the tailings may be less heterogeneous than suggested by ore distribution since Halverson (1990) notes that careful monitoring was done for Sb. Mixing of high and low grade Sb stopes was conducted to keep grades below 0.75%, since operation above this level leads to formation of problematic Sb sulfates (Halverson 1990).

While some of the gold at the Con mine is refractory, a significant amount of ore produced at various times during the life of the Con Mine was free milling (Table 1-1). Pyrite is ubiquitous within both free-milling and refractory ores at the Con mine, while arsenopyrite is noted as the dominant sulfide mineral in refractory ore and accessory in free-milling ore (Armstrong 1997). Pyrite in all ore zones at Con contain As-bearing and As-poor pyrite with As content ranging from below EPMA detection limits to 5.49 wt.% As and sometimes exhibit zoning within individual grains. Arsenopyrites at Con, as analyzed by Armstrong (1997), are often As deficient (typically $FeAs_{0.9}S_{1.1}$), although some approach or very slightly exceed the stoichiometric ideal (FeAsS).

1.3.2 Ore Processing

At the Giant mine, refractory gold ore was roasted at elevated temperature to breakdown arsenopyrite and release submicroscopic gold. Milling involved crushing, grinding, flotation to mechanically liberate and concentrate the gold and gold-bearing sulfides. The concentrate was roasted to decompose the gold-bearing sulfides producing porous Fe oxides amenable to cyanidation for extraction of the gold (Tait 1961).

Ore processing at the Con Mine was similar to the Giant Mine until approximately 1970 and included the flotation and roasting of a sulfide concentrate (Table 1-1). By 1970 greater

quantities of free milling ore were encountered at depth in the mine, the roaster was in a poor state of repair and the storage capacity of As trioxide in the two concrete lined As storage ponds had been reached. Thus, the refractory ore milling circuit (flotation and roasting) was shut down (Martin 1990). Between 1982 and 1989 Con produced and sold approximately 7,000 tons of high grade As trioxide refined from As trioxide sludge in the storage ponds using a hot water acid leach vacuum crystallization technique (Martin 1990). In 1993, a flotation and autoclave circuit was added in parallel to the free milling circuit to again process refractory ore. In addition, the autoclave operation was designed to process remaining As trioxide sludge and stock-piled calcine from the pre-1970s roasting operation along with the ore (Geldart *et al.* 1992).

Due to the larger scale and longer duration of operation of the Giant mine roaster, it is generally implicated as having a broader impact in the region in terms of aerial extent and magnitude of As deposition. However, a study in the mid 1970s (Hocking *et al.* 1978) indicated that the emissions from Con at that time were 1/3 that of Giant and not 1/7 as predicted from stack emissions data. Remobilization of As (presumably due to wind action) from the As storage ponds was implicated to explain the discrepancy. It should also be noted that the Negus Mine appears to have roasted ore after 1947, but the scale, timing and the effectiveness of gas treatment (if any) has never been established (Lord 1951, Martin 1990).

1.3.3 Gold Ore Processing and Environmental Issues: The Giant Mine Case

The milling of As-bearing ores can result in a complex distribution of As adjacent to mines involving both natural and anthropogenic inputs. Arsenic in metalliferous mining areas has been studied for some time (eg. Amasa 1975, Bamford 1990, Li & Thornton 1993) and continues to be the focus of recent, and on-going research (eg. Martin & Pedersen 2002, Savage *et al.* 2000, and Williams *et al.* 1996). Yellowknife, NWT has been the subject of many studies related to As in the environment and human health, which began as early as 1949 (CPHA 1977) and continue

today (eg. Koch *et al.* 2000, Andrade *et al.* 2006).

The case of the Giant Mine in Yellowknife, highlights a complex example of the redistribution of previously isolated natural As (a largely refractory gold ore containing arsenopyrite), into more available environmental forms and compartments (soils, sediments, tailings and As trioxide dust) over the span of >50 years. The complexity at Giant originates from the roasting of an arsenopyrite-bearing, refractory gold ore, which decomposed the sulfide to a porous Fe oxide residue and produced As trioxide and sulfur dioxide off-gases in the process.

1.3.3.1 Aerial Emissions from Sulfide Roasting at Giant

Roasting at the Giant Mine probably released in excess of 7,000 tonnes of As to the surrounding environment via stack emissions in the first few years of operation (2.75 years x 7.3 tonnes As/day, GNWT, 1993. To put this in perspective, at 1990s emission rates (3 t/year, Environment Canada 2006) it would take 2300 years to release the quantity of As released in the first few years of operation at the Giant Mine even though the mine was a relatively small operation at the time (Table 1-1).

Arsenic deposition rates were calculated over a large study area in the Yellowknife region ("many square miles") in the 1970s. The average As deposition rate across the study area was determined to be 10 pounds per square mile per month with up to 3 times these amounts within 0.5 miles of the Giant Roaster (CPHA 1977). The average deposition rate for total particulate matter was 11 tons per square mile per month. A deposition rate of 106 pounds per square mile per month was reported for the mid-1950s (deVilliers & Baker referenced in CPHA 1977). Since the "mid-1950s" post-dates installation of gas treatment systems at Con and Giant, the magnitude of As emissions to the region before 1951 is likely greater. The CPHA Task Force report (CPHA 1977) also states that deposition rates inside the Giant mine property measured as high as 564 pounds

per square mile per month during a snow survey in 1975. The roaster began operation in January 1949 and roaster gas treatment did not begin until October 1951 (Tait 1961). The study by Hocking *et al.* (1978) notes that about 1/3 of the land area in the region is "bare rock". However, this apparently has not been factored into the understanding of the fate of As emitted from roaster stacks in the region. There apparently has been no directed study at determining the fate of the As released to soils or outcrop surfaces in the region via stack emissions. Lichens on bedrock and soil as well as soil concentration profiles versus depth (3 horizons) were collected as part of the Hocking (1978) study.

Without taking into account subsequent redistribution (e.g. solubilization, volatilization, and wind and groundwater transport processes) the above review means that measuring soil content in the 1970s and today is still most influenced by early As emissions (1949 to 1951 and to a lesser extent 1951 to 1958). It also implicates other roasting operations without gas treatment as important to consider even if they were short lived (i.e. Con and Negus). The aerially distributed As is often considered as agglomerated particles of relatively soluble As trioxide particulate (probably condensed before leaving the stack) (Hocking *et al.* 1978). However, given the quantities of particulate matter collected in the Hot ESP and the baghouse on a tonnage basis after 1958 (Pawson (1973) suggests on average 10.5 tons ESP dust and 25 tons of baghouse dust), it is likely that aerial dispersed As emitted prior to gas treatment contained a significant quantity of lower solubility and complex As particulate (akin to that later collected by the Hot ESP).

1.3.3.2 Overview of Giant Mine Tailings

Most of the gold mined at Giant was refractory and hosted in arsenopyrite. The ore was crushed, subject to froth flotation, and the concentrate roasted at 500°C prior to cyanidation to extract the gold. During the first 3 years of mine operation (1948 to 1951) tailings were discharged onto the shores of Yellowknife Bay (Figure 1- 2) without treatment. After 1951 tailings were discharged

into a lake on the mine site (Bow Lake) and other low-lying areas. Sometime in the 1950s (when the natural capacity of the basin was exceeded) a series of dams were constructed across low-lying areas to increase tailings storage capacity (beginning with Dam 1, Figure 1-2). These were probably unengineered waste-rock structures. Beginning in the 1970s a series of engineered "clay core" dams were constructed, eventually resulting in the present day, North, Central and South tailings ponds (Figure 1-2). The Northwest tailings pond was constructed in 1987 to contain new tailings as well as tailings from the Tailings Retreatment Plant (TRP) that was operated briefly in 1988 and 1989. The tailings reclamation left the large depression in the south half of the North Pond adjacent to South Pond (Figure 1-2).

To understand the physical and chemical makeup of tailings at the Giant Mine, it is important to recognize that the above process has generated essentially three tailings streams that discharged the bulk of the tailings solids. The streams are flotation tailings, cyanided calcine residue and Cottrell tailings (cyanided electrostatic precipitator dust). The three streams vary substantially from each other in total tonnage, As content and mineralogy (Table 1-4). Flotation tailings are high tonnage, and relatively low in As, which is expected to be present predominantly as arsenopyrite. The lower tonnage streams (namely calcine residue and Cottrell tailings) carry higher concentrations of As as roasted products of the sulfide concentrate (eg. Fe oxides). The apparent variation in As content among the three waste streams over time is interesting and may be explained by changes in milling process that occurred (eg. improved flotation of arsenopyrite would decrease As in flotation tailings). It is known that cyanidation of the flotation tailings was completed between 1955 and 1967 suggesting a different flotation tails character in that time (Halverson 1984). However, sampling methods may also explain some of the difference, so caution should be exercised when interpreting observed changes in the As loading over time.

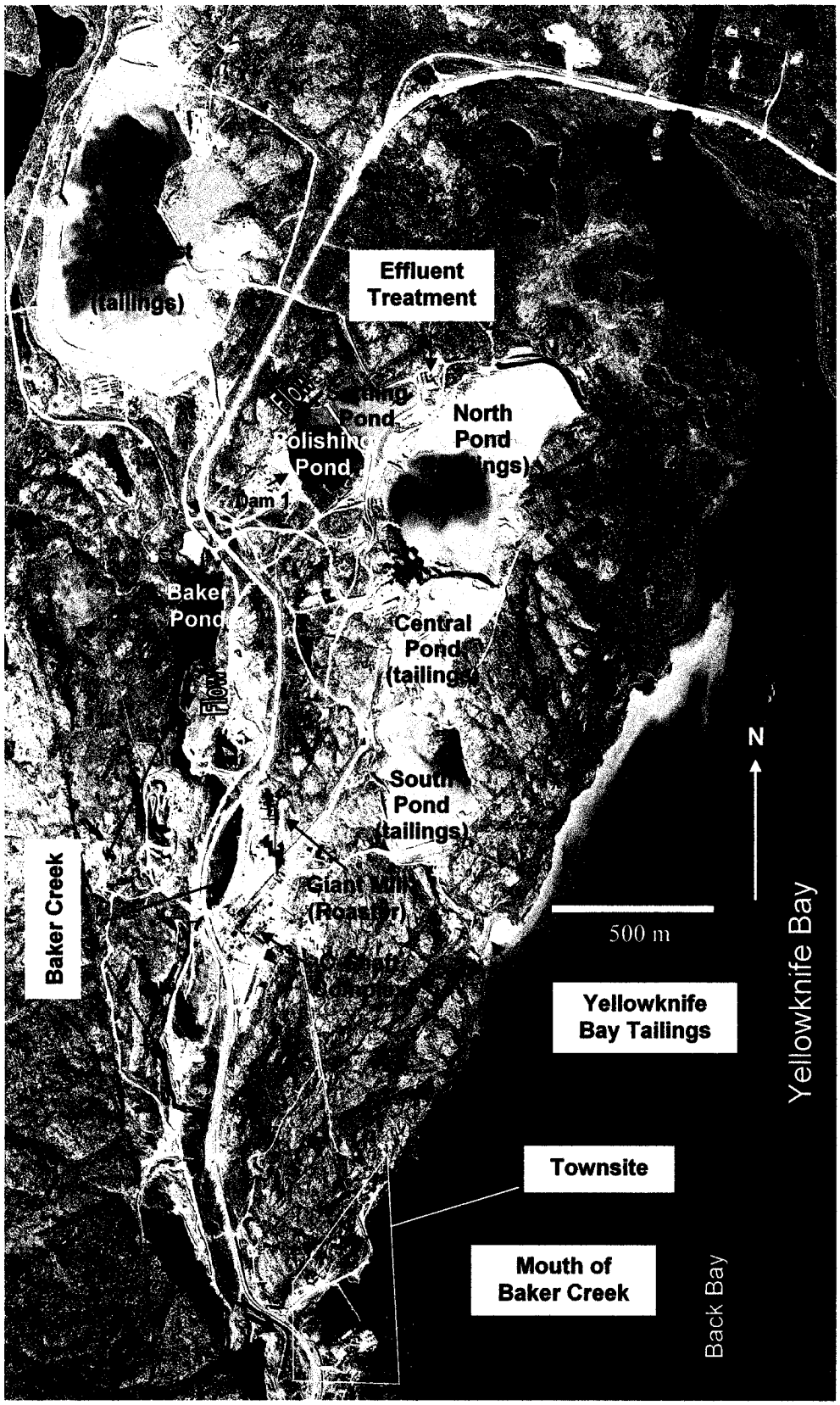

Figure 1-2. Giant Mine Site

Table 1-4 – Arsenic contributions from the main solid effluent streams at Giant

Tailings Stream	Year	Approximate Discharge Rate (tpd)	Arsenic Concentration (wt.%)	Arsenic Loading (tpd)
Flotation (70-80% <0.075 mm)	1999	1000	0.09	0.9
	1963	794	0.28	2.2**
Calcine Residue (90% <0.045 mm)	1999	170	1.8	3.4
	1963	122	1.2	1.5**
ESP Residue (90% <0.014 mm)	1999	9	4.4	0.4
	1963	9	6.2	0.6

tpd = dry tonnes per day. Arsenic loading data from Walker & Jamieson 2002. * Other as yet unidentified As phases may be present. ** Estimated total loading. Tailings were cycloned for mine-backfill from 1957 to 1976 removing approximately 50% of the coarsest material and an unknown proportion of As, leading to an overall decrease in grain-size and increase in calcine and ESP dust.

Specific modifications and improvements were also made at various times over the life of the mill. Some of the process changes are likely to have changed the physical and chemical characteristics of tailings discharged at different times. Variations in ore mineralogy as well as tailings management practices at the time of discharge may also be important. Several early publications, namely Grogan (1953), Tait (1961), and Foster (1963), reveal specific mill process and tailings management information that is helpful in understanding the nature of the early tailings and the Yellowknife Bay tailings specifically. This information is summarized in Appendix A.

1.3.3.3 Tailings Impacts on Yellowknife Bay and Sediment Quality

In addition to the Yellowknife Bay tailings, it is evident from a number of sources that fine grained tailings material (in addition to dissolved arsenic) has been discharged to Back Bay via Baker Creek. Additional detail on this information is provided in Appendix A.

Based on a review of all of the data, a brief chronological interpretation of tailings discharge to Yellowknife Bay can be discerned from the information provided in Appendix A. Beginning sometime around May 1948, flotation tailings were discharged directly to Yellowknife Bay. Calcine residue tailings would not have been produced until January 1949 and any discharges of calcine residue would have occurred after this time. Stockpiling of the calcine residue was common practice in the early years of operation and likely led to a significant reduction in the quantity of calcine residue tailings discharged directly into Yellowknife Bay. This is consistent with Giant staff reporting in 1984 that the flotation portion of early tailings (1948 to 1951) may be "the beach" at Yellowknife Bay (Halverson 1984). However, the potential exists for intermittent discharges of calcine residue tailings between 1948 and 1951. These intermittent discharges are more likely to have occurred in the winter months when difficulties were encountered in stockpiling (Tait 1961).

Details on the implementation of off-gas treatment at Giant (Foster 1963) suggest that the Hot Cottrell tailings would not have been routinely discharged with the regular tailings until late 1958 or early 1959 (a possible one time discharge could have occurred in 1955 during testing). Cold Cottrell units installed in 1951 were operated to collect the dust and also condense the As vapour. The combined dust and As trioxide was pneumatically pumped to underground storage in vaults. Therefore Yellowknife Bay tailings are not expected to contain a Cottrell tailings component since the Yellowknife Bay discharges occurred between 1948 and 1951.

However, fine dispersal of tailings material throughout Yellowknife Bay is possible via the tailings decant processes described in Appendix A. The high concentrations of As present behind the breakwater at the mouth of Baker creek confirm this as does the recent work of (Andrade 2006). It is also worth mentioning that the entire character of the mouth to Baker Creek has

changed since the beginning of mining at Giant. Early air-photographs show open water, while today it is choked with As- and Sb-bearing sediment and extensive weed growth in the summer.

The calcine residue and Cottrell waste streams may be especially important with respect to As-bearing fines deposited in Baker Creek and Yellowknife Bay since i) they are on average finer grained (silt sized and finer) than the flotation tailings, and ii) they contain high concentrations of As in a form (eg. roaster-derived Fe oxides) that is poorly characterized.

It is also important to note that the character of the calcine residues from hearth roasting produced before 1958 may be different than the later fluosolids roasted residues. Calcine residue discharged to Yellowknife Bay between 1948 and 1951 is expected to be wholly generated by hearth roasting (first fluosolids roasting commenced in 1952).

In summary, the Yellowknife Bay tailings depositional history and the present tailings distribution are likely to be very complex given the following:

- potential heterogeneous nature of the tailings (intermittent and variable calcine residue content at time of deposition)
- seasonally varying depositional processes (frozen vs. unfrozen discharge environments at Yellowknife Bay), and
- subsequent erosional and long-shore drift processes.

In particular, it is also important to realize that fine-grained tailings are also likely dispersed throughout a large area of Yellowknife Bay (probably concentrated most heavily around the Baker Creek outlet) due to the historic practice of discharging decanted tailings water through Baker Creek. A study of contamination of water, sediment and fish in 1992 and 1993 (Jackson *et*

al. 1996) indicates As concentrations of 1500 to 2500 ppm in sediment from the Baker Creek outlet at Back Bay. This and other studies (eg. Mudroch *et al.* 1984) and information summarized in Appendix A, formed the framework for the recent work by Andrade (2006) on the Yellowknife Bay tailings and sediments and continuing work by Fawcett (2005).

In the last years of operation (1994 to 1999) the Giant mine still released in excess of three tonnes per year of As to the Yellowknife region via stack emissions, and more than 0.5 tonnes per year in treated tailings decant water to Baker Creek which drains to Yellowknife Bay (Environment Canada 2002). These emissions compare to a total over the life of the mine of up to 7000 tonnes of As to the environment via stack emissions prior to 1951 (see above), some 50,000 to 80,000 tonnes of As released with tailings (~16 million tonnes of tailings at approx. 0.3 to 0.5 wt. % As[1]) and a total of 142,000 tonnes of As (237,000 tonnes As trioxide dust at ~60% As (SRK 2002)) stored in underground stopes and chambers at the mine site between 1951 and 1999. The As stored underground has been the subject of a public consultation and engineering review managed by Indian and Northern Affairs Canada since 1999 (SRK 2002). Present plans are to re-establish permafrost and prevent groundwater flow, by refreezing ground with thermo-siphons.

Of the estimated tonnage of As (50,000 to 80,000 tonnes) in the tailings, an unknown quantity of As has been redistributed to surrounding sediments by spills and poor tailings decant management (discharge of excess water from the tailings impounds) especially in early years of mine operation (Berube *et al.* 1974). Back Bay sediments (Figure 1-2) downstream of the Giant Mine tailings decant into Baker Creek, have been know to contain As concentrations in excess of

---

[1] The estimate of arsenic tonnage in the tailings is at best order of magnitude based on very limited data, but the values are reasonable when compared to an arsenic balance prepared in the early 1960s (Grainge, 1963), which shows ~4 tonnes per day of arsenic in the tailings stream in comparison to 15 tonnes per day of arsenic in baghouse dust.

1500 ppm since the 1970s (CPHA 1977). Separation (cycloning) of the coarse tailings fraction for use as mine backfill between 1957 and 1985 has also reduced the As tonnage in the tailings ponds by an unknown amount and is a second source of underground As now being considered along with As trioxide dust (SRK 2002).

1.3.3.4 Tailings Effluent Treatment

Commencing sometime before 1965 (Cross 1987), the high As tailings streams from the calcine and ESP circuits were limed in an attempt to stabilize the As (Pawson 1973 and Halverson & Raponi 1987). There is conflicting information on what the form of the precipitate from this treatment may have been. Pawson (1973) suggests Fe arsenate with lesser calcium arsenates or possibly Fe orthoarsenites. Halverson & Raponi suggest the product was calcium arsenite 75% and calcium arsenate 25%. Regardless of the form, this may represent a significant change in the tailings deposited at that time. The stability of these Ca-As (or Ca-Fe-As) oxides have been questioned (Halverson & Raponi 1987). In 1981 an effluent treatment plant utilizing alkaline chlorination went into operation to treat As, cyanide and dissolved metals (copper and zinc). The treatment plant treated all tailings decant water prior to discharge into Baker Creek and operated roughly from spring thaw to freeze up (May to October). Modifications to the effluent treatment plant were made in 1990 converting the use of chlorine as an oxidant to hydrogen peroxide treatment (Royal Oak Mines 1992). The treatment plant continues to operate even though the mine is closed in order to treat mine water and surface water runoff (Fawcett *et al.* 2006).

1.3.3.5 Potential for Sulfide Oxidation (Mine Tailings and Waste Rock).

Acid rock drainage from sulfide-bearing mine tailings and waste rock can result in mobilization of As along with a range of dissolved metals (eg. Cu, Ni, Pb and Zn) in low pH groundwater. Neutral drainage systems (those containing excess carbonate) have historically received less attention due to the generally lower mobility of most metals in neutral pore-waters. However, in

contrast to the metals, anionic complexes of As can be mobile over a wide range of pH and Eh. This is especially important when considering As-bearing hydrothermal gold deposits, since they often contain only a relatively small amount of sulfide and a significant amount of carbonate.

1.4 Scope of Research

It is clear from much of the work being carried out on As cycling, mobility and bioavailability, that the limited understanding the solid phases in the environment can be a significant limitation in many studies. In particular, there is little understanding of the form of As in the calcine and yet it constitutes a significant portion of the As in the tailings (Table 1-4) and may also be particularly important as a component of the off-site sediment As load. Therefore, a study of the form of the As in the calcine and calcine component of the tailings was to be a major focus of this work.

The application of synchrotron methods and particularly XANES to characterize the oxidation state of As in solid-phase samples was evaluated as a high priority technique for this study. The timely addition of μXRD at NSLS beamline X26A, where much of this analytical work was done, significantly expanded the capabilities of the grain-by-grain analytical approach we were developing.

1.4.1 Goals and Objectives

The principal goals of this thesis were the following.

- Evaluate the suitability and effectiveness of applying rapidly advancing synchrotron-based micro-analytical techniques such as μXRD and μXANES to complex environmental matrices including gold mine tailings, gold roaster mill products and mine waste rock from the Giant mine site.

- Characterize the principal form(s) of As in the roaster calcine residue and evaluate As behaviour in the tailings environment over time.
- Characterize the As in waste rock fill material from the Giant mine Townsite with a particular focus on potential As mobility and bioavailability from a mineralogical perspective.

Specific objectives of the research were:

- investigate specific aspects of past and recent mining, milling and environmental management practices at Giant and Con mines in order to understand the sources of As dispersal to the environment at and adjacent to the mine sites (largely described in the preceding sections of Chapter 1),
- develop a grain scale approach (10 μm scale) for solid-phase As speciation in thin sections using conventional and synchrotron-based methods,
- identify and characterize the As-bearing solid phases in tailings and mill products from the Giant mine, and
- identify and characterize As-bearing solid phases in Giant mine townsite "soils" especially the waste rock fill materials used in roads and lake-front fill that contain high As concentrations (>1000 ppm).

The outcome of this research was expected to provide:

- a detailed understanding of the solid-phase As speciation in As-bearing mine wastes originating at the Giant mine,
- an understanding of the potential effects of weathering and disposal environment on the As-bearing phases, and

- an improved understanding of As dispersal to areas adjacent to the Giant and Con mines that will aid in directing future research into solid-phase As speciation, not only at the mine sites, but in the surrounding environment (including soils and sediments).

Chapter 2 of this thesis is from a published manuscript (Walker *et al.* 2005) which describes the methodology of the grain scale analytical approach and synchrotron techniques applied in the context of two specific samples from the Giant Mine. Chapter 3 is a manuscript in preparation for journal submission that presents the overall findings on As speciation in the Giant mine tailings based on the grain scale analytical work and sequential selective extractions. Chapter 4 is a manuscript in preparation for journal submission that documents the characterization of weathered As-bearing sulfides in the Giant Townsite waste-rock fill materials and relates the mineralogy to sequential selective extraction results. Chapter 5 discusses the experience gained in applying the synchrotron methods and Chapter 6 provides the overall summary, principal conclusion and recommendations for further work.

Chapter 2 - The Speciation Of Arsenic In Iron Oxides In Mine Wastes From The Giant Gold Mine, N.W.T.: Application Of Synchrotron Micro-XRD And Micro-XANES At The Grain Scale

2.1 INTRODUCTION

The mobility and toxicity of As depend on its speciation (chemical form and oxidation state). In the dissolved phase, As is most often present as arsenate ($H_2AsO_4^-$ or $HAsO_4^{2-}$) or arsenite ($H_3AsO_3^0$), with arsenate being the more oxidized and thermodynamically stable form at ambient conditions. However, disequilibrium of As species is well documented (Inskeep *et al.* 2002, Smedley & Kinniburgh 2002), and both reduced and oxidized forms commonly occur together. This fact is important, as arsenite is generally regarded as the more mobile (Masscheleyn et. al. 1991) and more toxic in the environment (Naqvi *et al.* 1994, Winship 1984).

The concentrations of specific dissolved species present in pore water and groundwater are a measure of As mobility. However, the solid components of the sediments, soils and mine-waste are the ones that provide the geochemical or biogeochemical substrate that controls As partitioning to the aqueous phase. In addition, mining and metallurgical processing (including smelting and roasting of ores) produces fine particulate As-bearing solid phases that can be transported and deposited in the local and regional environment by aerial and hydraulic processes (Berube *et al.* 1974, Hocking *et al.* 1978, Ragaini *et al.* 1977, Mok & Wai 1990, Moore & Luoma 1990, Henderson *et al.* 1998, Reimann *et al.* 2000). It is important to understand the solid-phase speciation of As in mining and metallurgical products, as it may differ from the background speciation, or from solid phases produced by post-depositional adsorption or precipitation reactions. The multiple origins of As-bearing phases in soils and sediments adjacent to mining

and metallurgical operations suggest that a grain scale micro-analytical approach may be particularly well suited for determining As speciation in these complex materials.

In the present study, we establish a method to investigate the solid-phase speciation of As in silt-sized soil, sediment and tailings particles. We have combined powder XRD and bulk XANES with optical microscopy and grain by grain micro-analysis using EPMA, and synchrotron μXRD and μXANES. We highlight findings of complex As speciation in roaster-derived Fe oxide phases from the Giant mine, Yellowknife, Northwest Territories, and show the utility of applying synchrotron-based micro-analytical techniques at the grain scale (20 to 50 μm). Grain-scale analyses clarify potential ambiguities that would otherwise exist in these materials based on bulk analyses and petrography alone.

2.2 Background Information

In studying areas influenced by mining and metallurgical processing, it is important to distinguish between primary and secondary phases (Jambor 1994, Jambor & Blowes 1998, Manceau *et al.* 2002). Primary phases are those that originate from the milling process (both unreacted and reacted minerals and metallurgical products), and secondary minerals are those formed by reactions following deposition in the environment (*e.g.*, weathering or precipitation). Metallurgical products are designated as primary anthropogenic phases in order to distinguish between anthropogenic influences (metallurgical chemical reactions in the mill) and natural geochemical processes (Manceau *et al.* 2002). Observing physical or chemical changes to primary As-bearing phases in the environment may provide evidence of the long-term stability or behaviour of As in the environment. Secondary As-bearing minerals or As sorbed to other primary or secondary minerals is direct evidence of the attenuation of As in soils, sediments and mine waste (*i.e.*, sequestering by solid phase transformation, or removal from the aqueous phase by sorption or precipitation).

For a typical gold roasting operation, the primary phases would therefore include ore minerals (*e.g.,* arsenopyrite and pyrite), and gangue minerals (*e.g.*, quartz, other silicates and carbonates) and anthropogenic solid reaction products produced during milling (*e.g.*, hematite (α–Fe_2O_3) and maghemite (γ–Fe_2O_3) derived from the thermal oxidation of pyrite and arsenopyrite).

2.2.1 Solid-phase speciation of As in geochemical cycling, fate and bioavailability

Bonding in As-bearing minerals is dominantly ionic where coordinated with oxygen and covalent where coordinated with sulfur, Fe or itself (Greenwood & Earnshaw 1998). Arsenic in both ionic and covalent solids can exhibit a wide range in oxidation number: +5 for arsenates (*e.g.*, scorodite, $FeAsO_4{\cdot}2H_2O$) and +3 for arsenites (*e.g.*, arsenolite, As_2O_3 and schneiderhohnite, $Fe^{II}Fe^{III}{}_3As^{III}{}_5O_{13}$), +3 for orpiment ($As_2S_3$), +2 for realgar ($As_4S_4$), 0 for elemental arsenic (As), -1 for arsenopyrite and -2 for westerveldite (FeAs). Arsenic of different oxidation-states can also be incorporated in solid solution in mineral phases. For example, As^{-I} substitutes for S in pyrite (*e.g.*, Simon *et al.* 1999 and Savage *et al.* 2000), and AsO_4 substitutes for SO_4 in jarosite ($KFe_3(SO_4)_2(OH)_6$) (Dutrizac & Jambor 2000, Savage *et al.* 2000, Paktunc & Dutrizac 2003, Savage *et al.* 2005). Arsenate, and in some cases arsenite, can also sorb strongly onto clay minerals, and oxyhydroxides of Fe, Al and Mn (Smedley & Kinniburgh 2002, Hering & Kneebone 2002, and references therein). Bostick & Fendorf (2003) have shown that under aqueous reducing conditions, arsenite can be reduced to form an arsenopyrite-like surface precipitate on the surface of Fe sulfides.

Whether sorbed or structurally bound, understanding the kinetics and mechanisms of release of As in the context of equilibrium relationships involving solids and solutions is necessary to evaluate short- and long-term mobility and bioavailability (Huang & Fujii 1996, Hering & Kneebone 2002). For example, high surface-area As-bearing Fe oxyhydroxides, which are

amorphous or poorly crystalline, may recrystallize to more stable phases and desorb As (Fuller *et al.* 1993, Waychunas *et al.* 1993, Smedley & Kinniburgh 2002, Paktunc *et al.* 2004). However, such processes may be slow in nature owing to the presence of strongly surface-sorbed or coprecipitated ions including arsenate (Cornell & Schwertmann 1996). Also, redox conditions can profoundly affect partitioning of As between aqueous and solid species (*e.g.*, Hering & Kneebone 2002, Smedley & Kinniburgh 2002, Cummings *et al.* 1999, Nickson *et al.* 2000, Harvey *et al.* 2002), an important consideration in natural environments where biogeochemical conditions are rarely static.

With respect to bio-availability of As that has been orally ingested by humans, it is clear from existing work that solid phase As is less bioavailable than As in solution (Ruby *et al.* 1999, Valberg *et al.* 1997). However, in the solid state, the amount that is bioavailable depends on a number of factors, including oxidation state, mineralogy, grain size, surface area and morphological properties, such as encapsulation or rinding of grains (Ruby *et al.* 1999, Bhumbla & Keefer 1994).

2.2.2 Anthropogenic iron-arsenic oxides

Anthropogenic As-bearing Fe oxides have been identified in the environment (soils, sediments, tailings and house dust) adjacent to sulfide smelting and roasting operations (*e.g.*, Davis *et al.* 1996, McCreadie *et al.* 2000). Roasting of pyrite and arsenopyrite produces Fe oxides with concentric or porous 'spongy' texture depending on the pathway (formed by way of a pyrrhotite intermediate phase or not) and temperature of formation (Carter & Samis 1952, Jorgensen & Moyle 1981, Arriagada & Osseo-Asare 1984, Robinson 1988, Grimsey & Aylmore 1992, Dunn *et al.* 1995). However, there is limited understanding of the solid-phase speciation of As in Fe oxides derived from roasting. The presence of an unidentified non-sulfide As-bearing phase or phases has been inferred based on a sizeable excess of As to sulfur in some calcines (*e.g.*,

Arriagada & Osseo-Asare 1984). Roaster-derived Fe oxides are an example of primary anthropogenic As-bearing solids that have a high As content (several weight percent) and have little analogy to better studied naturally occurring primary minerals such as arsenopyrite and secondary minerals such as As-bearing Fe oxyhydroxides and As sulfides.

For many low-temperature geochemical systems, formation of Fe oxides and oxyhydroxides as amorphous or crystalline nanoparticles (*i.e.* 1 to 100 nm in diameter, Waychunas 2001) is expected over short to medium time scales (Banfield & Zhang 2001, Waychunas 2001, Hochella 2002). Furthermore, industrial methods of Fe oxide production at elevated temperatures also produce nanocrystalline Fe oxides (*e.g.*, Morjan *et al.* 2003, Deb *et al.* 2001). Recent experiments, by Eneroth & Koch (2003), determined that thermal oxidation of Fe sulfides (pyrite and marcasite) can result in small sizes (15 to 60 nm) of the average crystallite sizes in the resulting Fe oxides. If roaster- or smelter-derived phases (grains) are nanoparticle composites, they may exhibit modified phase-stability relationships and different reaction kinetics in comparison to their microscopic and macroscopic counterparts (Banfield & Zhang 2001, Navrotsky 2001).

2.2.3 Roasting of gold ore at the Giant mine

Mineralization at the Giant mine, Yellowknife, Northwest Territories, occurs within shear zones as disseminated sulfides in broad silicified zones or quartz carbonate veins bounded by muscovite or chlorite schist (Boyle 1960, Ellis & Hearn 1990). The gold at the Giant mine is refractory, being mostly incorporated submicroscopically within arsenopyrite, making it unavailable to conventional cyanide extraction. To access this "invisible" gold, ore milling at Giant mine included grinding, flotation, roasting of the flotation concentrate followed by cyanidation (More & Pawson 1978). The roasting of gold ore is a thermal oxidation process that decomposes sulfide minerals such as pyrite and arsenopyrite into porous Fe oxides including hematite, maghemite or

magnetite, to make the ore amenable to cyanidation (Gossman 1987, McCreadie *et al.* 2000). Roasting at the Giant mine commenced in January 1949 (Grogan 1953) and continued until the mill closed in late 1999.

Roasting at the Giant mine has produced a number of As-bearing wastes including As trioxide baghouse dust, electrostatic precipitator dust, and calcine residue tailings (cyanidized roasted sulfide concentrate). Baghouse dust has been stored in underground stopes and chambers since 1952 and is the subject of critical evaluation for remediation at the present time (SRK 2002). It has been estimated that some 7900 tonnes of As were released to the environment by stack emissions between 1949 and 1952, since roaster off-gases were not treated at that time (unpublished Environment Canada report referenced to by Hocking *et al.* 1978). With the exception of the As trioxide dust, roaster-derived wastes have generally been discharged with flotation tailings along with mine and mill water. On a dry tonnage basis, the calcine residue tailings constitute only some 10% of the total tailings discharged, but approximately 70% of the total As by weight (Walker & Jamieson 2002).

2.2.4 Analytical Approach

X-ray absorption spectroscopy (XAS) is effective at determining both oxidation state by X-ray absorption near edge structure (XANES), and coordination state by extended X-ray absorption fine structure (EXAFS). The XANES approach is capable of determining oxidation states of As by resolving small shifts in the energy position of the As K absorption edge (Fendorf & Sparks 1996). The ability to detect As^{III} bearing phases may be particularly important since they are generally linked to lower stability and higher toxicity.

Methods for characterization of solids routinely combine grain scale analyses such as optical microscopy, scanning electron microscopy (SEM) and electron-probe microanalysis (EPMA)

with results of bulk analyses such as X-ray diffraction (XRD). Bulk XAS methods have also been successfully applied for the characterization of As-bearing phases in soils (*e.g.*, Morin *et al.* 2002) and mine waste materials (*e.g.*, Paktunc *et al.* 2003, Morin *et al.* 2003, Savage *et al.* 2000, Foster *et al.* 1998). Comparatively fewer authors (*e.g.*, Strawn *et al.* 2002, Paktunc *et al.* 2004) have utilized μXAS methods in As focused studies. A comprehensive discussion of methods of solid-phase speciation for metals and metalloids, including application of synchrotron μXAS methods can be found in Manceau *et al.* (2002).

2.3 EXPERIMENTAL

2.3.1 Samples

Materials selected for this study include: cyanidized roaster calcine residue (hereafter referred to as calcine), and a calcine-rich horizon from tailings deposited on the shore of Great Slave Lake about 1950 (hereafter shoreline tailings). The selected tailings-hosted horizon is a subsample of a core collected as part of a larger suite of mine-tailings samples obtained at the site in July 1999. Coring was accomplished by hand driving aluminium tubes (wall thickness 1.6mm) with a drop hammer assembly. The tubes were extracted, immediately cut at the top and bottom to remove any open air space, sealed and placed in coolers with ice packs. Staff at the Giant mine provided mill samples as slurries in one-litre sealed containers. All samples were frozen shortly after collection (to preserve solid phases from further reaction) and shipped in coolers to laboratory facilities, where they were kept frozen until preparation for analysis.

In order to prepare thin sections, samples were thawed and air-dried at room temperature. Polished thin sections were prepared as intact specimens (plugs extracted from tailings core to preserve stratigraphic relationships) and grain mounts (mill products) using As-free silica glass slides and room temperature set epoxy (Sealtronic 21AC-7V by Industrial Formulators), and

without the use of added heat or water. Oil was used for all grinding and polishing. Sections were polished to a final thickness of approximately 30 to 40 μm. The final thickness of sections was determined by measuring edges of polished sections with a micrometer. The slightly thicker sections (standard sections are usually 20 to 30 μm) were necessary to minimize stripping of the fine-grained sections from the slide during final grinding. For some samples, a second "detachable" thin section was made from the same off-cut to facilitate transmission mode μXRD which requires removal of the glass slide substrate from beneath the thin section. The preparation of these thin sections was the same as the other sections, except for the following modifications. Each section was polished and fixed to a prefrosted glass slide using Krazy® glue instead of epoxy. Grinding and polishing were completed in the same manner as the regular sections except that the final polished thickness was up to 50 μm. This thickness ensured a robust specimen when the glass slide was removed. Following petrographic examination and target location (see below), the thin section was immersed in an acetone bath (ACS grade) until complete separation of the sample from the slide. Detachment time seems to depend on sample grain size and ranges from 20 minutes for coarser-grained sections to several hours for finer-grained sections. The detached sample was allowed to dry, oriented and carefully pressed on Kapton® tape and placed into a 35-mm cardboard slide holder for analysis. Kapton® mounted sections were later fixed back onto glass slides using double-sided tape for characterization by EPMA.

Thin sections were inspected and photographed under transmitted and reflected light to identify potential As-bearing phases and to map out targets for microbeam analysis. Target locations were catalogued using coordinates from a scanned image of the thin section and microscope photographs at multiple scales (Figure 2-1) to ensure that the small grains (generally < 50 μm diameter) could be relocated for subsequent analyses on several different micro-beam instruments.

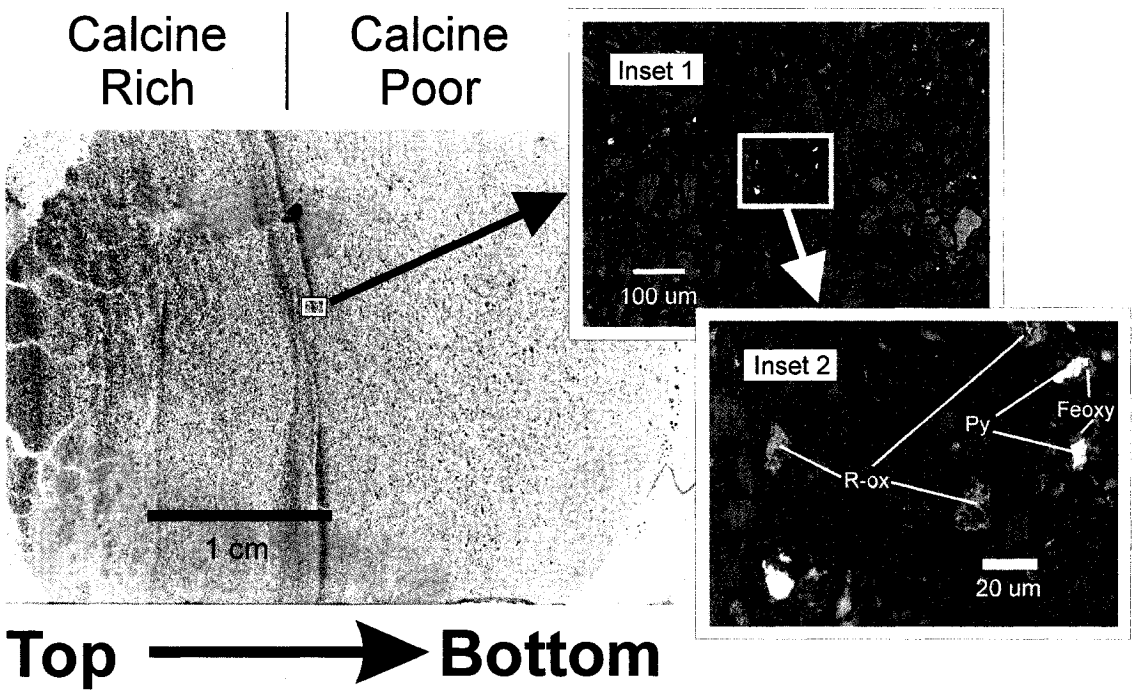

Figure 2-1. Thin section scan showing calcine layer in shoreline tailings. High resolution thin section scan of 50-year-old stratified shoreline tailings subsampled from core taken adjacent to Yellowknife Bay. Insets 1 and 2 are plane-polarized reflected light photomicrographs that provide progressive magnification of one of the darker silty layers. Darker layers are calcine-rich and contain As-bearing roaster Fe oxides (R-ox, Inset 2). Two grains of weathered pyrite (Py) with As-bearing Fe oxyhydroxide rims (Feoxy) are identified for comparison. Targets and reference points are recorded as coordinates in mm from scans of the thin sections. Maintaining a consistent orientation allows target spots to be readily located on any micro-beam instrument with an X,Y coordinate stage. Photos at multiple scales provide backup for relocating grains.

2.3.2 Analysis using μXANES and μXRD

Synchrotron analysis was conducted with the hard X-ray microprobe, X26A, at the National Synchrotron Light Source (NSLS), Brookhaven National Laboratory. A 350-μm collimated monochromatic beam is focused to approximately 10 μm in diameter using a system of Rh-coated Kirkpatrick-Baez mirrors (Eng *et al.* 1995). A monochromatic beam is achieved using a Si(111) channel-cut monochromator. Instrumental resolution is approximately 3.5 eV with reproducibility of the edge position at better than 1 eV. All the μXANES experiments were made by scanning through the As K edge (11,867 eV) in fluorescence mode with a Si(Li) detector. MicroXRD experiments are imaged in 2D, in transmission mode using a Bruker SMART 1500 CCD diffractometer with a fiber optic taper, in high-resolution mode at 1024x1024 pixels.

Thin sections and standards are placed in cardboard slide holders and fixed by thumb-screws into the vertical plastic sample holder oriented at 45° to the beam in the horizontal plane. This geometry results in an elliptical surface footprint of the beam on the sample (10 μm in the vertical x 15 μm in the horizontal). Beam penetration through the sample is approximately cylindrical. The small grains being analysed in these materials (<50 μm) can result in spatial inhomogeneity under the beam especially since grain depth in the sections can be less than the full thickness of the section (30 to 50 μm). This potential inhomogeneity is handled by observing the sections in transmitted as well as reflected light and by comparing μX-ray fluorescence maps (Fe and As) to scaled photos of thin sections. Two or three analyses can then be conducted through the core and rim of grains or in regions selected to either investigate or avoid unidentified material buried in the section.

XANES analysis was conducted by scanning across the absorption edge region (11,830 to 11,970 eV) in three segments with a 2- to 4-second dwell time by increment. The step increment was 5 eV in the pre- edge region (11,830 to 11,850 eV), 0.4 eV across the edge (11,850 to 11,890 eV) and 2 eV in the post-edge region (11,890 to 11,970 eV). Primary standards were routinely run, to correct for any shifts in edge position that might occur over time (total range less than 1.5 eV). Each spectrum was normalized to an incident beam flux measured by an upstream ion chamber, pre-edge background corrected at 11,840 eV, and then normalized to the edge-step (intensity at 11,960 eV). Normalization was done at approximately 100 eV above absorption edge owing to the significant post-edge oscillations that vary significantly among the various As standards. Standard materials (Table 2-1, Figure 2-2) were selected to cover a wide range of oxidation states. To manage self-absorption effects, only the suspended (finest) fraction was retained and mixed with boron nitride (99.9% < 1 um) to obtain a total As concentration of approximately 4% (w/w). Since arsenic trioxide is slightly soluble in ethanol, an additional dry ground standard of this material was prepared, but there was little difference in the resulting XANES scans. Realgar is known to undergo light-induced transformations to a number of other As_4S_4 polymorphs (Bonazzi, *et al.* 1996). To minimize the potential for such reactions, the realgar was stored in the dark immediately following preparation and until analysis. However, no attempt was made to track possible transformations. Each mixed standard and boron nitride was dispersed as a thin layer onto Kapton tape for analysis.

For μXRD, the incident x-ray beam was tuned to 11,950 eV (1.0375 Å). The distance between the camera and the thin section was fixed at approximately 17 cm, which yielded a calibrated range of *d*-values between 2 and approximately 10 Å. Detector calibration was made using SRM 674a diffraction standard α-Al_2O_3. Calibrations and corrections for detector distortions (camera-sample distance, the camera tilt and rotation, and the beam center on the camera plane) were done

Table 2-1. Standards for μXANES analysis

Primary Standard	Formula	Source/Locale	Edge Position† (eV)	Normalized peak intensity
Scorodite	$FeAs^{V}O_4 \cdot 2H_2O$	Laurium Greece [M6303]	11,873.9*	3.2
Arsenolite	$As^{III}_2O_3$	J.T. Baker reagent	11,870.0*	2.9
Arsenopyrite	FeAsS	Mina La Bufa, Mexico [M5579]	11,867.0	2.2
Secondary Standard	**Formula**	**Source/Locale**	**Edge Position†‡ (eV)**	**Normalized peak intensity**
Sodium arsenate	$Na_2HAs^{V}O_4 \cdot 7H_2O$	J.T. Baker reagent	11,873.5	3
Sodium arsenite	$NaAs^{III}O_2 \cdot 4H_2O$	J.T. Baker reagent	11,870.2	2.6
Schneiderhohnite	$Fe^{II}Fe^{III}_3As^{III}_5O_{13}$	Urucum, Minas Gerais, Brazil	11,869.8	2.7
Orpiment	As_2S_3	Moldawa, Banat, Hungary [M7719]	11,868.2	3.5
Realgar	As_4S_4	Hunan Realgar Mine, Shimen, Hunan Province, China [M9900]	11,867.7	2.7
Elemental arsenic	As	Sampson Mine, Andreasberg, Harz Mountains, Lower Saxony, Germany [M72]	11,867.0	1.7

[Mxxxx] = Miller Museum Reference, Department of Geology Queen's University.
† Edge position at first derivative maximum relative to arsenopyrite set at 1,867.0.
* Estimated error based on multiple repeat analyses relative to arsenopyrite is better than ~0.4 eV.
‡ Edge positions of secondary standards based on one or two analyses relative to arsenopyrite standard.

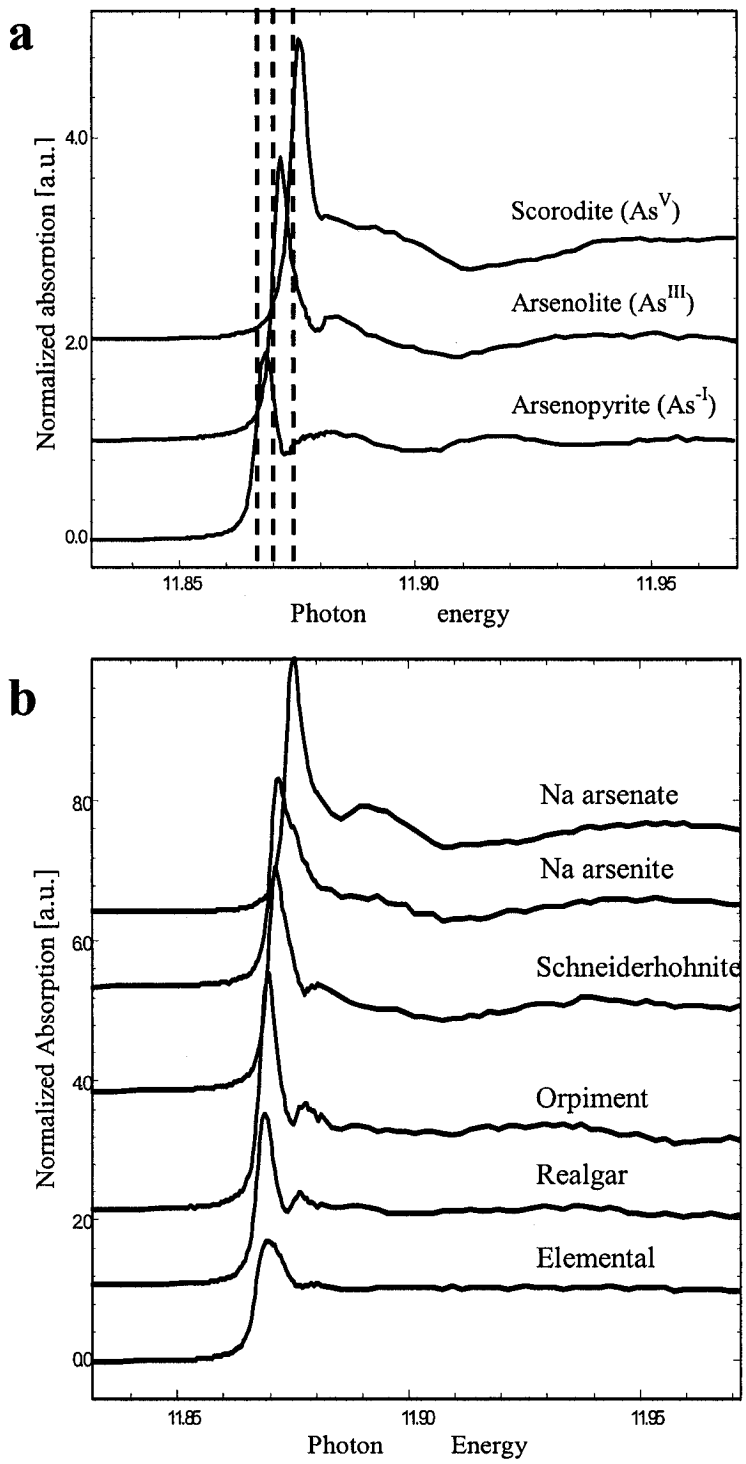

Figure 2-2. Micro-XANES spectra of standards. a) Primary standards. Vertical dashed lines indicate edge position at first derivative maximum for arsenopyrite (left), arsenolite (middle), and scorodite (right). b) Secondary standards. All spectra are spread vertically for purposes of presentation only.

using Fit2D™ software (Hammersley 1998). The two dimensional patterns were manually inspected to identify the types of reflections present (rings or points). The *d*-values of unknowns were determined by integration of the two-dimensional pattern to produce a simulated powder-diffraction pattern. Resolution is about 0.2° 2θ, as measured by integrated peak widths (FWHM) for the α-Al_2O_3 standard. Unknown phases were identified by comparison with reference powder-diffraction patterns (ICDD 2003).

The experimental conditions in this case utilize monochromatic X-rays without randomization of grain orientation under the beam. Under these conditions, well-defined Debye-Scherrer rings are only obtained where the average size of mineral crystallites is small relative to the diameter of the incident beam and where their orientation is sufficiently random (He 2003 & Manceau 2002). Where this is not the case, crystals at diffracting conditions show portions of reciprocal lattice nets *i.e.,* individual spots, arcs or spotty rings representing discrete diffracted beams.

2.3.3 Bulk X-Ray diffraction and bulk XANES

Duplicate samples of the mill calcine (subsample of cone-and-quarter split of M2M) and shoreline tailings (representative sample taken perpendicular to bedding in same interval as CB1bS3) were submitted for bulk X-ray diffraction analysis. Analysis utilized a Philips X'Pert MPD fitted with a Co tube operated at 45 KV and 40 mA, with 0.2 rad soller slits, a 20-mm sample mask, 1/2° divergence slit, K_β filter and X'Pert detector. Samples were mounted dry on glass discs rotated at 1/2 revolution per second with a scan rate of 20 seconds per step, from 5° to 90° 2θ. The material of stratified shoreline tailings was sampled and analyzed in two parts. The first represented the upper, more calcine-rich portion, and the second the less stratified, lower calcine content portion (Figure 2-1).

Bulk XANES analysis was completed with the mill calcine mounted as a thin powder on Kapton

tape using similar analytical conditions as those for μXANES described above, but using an unfocussed beam approximately 0.12 mm^2 (0.35 mm x 0.35 mm). Three random locations were analyzed (single scan each) and averaged after confirming similar spectral shapes for each domain.

2.3.4 Linear-combination fitting of XANES data and PCA analysis

The shape of both bulk and μXANES spectra suggested the presence of multiple oxidation states within the target roaster Fe oxide grains (Figure 2-3). We found, however, that linear combination fits with certain standards of different oxidation states (model compounds) gave reasonable fits for the unknown spectra. Linear combination fitting was made using WinXAS™ v.2.3, and

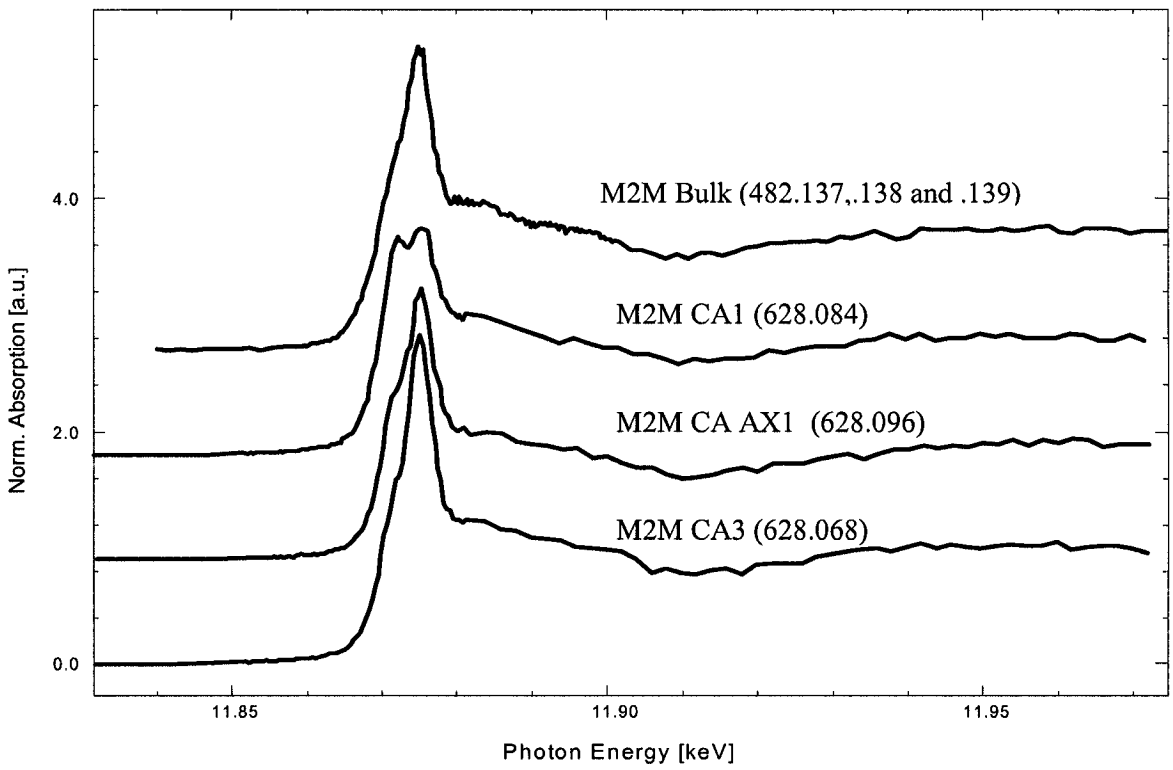

Figure 2-3: Selected XANES spectra from calcine sample (M2M). The XANES spectrum of the bulk sample suggests the presence of As in more than one oxidation state. Analysis of individual grains of Fe-oxide also show the presence of more than one oxidation state, with different spectral shapes indicating a variation in oxidation state proportions from one grain to another (see Table 2-4).

procedures modified from those described in Ressler *et al.* (2000). Fits may not yield quantitative concentrations since the actual As species have yet to be determined. However, the proportions calculated on the basis of a consistent set of standards are useful to highlight variability both within and between grains, and between samples. Reported percentages of each model compound in fits are absorption-corrected amounts (normalized to 100%), as calculated by WinXAS. Totals before correction were in the range of 95% to 105%, and generally greater than 98% and lower than 102%. Fitted model spectra at 5% or less gave little noticeable improvements to fits. Analysis of control mixtures of model compounds in macroscopic XAS studies have shown the precision of similar fit procedures to be approximately 10 % (*e.g.,* Foster *et al.* 1998).To increase objectivity in the linear-combination procedure of fitting, a principal component analysis (PCA) was conducted using routines in the WinXAS™ software in a manner similar to that described in Ressler *et al.* (2000). A total of 14 spectra from M2M were selected for PCA analysis to cover the range of spectral shapes encountered (Figure 2-3). All spectra were normalized, calibrated and sectioned to include only the immediate-edge region (11,850 to 11,900 eV). Results of the PCA analysis indicate that at least three components are necessary to fit the data. The first two components accounted for 82 % of the fit, and three components accounted for 85 %. Transform fits were then applied to the standard spectra (Ressler *et al.* 2000), and a quality of fit determined by visual inspection and the residual values calculated by the WinXAS™ software (Table 2-2).

Transform fits for the arsenite and arsenate model compounds gave generally good fits over the edge (white line peak), but diverged in the region above the edge (Table 2-2). The model compounds (primary and secondary standards) thus may not be specifically present in the unknown spectra, but that the strength and position of the white line for a given oxidation state (especially As^{III} and As^{V}) are characteristic within the unknown spectra. Transformed spectra for lower oxidation state standards and orpiment were noisier than for the arsenate and arsenite

transforms. This may be due to the lower abundance (or absence of) low oxidation state species in the unknown spectra.

Table 2-2 - Selection of Model Compounds for Linear Combination Fit XANES Analysis

Standard	Formal As oxidation state	Residual of transform fit in PCA*	Quality of transform fit**		Selected for linear combination fit XANES analysis
			At the edge	Above the edge	
Scorodite	**+5**	**3.2**	**1**	**2**	**Yes**
Na arsenate	+5	8.0	1	3	No
Arsenolite	**+3**	**5.7**	**1**	**2**	**Yes**
Schneiderhohnite	+3	3.9	1	2	Yes
Na arsenite	+3	5.1	2	2	No
Orpiment	+3	9.7	3	2	No
Realgar	+2	4.6	2	2	Yes
Elemental As	0	6.1	2	3	No
Arsenopyrite	**-1**	**5.4**	**2**	**2**	**Yes**

* Residual as % under PCA target transformation routine in WinXAS™.
** Visual assessment of transform fit. 1=little to no deviation, 2=deviation, 3=poor fit.
Standards in bold are model compounds used in linear combination fit results presented in this paper.

On the basis of the PCA (Table 2-2), model compounds were selected for linear combination XANES analysis of unknown spectra. We selected scorodite to represent As^{V} species, arsenolite and schneiderhohnite representing As^{III} species, and arsenopyrite and realgar representing lower oxidation state compounds. The selected model spectra were initially applied in iterative trials, using different combinations of the above model spectra. All spectra were constrained to ±0.4 eV energy shifts during the fits. Schneiderhohnite and arsenolite gave slightly different but reasonable fits as As^{III} models. Where a lower oxidation-state compound was required to improve the fit, both realgar (edge at 11,868 eV) and arsenopyrite (edge at 11,867 eV) gave reasonable results. These trials indicated that there was no overall improvement in the fits where

schneiderhohnite and realgar were used instead of arsenolite and arsenopyrite, even though the former compounds exhibited lower residuals in the PCA transform fits (Table 2-2). For consistency, arsenopyrite (As^{-1}) was chosen as the low oxidation state model compound in subsequent analyses, on the basis of the presence of relic arsenopyrite and As-rich pyrite in the tailings. Similarly, arsenolite was chosen as the As^{III} model compound in preference to schneiderhohnite, since it is a major by-product of the roasting process.

2.3.5 Electron-probe micro-analysis (EPMA)

Electron probe micro-analysis was used to quantify total As content in individual grains of roaster Fe oxide. Analytical conditions for EPMA comprise an accelerating voltage of 15 kV, a take-off angle of 52.5°, an emission current of 100 mA, a beam current of *ca.* 40 nA, and analysis using energy-dispersive mode. Primary analytical standards for EPMA included scorodite from Laurium, Greece, for As, alunite from Marysville, Utah (Stoffregen & Alpers 1987) for S, kaersutitic amphibole for Na (Smithsonian USNM 143965) and a synthetic glass for Fe, Al, Mg, Ca, and Si (US National Bureau Standards 470). Synthetic magnetite and arsenolite were used as secondary standards to ensure accurate determination of Fe and As.

2.4 RESULTS

2.4.1 Petrography

The roaster calcine (M2M) contains predominantly silt-sized porous textured Fe oxides (maghemite and hematite) among fine sand and silt gangue (quartz, carbonates and silicates). The bulk texture of the calcine is grain supported, but poorly sorted with a fine opaque matrix that probably comprises mostly submicrometric roaster Fe oxides. The shoreline tailings sample (CB1bS3) is stratified fine sand comprising mostly quartz, carbonates and silicate gangue, with red-brown silt interbeds that contain numerous silt-sized roaster Fe oxide grains.

Both the mill calcine and the shoreline tailings contain roaster-derived Fe oxides with concentric and spongy textures (Figure 2-4). Some concentric textured Fe oxides rim pyrite in both the mill calcine and the shoreline tailings. Similar rims surrounding relic arsenopyrite are rarely observed in the mill calcine. A pyrrhotite-like phase is also present at low abundance in the mill calcine as free grains, rims on pyrite and porous cores surrounded by concentric Fe oxide. Pyrrhotite is an uncommon component in ore from the Giant mine, but is an expected intermediate product in the roasting of both pyrite and arsenopyrite (Arriagada & Osseo-Asare 1984, Dunn *et al.* 1995).

Iron oxides in the mill calcine are also fragmented in some cases. This may be due to subsequent regrinding prior to cyanidation or explosive fracturing during roasting (Dunn *et al.* 1995). Some pyrite in the shoreline tailings also exhibits weathering as Fe oxyhydroxide rims in both calcine-rich and calcine-poor zones. Under optical microscope, very few roaster Fe oxide grains exhibit bright red internal reflections characteristic of hematite and even fewer exhibit a brownish hue more characteristic of magnetite.

2.4.2 Bulk XRD patterns

XRD patterns for the mill calcine (M2M) and the shoreline tailings (CB1bS3, calcine-rich and calcine-poor zones) are shown in Figure 2-5. Bulk XRD results have confirmed the presence of quartz, muscovite, chlorite and dolomite as the dominant crystalline phases in both the mill calcine and shoreline tailings, consistent with gangue mineralogy of the Giant ore and petrographic observations. Minor phases including calcite, plagioclase and rutile have been identified by the presence of one or two major peaks. Maghemite (or magnetite) and pyrite are additional major components in the XRD pattern for the mill calcine (Figure 2-5). Identification of maghemite instead of magnetite is based primarily on petrographic observations (see Discussion below). The broad peaks exhibited by maghemite are indicative of poor crystallinity. Hematite is not observed in the XRD trace of the mill calcine. However, the two

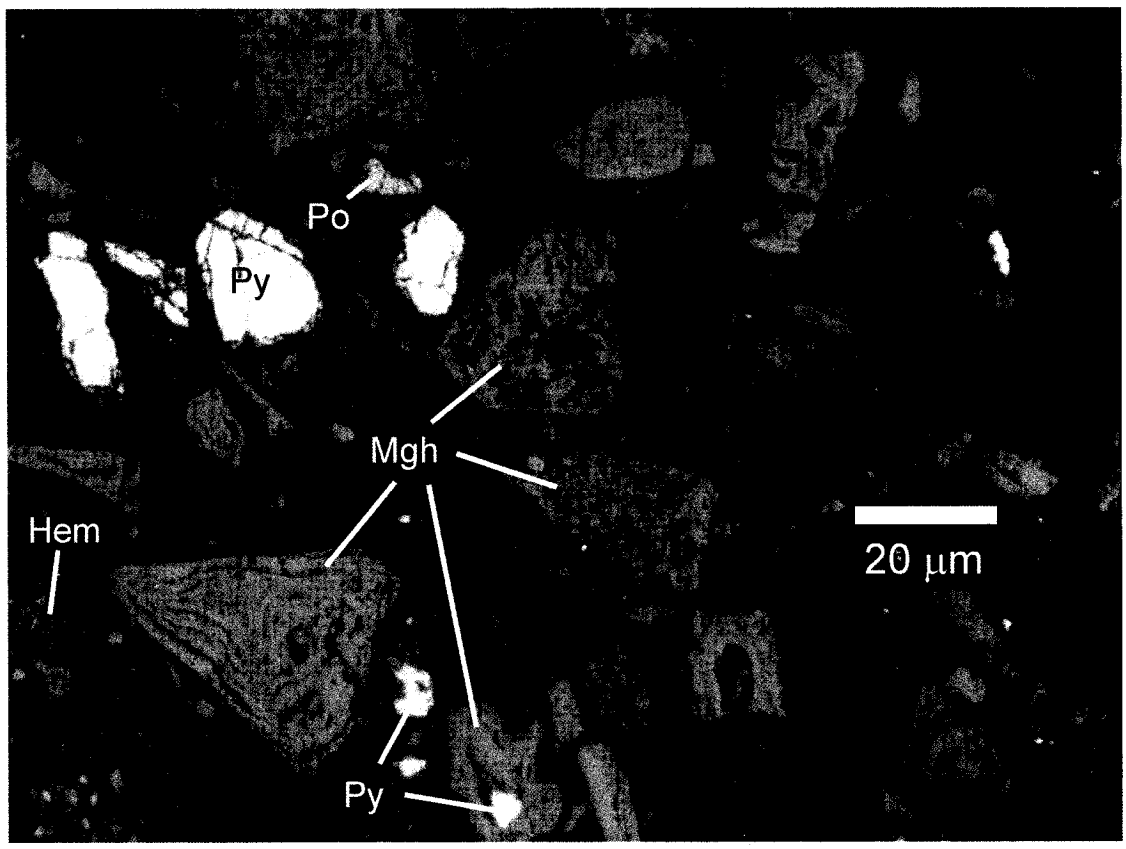

Figure 2-4. Reflected-light photomicrograph of calcine residue (roasted sulfide concentrate) from the Giant mine. Grey grains are As-bearing roaster Fe-oxides that exhibit spongy and concentric textures. Roaster Fe-oxides are mostly maghemite (Mgh) with some hematite (Hem) that exhibits red internal reflections. Bright grains are relic sulfides including yellowish white pyrite (Py) and brownish white pyrrhotite (Po).

strongest reflections for hematite (*d*-values for 104 at 2.70 Å and 110 at 2.52 Å) may be obscured by the 200 peak of pyrite at 2.71 Å and the 311 peak of maghemite at 2.52 Å. Maghemite is also clearly identified in the calcine-rich portion of the shoreline tailings (Figure 2-5).

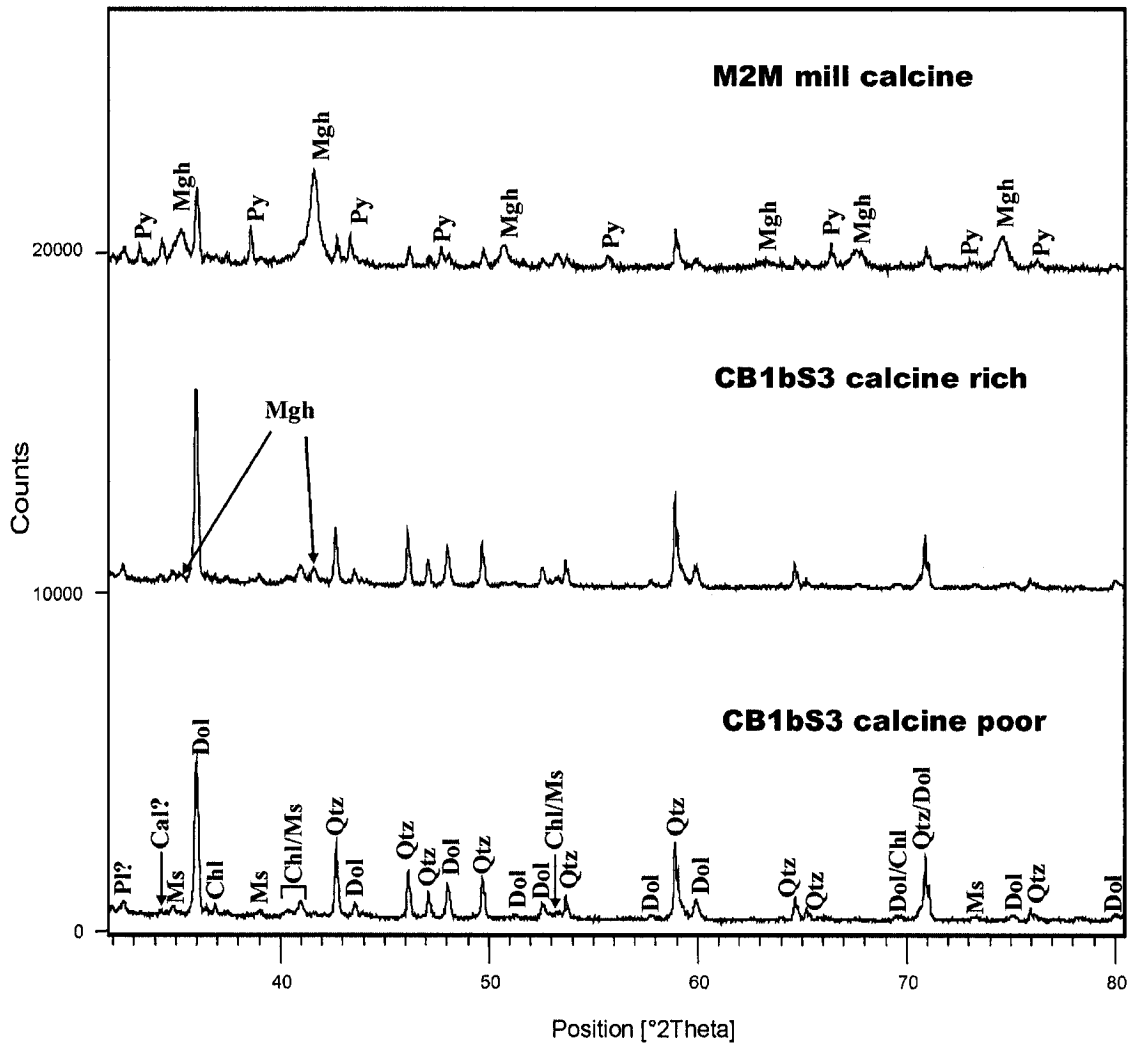

Figure 2-5. Bulk X-ray diffraction results highlighting the key interval for maghemite reflections (32° to 75° 2θ). Selected peaks for major phases (gangue) in this interval are labeled in the calcine-poor shoreline tailings (bottom, CB1bS3 calcine-poor). Pyrite and maghemite peaks are labeled in the mill calcine scan (top, M2M mill calcine). Maghemite is only weakly detected in the calcine-rich shoreline tailings (middle, CB1bS3 calcine-rich) and not detected in the calcine-poor sample as expected. Scans are displaced vertically for purposes of presentation. The major peaks for quartz, chlorite and muscovite all occur at lower 2θ angles than the interval shown.

2.4.3 Bulk XANES of mill calcine

The XANES spectrum for the bulk sample of mill calcine is shown in Figure 2-3. Mixed As oxidation states including As^{-I}, As^{III} and As^{V} are identified with contents of 9, 32 and 59%, respectively, by linear-combination fits of the reference spectra. The As^{-I} detected by XANES can be attributed to relic As-rich pyrite and arsenopyrite in the calcine, on the basis of their identification by petrography and bulk XRD. However, As^{III} and As^{V} cannot be attributed to a specific phase or phases.

2.4.4 EPMA data

No evidence of a distinct As-rich phase was found in high-resolution back-scattered electron images of either spongy or concentric-textured Fe oxides. Targets for point analyses were chosen to include both thick, concentric layers and "webs" within spongy grains. The As content of the roaster Fe oxide grains established by EPMA ranges from <0.5 to 7.6 wt. % As (Table 2-3), with the highest As concentrations in the recent mill calcine. Grain-specific analytical results are presented in conjunction with μXANES and μXRD results, which follow.

Table 2-3 - Electron Probe (EPMA) Results

	Calcine Residue (M2M)	Shoreline Tailings (CB1bS3)
# grains analysed	27	15
# analyses *	63	32
	wt. % As	wt. % As
Mean	2.9	1.3
Standard Deviation	1.7	0.6
Maximum	7.6	2.9
Minimum	<0.5	<0.5

* Between 1 and 4 analyses per grain depending on size.

2.4.5 μXANES and μXRD of roaster iron oxide grains

As in the case of bulk XANES, As in mixed oxidation states is also detected within individual grain analyses of roaster Fe oxides (Figure 2-3). Linear-combination best-fit XANES results for the spectra in Figure 2-3 (Table 2-4) generally show little As^{-I} (<15%), and a greater amount of As^{III} and As^{V}. Pentavalent As is usually the dominant oxidation state observed for most grains, but As^{III} constituted up to 52% of individual samples. Analysis of three opaque areas in the matrix of the mill calcine (*e.g.,* Figure 2-3, Table 2-4) confirms the same mixed oxidation-state (As^{III} and As^{V}) relationship, with typical concentrations of 40% As^{III} and 60% As^{V} and less than 5% As^{-I}. As previously noted, fitted model spectra at 5% or less gave little noticeable improvements to fits; values are included for consistency, however.

A further confirmation of the predominance of maghemite relative to magnetite is found in some μXRD maghemite patterns, which include a faint reflection (Debye-Scherrer ring) at 5.9 to 6.0 Å. Reference patterns of maghemite include a weak peak at approximately 5.9 Å, which is not present in magnetite.

A number of analytical results for discrete grains combining μXANES and μXRD are shown in Figures 2-6, 2-7 and 2-8. Maghemite is, by far, the most common phase identified by μXRD of roaster Fe oxide grains (*e.g.,* Figure 2-6) in both the calcine residue and shoreline tailings. Well-defined Debye-Scherrer powder patterns are observed for all μXRD images of roaster Fe oxides (*e.g.,* Figures 2-6b,c), indicating that the average size of mineral crystallites is small relative to the diameter of the incident beam. As previously stated, individual crystallites at the beam scale under monochromatic X-rays would show up as discrete points or spotty rings, not the smooth rings observed for these grains. Roaster Fe oxide grains are therefore interpreted to be polycrystalline nanoparticle composite grains. This is also consistent with the broad peaks

Table 2-4. Results of Linear Combination XANES Fits of Spectra in Figure 2-3

Standard	M2M CA3 (628.068) %	M2M CA AX1 (628.096) %	M2M CA1 (628.084) %	M2M (Bulk) %
Arsenopyrite (As^{-I})	4	5	14	9
Arsenolite (As^{III})	27	37	52	32
Scorodite (As^{V})	69	58	34	59
Total As* (% w/w)	1.3 to 1.6	n.a.	1.5 to 2.2	2.5**
Description	Porous maghemite	Submicron matrix	Concentric maghemite rim on pyrite	Calcine powder on Kapton

* Total As by EPMA except at indicated. Range given as maximum and minimum of 2 or more analyses.
** Total arsenic in bulk calcine sample (M2M) (Walker & Jamieson 2002).
n.a. – not available.

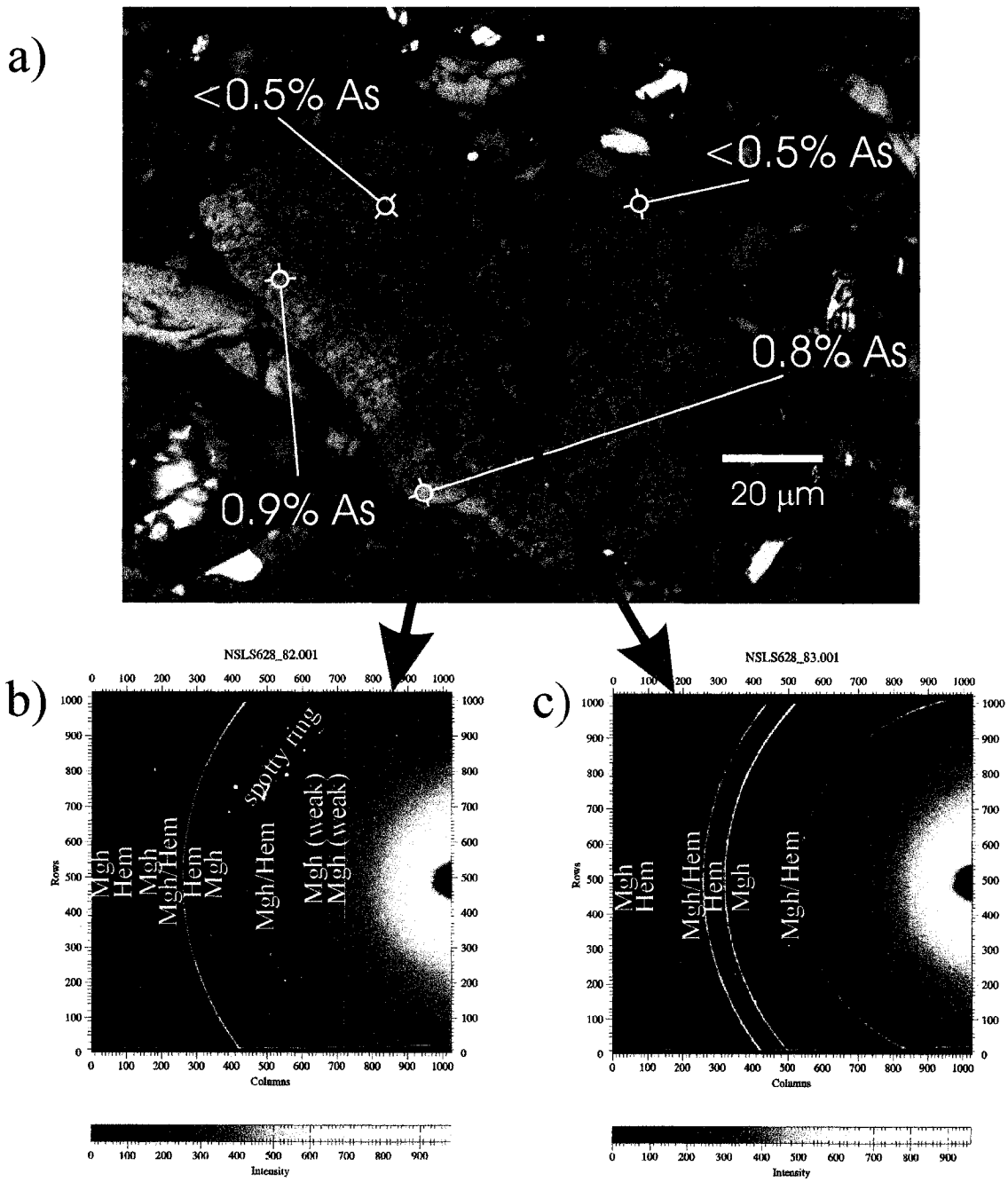

Figure 2-6: Micro-XRD results of a hematite-rich grain exhibiting red internal reflections. a) Photomicrograph of target grain with total As by EPMA indicated in white. Red ellipses indicate inferred footprint of the beam on sample for µXRD analysis. Micro-XRD patterns for two analysed spots are shown below (b and c). Both XRD patterns show the presence of maghemite and hematite. More hematite occurs in the region exhibiting red internal reflections (c). The hematite rings in (c) are uneven in intensity, which suggests the presence of coarser hematite crystallites. The spotty ring in (b) is probably due to reflections from fine gangue minerals, including chlorite, muscovite and quartz.

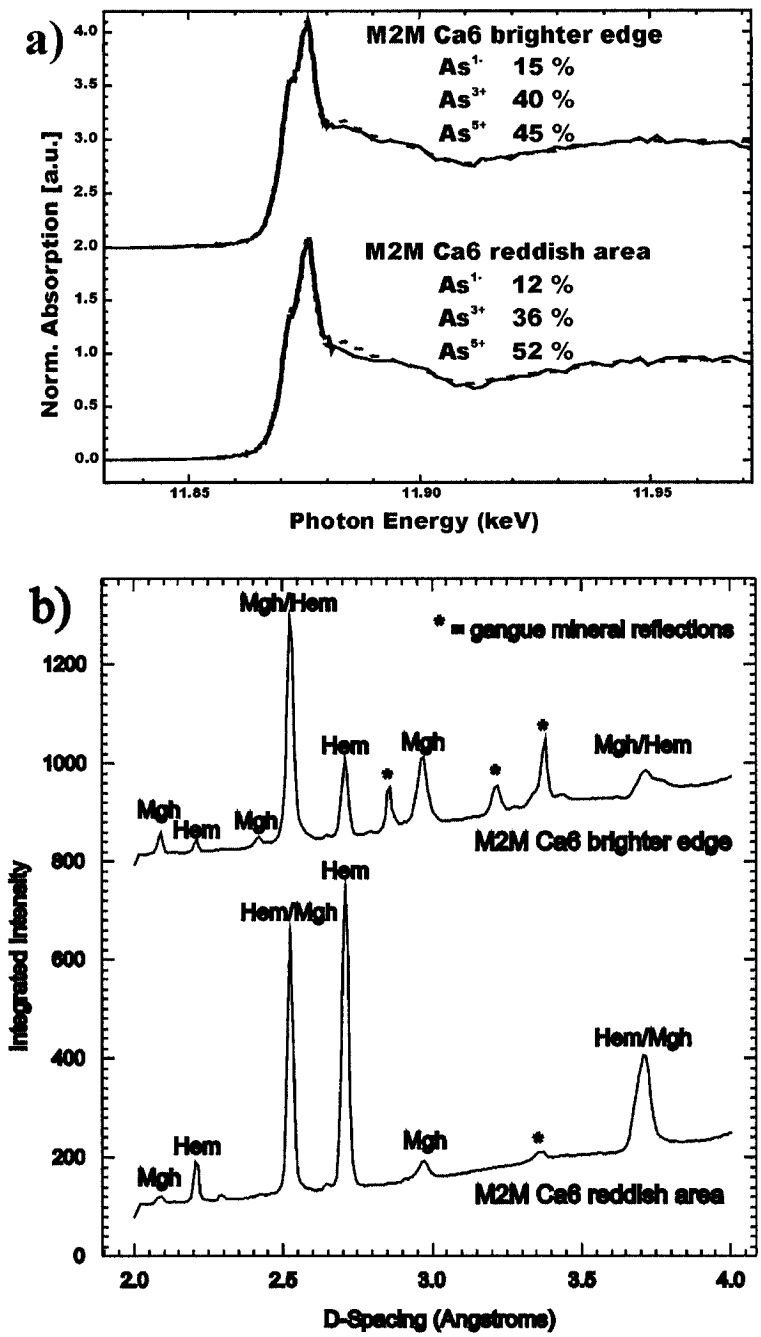

Figure 2-7. Comparison of micro-XANES and micro-XRD for mixed hematite and maghemite grain in Figure 2-6. a) XANES results. Solid line is experimental data and dashed line is linear combination best fit. Only minor differences are evident in XANES results for maghemite-rich area (a, top) and hematite rich area (a, bottom). Integrations of the micro-XRD patterns (Figure 2-6b,c) clearly show the bright edge is maghemite-rich (b, top) and the area with red internal reflections is mostly hematite (b, bottom). It should be noted that more maghemite is present in the analysis of the reddish area than would appear from the integrated pattern (b, bottom) owing to the overlap of the second strongest peak of hematite and the strongest peak of maghemite 2.52 Å.

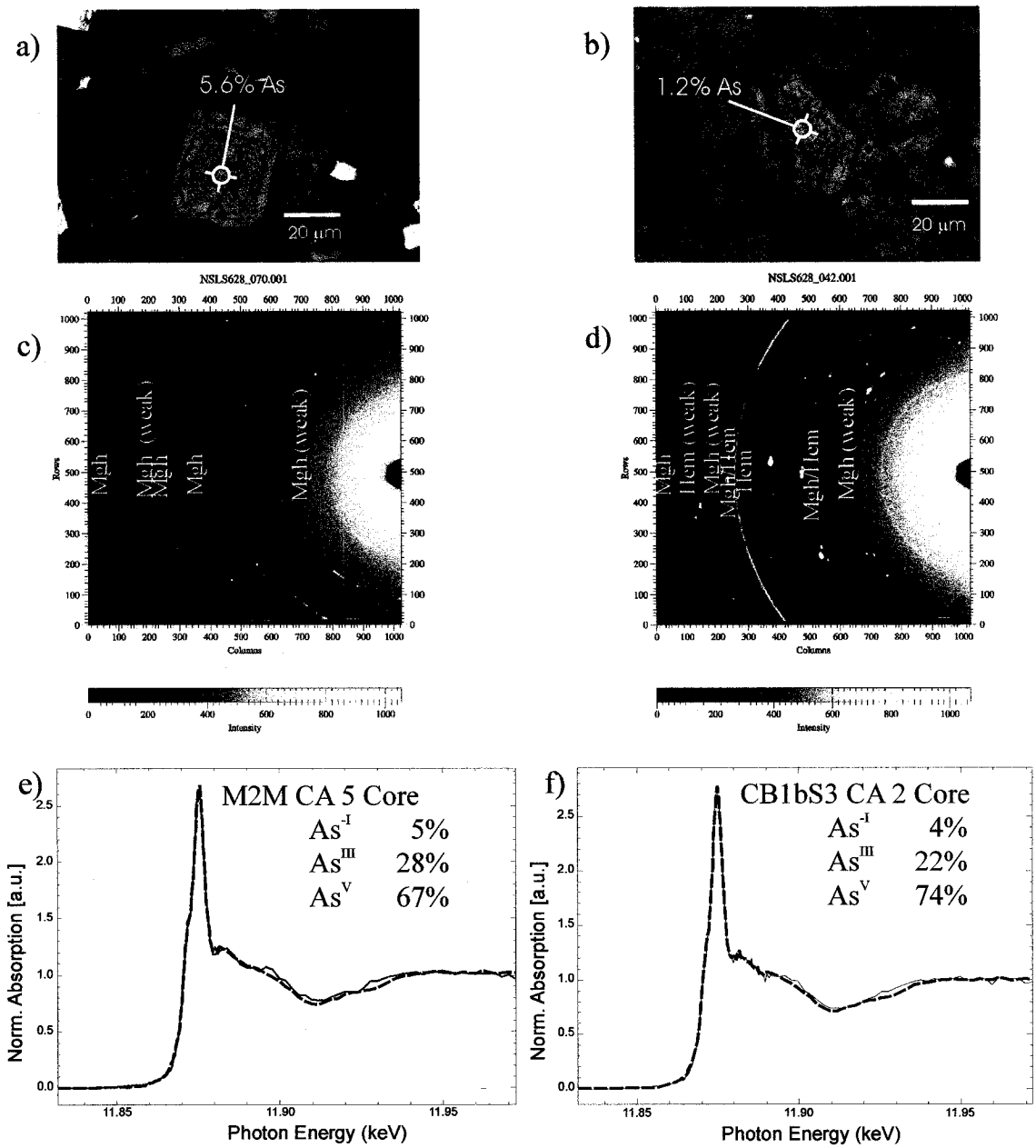

Figure 2-8. Selected analyses of two grains of roaster Fe-oxides. a) Reflected- light photomicrograph of square concentric roaster Fe-oxide from calcine sample (M2M). Total As by EPMA (designated in white). b) Transmitted- and reflected-light photomicrograph of target grain from shoreline tailings sample (CB1bS3). Total As by EPMA as indicated. c) micro-XRD image of target in a) (red ellipse). Pattern is maghemite. Three arcs in lower-right hand corner are chlorite reflections. d) Micro-XRD image of target in b) (red ellipse). Pattern is a mixture of maghemite and hematite. e) Micro-XANES analysis of target in a) (red ellipse). Sample spectrum is in red, dashed line is best-fit linear combination for result shown. f) Micro-XANES analysis of target in b) (red ellipse).

observed by bulk XRD for maghemite in the mill calcine (Figure 2-5).

Analyses confirm that for M2M (calcine), only grains exhibiting a spongy texture and red internal reflections contain hematite. The low modal abundance of these particles in the thin sections has limited the number of analyses of hematite grains to two. The analyses indicate that these grainsare a mixture of maghemite and hematite, not just hematite (Figures 2-6 and 2-7b). No discrete As-bearing phases were identified by μXRD of roaster Fe oxide grains, even for grains with As content in excess of 5% (w/w) (Figure 2-8a,c). A maghemite grain mixed with hematite has also been observed in a grain in the shoreline tailings without obvious spongy texture or red internal reflections (Figure 2-8b,d).

A close inspection of individual Debye-Scherrer rings for hematite (Figures 2-6c, 2-8d) reveals that they vary in intensity, in contrast to the rings for maghemite (Figures 2-6b and 2-8c), which seem smoother. This is qualitative evidence of coarser crystallites of hematite than crystallites of maghemite, even when both minerals are present together within the same grain.

A mixture of As^{III} and As^{V} is consistently evident in maghemite grains with concentric and spongy textures, for both high and low As content, with or without the presence of hematite, and for fresh calcine and 50-year-old subaerial (oxic) shoreline tailings. In the shoreline tailings, this mixed oxidation state relationship contrasts distinctly with As associated with Fe oxyhydroxides in the same thin section and even within grains located within 30 μm of each other (Figure 2-9). The As-bearing Fe oxyhydroxide weathering-induced rims on pyrite show only As^{V} with very little (if any) As^{III}. The As^{-I} associated with Fe oxyhydroxide grain in Figure 2-9 varies with the position of the beam on the grain (data not shown) and is consistent with As^{-I} associated with the pyrite core. Three XANES analyses for this grain yielded similar results to those in Figure 2-9

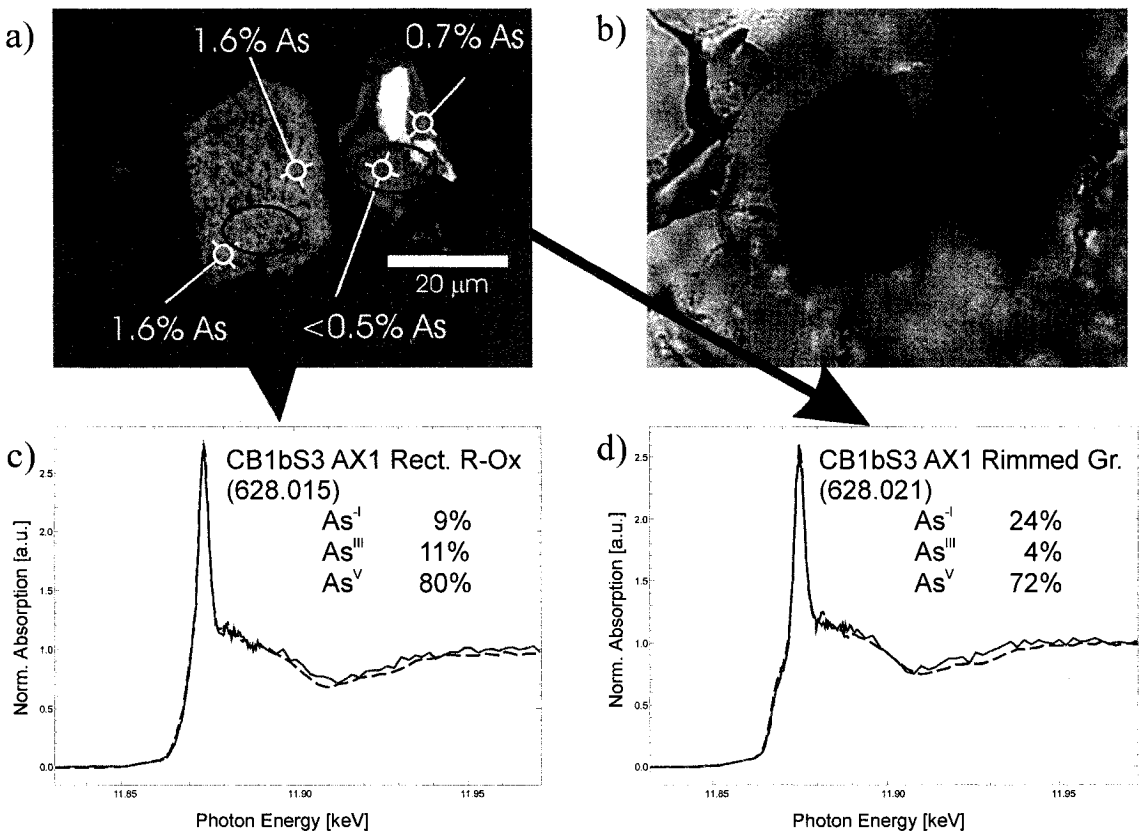

Figure 2-9. Comparison of As oxidation state in shoreline tailings grains of various origins. a) Reflected-light photomicrograph of roaster Fe-oxide (left) and weathered pyrite with Fe oxyhydroxide rim (right). Target locations of XANES analyses are red ellipses and EPMA analyses are indicated in white. b) Transmitted- and reflected-light photomicrograph of same area as in a) showing sizeable portion of the Fe-oxyhydroxide grain is buried in the section. c) Micro-XANES analysis of the roaster Fe oxide. Dashed line is linear-combination best fit for results shown. Solid red line is XANES scan. d) Micro-XANES analysis of the Fe oxyhydroxide rim. Of particular note in this case is that little or no As^{III} is detected in the Fe oxyhydroxide, in contrast to the roaster Fe oxide.

(As^{-I} from 13% to 24%), whereas in one scan, the As^{-I} determined amounts to 39%. For this latter sample, attempts to fit As^{III} yielded negative concentrations, which is strong evidence that there is no As^{III} in the Fe oxyhydroxide rim of this grain.

2.5 DISCUSSION

2.5.1 Roaster iron oxides

As already discussed, roaster-derived Fe oxides may consist of magnetite, maghemite or hematite. Magnetite and maghemite can be difficult to distinguish on the basis of XRD alone. Magnetite can be readily distinguished petrographically from hematite and maghemite on the basis of colour in reflected light (brown-grey versus blue grey). The distinction between maghemite and magnetite in this study is based on petrographic observation rather than XRD alone.

The presence of maghemite in the roaster tailings from the Giant mine is not unexpected, considering roasting was completed at 500 °C in two stages, firstly at a low partial pressure of O_2 and secondly at a high partial pressure of O_2 (More & Pawson 1978). The maghemite is probably formed by oxidation of a finely divided magnetite precursor (Cornell & Schwertmann 1996). Once formed, the maghemite is expected to transform to hematite between 370 °C and 600 °C, depending on its origin and foreign ion content (Cornell & Schwertmann 1996, and references therein). We are not aware of specific studies on the thermal stability of As-bearing maghemite; however, isomorphous substitution of Al for Fe in maghemite (Wolska 1990) is known to increase its stability. The ionic radius of As^{III} is between that of Fe^{III} and Al^{III}, structurally incorporated As may thus be possible and could increase the thermal stability of the maghemite. Further discussion concerning the speciation of As in the roaster Fe oxides is described below.

The low content of hematite in the Giant calcine is somewhat unexpected, since the second stage of roasting occurred with excess O_2, and roughly half of the sulfur as sulfide would have remained after the first stage of roasting (Jha & Kramer 1984). In the work by Eneroth *et al.* (2003), significant quantities of nanocrystalline maghemite were formed during the thermal oxidation of pyrite at 500 °C.

2.5.2 The speciation of arsenic in roaster iron oxides from Giant mine

Although nanocrystalline maghemite and hematite are clearly identified as hosts for the As in the roaster Fe oxides, there are a number of possible relationships between the As and the Fe oxides. Arsenic may be structurally incorporated into maghemite or hematite, surface sorbed to high surface area maghemite or hematite, or present as finely dispersed crystalline or amorphous As-bearing phase(s). The presence of both As^{III} and As^{V} adds another level of complexity to this relationship.

Only maghemite has been detected by μXRD in grains that have relatively high As content (*e.g.*, 5.6 wt.%, Figure 2-8a,c), although up to 1.5 wt.% As has been detected in a grain containing both hematite and maghemite (Figure 2-8b,d). The As in these nanoparticle composite grains thus is not present as a separate crystalline phase or phases. However, the dual oxidation state observed by μXANES opens the possibility of finely dispersed nanocrystalline phase(s) at lower abundance than suggested by the total As measured by EPMA. For example, if we assume that all of the As in Figure 2-8a (5.6 wt.%) is present as two nanocrystalline phases intergrown with maghemite, say scorodite (Fe arsenate) and schneiderhohnite (Fe arsenite), the calculated modal amounts would be 17% and 4 %, respectively. In such a case, we would expect detection of scorodite, but not necessarily schneiderhohnite. Therefore, the possibility of separate finely dispersed nanocrystalline phase(s) cannot be completely eliminated. Crystalline Fe arsenates

seem unlikely, considering the above calculation. Soluble phases such as the As_2O_3 polymorphs arsenolite and claudetite are also unlikely, as they would be expected to dissolve in the calcine regrind and wash circuit or cyanide leach circuit (More & Pawson 1978, Tait 1961).

Arsenate, a tetrahedral group, is not expected to enter the structure of hematite. (McCreadie *et al.* 1998). The greater flexibility of the defect spinel structure makes some arsenate solid-solution in maghemite a possibility, but this has not been tested, and the high charge (5+) would need to be balanced. The similarity in ionic radius of As^{III} to Fe^{III} and Al^{III} does suggest the potential for isomorphous substitution of arsenite in both hematite and maghemite. However, As^{III} in arsenite minerals (*e.g.,* arsenolite, claudetite and schneiderhohnite) exhibits trigonal pyramidal coordination with oxygen, whereas Fe is in octahedral coordination in hematite, and octahedral or tetrahedral coordination in maghemite. Sites suitable for As^{III} coordination may exist in the maghemite structure at defect sites where an Fe^{III} atom is missing as well as two or three of the coordinating oxygen atoms. The closest-packed nature of the oxygens of the spinel structure presents an opportunity for trigonal pyramidal coordination of As^{III} in such a defect.

It is possible that all of the As^{III} and As^{V} associated with these grains is strongly surface-sorbed as inner-sphere complexes, with the high concentrations of As being further evidence of the nanocrystalline nature (high surface area) of these grains. However, considering that these phases were formed at elevated temperature (approximately 500 °C) in the presence of an As-rich vapour, a structural association within the defect maghemite framework as well as a separate nanoscale X-ray amorphous phase (*e.g.,* Fe arsenate) or nanocrystalline phase (*e.g.,* Fe arsenite) cannot be completely ruled out. The speciation of the lower oxidation state As (edge <11,868 eV) in the roaster Fe oxides remains undetermined.

Investigating these roaster Fe oxides in the context of their likely nanoparticle nature is critical. In fact, recent synchrotron-excited photoelectron spectroscopy (SXPS) work by Schaufuss *et al.* (2000) on the oxidation of arsenopyrite at room temperature shows some striking similarities to our results, namely the presence of mixed oxidation-states at the surface of oxidizing arsenopyrite. At Giant mine, the oxidation would have proceeded much more rapidly at elevated temperatures, and we observe the presence of weight percent concentrations of mixed oxidation-states of As on Fe oxides derived not only from arsenopyrite, but also pyrite which has concentrations below one weight percent. However, the inferred high specific surface-area and nanoparticle nature of these grains suggest that a comparison with the SXPS results is appropriate. This would not be the case if the roaster Fe oxides had a macroscopic texture.

The total As contents in Fe oxides in the shoreline tailings are, on average, lower than those in the mill calcine (Table 2-3). Similarly, the lowest As^{III} contents (in the order of only 10%) are also observed in the shoreline tailings (*e.g.,* Figure 2-9). The roasting method differed at the time the shoreline tailings were deposited (Tait 1961), and it is not possible to determine whether the lower total As and lower As^{III} contents in the shoreline tailings are related to aging, leaching, processes of secondary mineralization, or the different conditions of roasting.

2.6 CONCLUSIONS

2.6.1 Arsenic speciation in roaster iron oxides

Roaster-derived Fe oxides from the Giant mine contain up to 7 wt. % As. The As in these grains is present in mixed oxidation-states, mostly as As^{III} and As^{V}. The As concentrations and ratio of As^{III} to As^{V} seem to vary with mineral association and age of tailings, but additional work is necessary to better elucidate these relationships. The persistence of maghemite and As^{III} in 50-year old subaerial tailings suggests that these As-bearing anthropogenic Fe oxides are stable

during prolonged exposure in an oxic environment.

Maghemite is metastable with respect to hematite. However, as pointed out by Majzlan *et al.* (2003), the small difference in free energies between these phases can be altered by small changes in chemical composition (*e.g.,* Al substitution or, perhaps in this case, As), or physical properties such as grain size. Alternatively, kinetic barriers may inhibit crystal growth or transformations. The presence of either structural or surface-sorbed As is likely to increase resistance to such transformations (Cornell & Schwertmann 1996). The significant amount of As^{III} remaining in the shoreline tailings roaster-Fe oxides after 50 years of exposure contrasts with the As^{V} association (*i.e.,* lack of As^{III}) observed for weathering rims of iron-oxyhydroxide on pyrite in the same material. The mixed oxidation-state of As and the nanocrystalline nature of these Fe oxides may have important implications when it comes to bio-availability and long-term stability, particularly under reducing conditions. Indirect evidence has been provided that other As-bearing roaster-derived Fe oxides are subject to microbially mediated reductive dissolution at the base of a tailings impoundment in Northern Ontario (Stichbury *et al.* 2000).

2.6.2 Coincident μXRD and μXANES

Monochromatic μXRD using a two-dimensional CCD detector can be a powerful tool that quickly confirms in a qualitative manner the scale of crystallites within complex particles under the synchrotron beam. Specifically, i) amorphous phases or individual crystals at the beam scale result in no reflections (except in the unique case of a single crystal oriented such that it satisfies the Bragg condition), ii) fine crystallites at the micron scale result in spots, spotty rings and arcs, and iii) nanocrystalline phases result in well-defined smooth rings. In this study, the broad peaks for maghemite in the bulk XRD pattern of the calcine suggest the existence of nanocrystalline maghemite. However, more dilute materials such as bulk tailings, sediments and soils will rarely

contain sufficient phases of interest to assess the degree of crystallinity using bulk XRD. More importantly, μXRD is capable of confirming the presence of low abundance crystalline phases (*e.g.*, hematite in this study) and the spatial relationship of multiple phases (*e.g.*, hematite and maghemite) that could not be determined by bulk XRD methods.

If linked with results from other synchrotron techniques such as μXRF and μXANES, the coincident collection of information on chemical composition, mineralogy and oxidation state at a 10-μm spatial resolution can be very powerful. In this case, the mixed As^{III} and As^{V} states have been shown to be present for concentric and spongy maghemite, with or without the presence of hematite and for a range of As content (<0.5 to 7 wt. % As). However, it is also apparent that for arsenic, low oxidation state species in low abundance relative to As^{III} and As^{V} are difficult to resolve, despite the difference in oxidation states. This is because the shift in edge position measured for a number of possible inorganic As-S compounds and elemental As by XANES is small (<2 eV), and they are at sufficiently low modal abundance that they are unlikely to be detected by μXRD.

The non-destructive nature of synchrotron radiation allows for subsequent analysis of the same targets by other microbeam techniques (such as EPMA in this case) or repeat analyses on the same grains at a later time. For As and other redox-sensitive species, the ability to rapidly measure mineralogy by XRD (minutes) and oxidation state by XANES (tens of minutes) provides a means to measure or monitor alteration of sensitive phases due to micro-beam influences (synchrotron or other techniques). As pointed out by Manceau *et al.* (2002), care must be exercised in preparing thin sections in order to eliminate or minimize the possibility of influences by the techniques of preparation on the speciation of solid phases. In this study, the results of bulk XANES analysis for calcine material confirm that the mixed oxidation-state of As observed

in individual grains is not a result of thin section preparation. In addition, such concerns are not limited to thin section preparation alone, but extend to all aspects of handling and techniques of preservation of solid samples. We believe that bulk and micro-analytical approaches similar to those described in this paper can be applied not only to solid speciation and characterization of solids, but also to further the understanding of potential effects of sample handling on solid-phase speciation.

Chapter 3 – Arsenic oxidation state heterogeneity and correlations with mineralogy in mine waste solids from Yellowknife

3.1 Introduction

Anthropogenic inputs of As to the environment are sizeable in comparison to natural inputs. Major sources of anthropogenic As in the environment are mining and smelting activities, and coal combustion (Han *et al.* 2003). In the past (especially between the late 1800s and mid-1900s) As pesticides saw widespread application on agricultural land (Bhumbla & Keefer 1994) and in the latter part of the 20th century chromated copper arsenate (CCA) wood preservatives were widely used.. A manufacturer-initiated voluntary phase out of CCAs for noncommercial uses implemented in the United States and Canada in 2003 may signal a trend to eventual replacement of CCA which is still the largest secondary use of As in the United States (Brooks 2005). However, raw material for secondary arsenic products (such as pesticides) has largely come as a byproduct of smelting activities. Thus continued reductions in secondary arsenic products will probably lead to increases in stockpiled As waste products. In addition, past industrial activities have already left widely dispersed As contamination in many areas (eg. Amasa 1975, Hocking *et al.* 1978, Ragaini *et al.* 1977, Mok & Wai 1990, Moore & Luoma 1990, Mitchell & Barr 1995, Henderson *et al.* 1998, Reimann *et al.* 2000). Arsenic may be transported as a gas in reduced form (AsH_3 and organic derivatives), but more often it is transported in dissolved form or in suspended particulates (in both air and water).

Pyrometallurgical processing of As-bearing ores has been conducted for centuries, sometimes for the purposes of extracting the As (Camm *et al.* 2003), but more often as a by-product of

production of other metals especially gold and copper (Gossman 1987, Vian *et al.* 1963). Arsenic volatility leads to partitioning of As from solid phases (eg. As-bearing pyrite (FeS_2) or arsenopyrite (FeAsS)) to gases at elevated temperatures during processing (primarily As_4, As_4S_4, As_2S_3 or As_4O_6 depending on the reacting atmosphere) (Chakraborti & Lynch 1983). Present practices require appropriate management and treatment to minimize release of As to the atmosphere, however in the past treatment technologies were less effective. Prior to the 1950s in many cases there was little to no treatment of volatilized As. Arsenic also remains to a variable extent in other mill wastes and products as dissolved As and solid phases that can include both unreacted sulfides, products of sulfide combustion and waste treatment residues. This means that pyrometallugical processing of As-bearing ores can result in a complex range of solid As-bearing phases with a range of solubilities and oxidation states distributed among different waste streams. This results in the potential release and transport of multiple As species in all environmental compartments (air, soil, surface water, groundwater and sediment) and often mixing of different waste stream components at the point of deposition. Understanding the fate of As in the environment therefore requires as much an understanding of the changing anthropogenic processing and waste treatment processes employed at a site over time as the transport mechanisms, and hydrogeochemical and biogeochemical processes that are active at the point of deposition.

Since at least the 1930s (Norwood 1939), metallurgists have sought to characterize the reactions and processes involved in the thermal decomposition of As-bearing sulfide ores for the purposes of making refractory gold amenable to cyanidation. Beginning in the 1980s (eg. Charkraborti & Lynch 1983) and continuing to the present day (Nakazawa *et al.* 2003b), research has also been directed at the mechanisms behind the retention of As in the roaster-calcine feeds to copper smelters. Arsenic poses additional metallurgical and environmental problems during the higher

temperature copper smelting process so it is generally removed in a pretreatment step such as roasting. The combined research efforts toward improving refractory gold extraction and identifying the mechanisms of As retention in the calcine have established the principal reactions and processes involved in the roasting decomposition of As-bearing pyrite and arsenopyrite ores. However, the mechanisms that retain As in the calcine are complicated and still poorly understood. This is due to the many solid and gas species involved, multiplicity of reactions that vary with temperature and roasting atmosphere, and the dynamic (non-equilibrium) nature of roasting environment (Chakraborti & Lynch 1985, Nakazawa *et al.* 1999a, Nakazawa *et al.* 1999b). Other than carefully controlled laboratory studies to confirm the gas solid reactions occurring during roasting (eg. Chakraborti & Lynch 1983), there are few environmentally-focused studies that have actually identified the As species remaining in roaster-calcines. The study by van Elteren *et al.* 2006 on calciner wastes from the 1800s is a notable exception. Metallurgical laboratory studies have directly identified or predicted the formation of relatively few retained As solid species (Fe_2As, FeAs, $FeAs_2$, $FeAsO_4$ and As_2O_5) for which there has been available thermodynamic data (Vian *et al.* 1963, Chakraborti & Lynch 1983). Some have acknowledged this limitation (Chakraborti & Lynch 1985) but to our knowledge there has been very little direct metallographic or petrographic study of As speciation in the calcines beyond confirmation of weight percent concentrations of As in roaster derived Fe oxides. When specific As phases are identified, they tend to occur at extremes in roasting conditions (eg. FeAs in Chakraborti & Lynch 1983). However, most (if not all) roaster-calcines retain As, typically at concentrations ranging from 0.1 to >2% As (1,000 to 20,000 mg/kg) (Vian *et al.* 1963, Lindkvist & Holmstrom 1983, Jha & Kramer 1884). As with all heterogeneous solid mixtures including soils, sediments and tailings these concentrations can be distributed in the form of relatively few high As content particles (eg. arsenopyrite), more numerous moderate concentration particles or a mixture of both. It appears that identifying the species of As in roaster calcines has been

hampered by the fact that other than relic arsenopyrite, the As bearing-phase or phases in these materials are finely dispersed within or surface-bound to complex nanocrystalline Fe oxides (Walker *et al.* 2005). This leads to a situation of a high abundance, but moderate to low concentration As phase or phases that are difficult to characterize, and explains why conventional petrographic approaches (eg. Grimsey & Aylmore 1992) have not been successful at identifying the solid As species retained in the calcine Fe oxides.

The objective of this study is to further the understanding of As speciation in the complex iron-oxides formed by roasting of mixed arsenopyrite and pyrite concentrates. Our previous work (Walker *et al.* 2005) has shown these Fe oxides to be micro-porous nanocrystalline composite grains of maghemite (γ-Fe_2O_3) and sometimes hematite (α-Fe_2O_3) with As contents of <0.5 to 7% As (w/w). The As in these nanocrystalline composite phases were mixtures of As^{III} and As^{V} in ratios that varied from grain to grain. This study specifically investigates the variation in As content and oxidation state with Fe oxide morphology (related to roasting conditions), mineralogy (maghemite and hematite), exposure in the environment (0 to 50 years) and type of tailings depositional environment (subaerial and subaqueous).

3.2 Synopsis of Gold Ore Roasting and the Samples Studied

Roasting of arsenical sulfide ores as already indicated has been implemented at numerous locations as a pretreatment for two common purposes: i) improve the cyanide extraction of refractory gold, and ii) remove As from copper ores prior to smelting. Traditionally rabbled hearth roasters (often referred to as the Edwards roaster) were employed in the roasting of refractory gold concentrates (Gossman 1987). In contrast, multi-hearth roasters were originally used in the pretreatment of copper ores (Lindkvist & Holmstrom 1983). Fluosolids roasting has been the preferred roasting technology for both gold and copper ore pretreatments since the 1950s. Fluosolids roasting is characterized by more even temperature and atmosphere control

than hearth roasting due to the fluidized bed of reacting calcine with variable retention times in the reactor (smaller particles generally have shorter retention times, however short circuiting can occur).

Details on the roasting operation at Giant from 1948 to 1999 have already been summarized (Chapters 1 & 2, Walker *et al.* 2005) and are not repeated here, except to highlight similarities and differences between Giant and the broader application of roasting arsenical ores. The main roasting operation at the Giant mine was two stage fluosolids roasting, where the first stage was conducted with an "air deficiency" that favored As removal, and the second stage was conducted with an excess of air (Tait 1961). This two-stage process is typical of roasting operations involving arsenopyrite. The terms "air deficiency" and "reducing" roasts are commonly used in the literature to describe the first stage roast, however in most operations (including Giant) the roasting is conducted in a self-sustaining (autogenous) manner with sufficient oxygen to maintain the reaction. Thus, the first stage roast is still largely oxidative driven by the exothermic reaction of sulfides. The temperature of roasting at Giant was tightly controlled with both the first and second stages kept at 500 °C with the use of spray water in the reactor vessels. This relatively low temperature of roasting at Giant is common for refractory arsenical gold ores although the second stage of roasting is often conducted at higher temperatures at other operations (typically 600 to 700 °C, Jha & Kramer 1984).

3.3 Samples and Methods

Solid-phase samples for this study include Giant mine mill products (flotation tailings, cyanided fluosolids roaster calcine and ESP dust) and tailings cores of various depositional ages that were sampled in 1999 at the Giant Mine, Yellowknife, Northwest Territories. Sample locations are provided in Appendix B. The earliest tailings sampled include calcine from an original Edwards hearth roaster that operated at the site in the first decade of mining at the site (1949 to 1958). A

sample of stockpiled roasted ore from the nearby Con Mine in Yellowknife is also included as an example of cyanided (Edwards type) hearth roaster calcine from another old roasting operation. A detailed description of the samples is included in Table 3-1 and field sampling methods are described by Walker *et al.* (2005) (Chapter 2).

The set of samples were submitted for sequential selective extraction (SSE) using the method developed by the Geological Survey of Canada (Hall *et al.* 1996a,b,c). SSE methods are operationally defined wet chemical extraction methods that attempt to measure elemental relationships to specific solid component types within the soil (or in this case tailings). The operationally defined fractions deemed most appropriate for this study included adsorbed/exchangeable, carbonate, amorphous Fe oxides, crystalline Fe oxides, sulfides and residual. Samples for more detailed micro-analytical work were selected on the basis of these results in conjunction with sample type (mill product, tailings), age, and depositional history.

The micro-analytical grain-scale approach and methods are largely based on those described in our previous work (Walker *et al.* 2005, Chapter 2). We have employed this approach to the generally silt sized and finer arsenic-bearing solids in the tailings and mill product samples. The work is guided by petrographic characterization of potential As-bearing phases using optical microscopy in transmitted and reflected light. This grain selection and targeting process was followed by synchrotron microanalysis as NSLS, Beamline X26A. Potential μXANES and μXRD targets were selected on the basis of i) observed mineralogical relationships to the roaster derived iron oxide phases (eg. Aspy-Fe oxide, Py-Fe oxide, Po-Fe oxide, Fe oxide without

Table 3-1 - Mill Product and Tailings Samples[a] Examined in This Study

Sample	Depth[b] (m)	Age[c] (years)	Description	Roaster Fe oxide Content[d]	Total As (mg/kg)	As in porewater[e] (mg/L)
CB1b S4	0.8	50	Subaerial shoreline tailings (brown silt)	tr.	1180	0.45
CB1b S3	1.0	50	Shoreline tailings (stratified brown reddish brown silt to very fine sand above brown fine sand)	tr. – 20%	2240	0.30
Stn5 S7	0.02	50	Submerged tailings (brown silty sand probably eroded and redeposited shoreline tailings)	< 1%	1070[f] (0 to 0.2 m)	0.2[g] (0.03 to 0.12 m)
Stn5 S8	0.3	50	Submerged tailings (grey silt probably original distal tailings from discharge before 1951)	< 1%	1200[f] (0.2 to 0.4 m)	4.0[g] (0.15 to 0.30 m)
CN4b S2/S3	4.1	~30	Grey fine silt with reddish-brown interbeds	Too fine to estimate	3280	0.58 (3.6 to 3.8 m)
CN2b S2/S3	0.5	~25	Grey fine silt with reddish-brown interbeds	Too fine to estimate	1500	2.54 (1.5 to 1.7 m)
CNW1a S2	0.2	1 to 2	Calcine rich strata in recent tailings	Up to 50%	4530	0.47 (0.8 to 1.5 m)
M1M	-	Direct from mill	Flotation tailings	0%	930	n.a.
M2M	-	Direct from mill	Calcine residue tailings	50%	24900	n.a.
CM1a[h]	Unknown	> 30 yrs	Stockpiled calcine	50%	n.a.	n.a.

[a] All samples from the Giant Mine, Yellowknife, NWT except as indicated. [b] Depth below tailings surface where applicable. For Stn 5 samples – depth below sediment water interface. [c] Estimated age of tailings based on sample location and historical site knowledge. [d] Visual modal estimate of roaster Fe oxide content of thin section. Range is given where sample includes discrete calcine rich layer(s). [e] Typical pore water concentrations in vicinity of solid samples (Appendix D, except where indicated). [f] Golder 2002. [g] From nearby pore water profile sampling in August 2003, Andrade 2006. [h] Sample of stockpiled (pre-1970) calcine residue from nearby Con Mine, Yellowknife NWT. n.a. – not analysed.

sulfide) and ii) grain morphology and reflectivity (microporous reflective, microporous with lower reflectivity, microporous with red internal reflections, concentric). Within each texture type there is a wide range of variation. Microporous grains may have coarse porosity, fine porosity or an almost massive appearance. Concentric grains may have thick layers or very thin layers with thick outer layers being quite common and attributed by others as representing relatively rapid initial oxidation followed by slower oxidation of the inner regions by restriction of gas migration through this outer rim or fractures within it (Arriagada & Osseo-Asare 1984). There are also some that are clearly compound grains and a few that seem to have a blocky (or reticular) appearance that is difficult to categorize as either microporous or concentric, but is probably a variation of the former. Given the wide range of textures, textural combinations and mineralogical associations observed, analysis of every variety was not conducted, but rather targets were selected on the basis of representation of the most common textures and specific mineral associations. Grain size was also a consideration since fine grains are difficult to analyse in isolation from other surrounding grains and matrix especially in calcine rich samples.

The synchrotron analysis was completed in essentially two rounds of work. The first was completed prior to installation of μXRD at the beamline so this data set contains only μXANES results on silica glass (As-free silica glass thin sections). The second round involved preparation of a selection of replicate thin sections (from the same off-cuts as the previous samples) using a removable thin section technique (Walker *et al.* 2005) that allows mounting of the thin sections on Kapton tape for transmission mode μXRD and coincident μXANES. XANES scans were collected according to methods described in Walker *et al.*(2005) using either a single element Si(Li) detector or multi element Ge detector (MED). Mixed oxidation state spectra were subjected to the linear combination fit routine of WinXAS™ to determine the proportions of As^{III} and As^{V} (Walker *et al.* 2005, Chapter 2). A single set of standard analyses collected on the 9

element MED (including arsenopyrite (As^{-I}), schneiderhohnite (As^{III}) and scorodite (As^{V})) was used for all fits. A set of standard spectra (same standards as MED) collected on the Si(Li) detector gave comparable fit results. The arsenopyrite standard was included in all fits to remove any component of background As in pyrite or arsenopyrite. Pyrite and arsenopyrite are not volumetrically homogenous within the beam intersected analytical volume, therefore inclusion of the arsenopyrite in all fits is meant to correct for this effect and improve the fit of As^{III} and As^{V} rather than quantify any relationship between As^{-I}, and As^{III} or As^{V}. As discussed in our previous paper (Walker *et al.* 2005) there is a possibility that reduced As phases other than As in pyrite or arsenopyrite may exist at low concentrations in some grains. If other reduced As phases are present their concentrations were low enough to escape detection in the linear combination fit routine. It is possible the improvement in fits observed in some cases with incorporation of a small component of As^{-I} could be related to such compounds instead of arsenopyrite, but the method is not capable of distinguishing between these lower oxidation state phases (Walker *et al.* 2005). Where negative concentrations were determined for As^{-I} during fits, zero concentration of this component was assumed.

EPMA was conducted on selected thin sections that contained abundant roaster Fe oxides in the coarse silt size range. Analytical conditions were the same as those described in Walker *et al.* 2005 with the exception that an additional secondary standard (schneiderhohnite) was used to check accuracy of results. The EPMA work was used to quantify the As content in grains previously analysed by μXRD and μXANES. Additional grains were analysed on a random basis generally from within the same field of view as the principal target grains. The objective of this was to increase the number of EPMA analyses.

The main As-bearing mineral in the ore is arsenopyrite, which is sub-equal in abundance with pyrite (Coleman 1957, Boyle 1960). Analysis of pyrite has been reported to contain up to 5.49 wt.% As in a deposit wide study at the nearby Con Mine of similar origin (Armstrong 1997). Analysis of over 99 pyrite grains in a previous study at the Giant mine by Chryssoulis (1990) identified a maximum of 3 wt.% and an average of 0.68 wt.% As. Twenty percent of the grains contained more than 1 wt.% and only two were below the detection limit of 0.01 wt%. Some As may also be associated with sulfosalts and especially as solid solution with Sb in tetrahedrite that has been identified in generally low abundance (Coleman 1957, Boyle 1960, Chryssoulis 1990, Armstrong 1997). For this study, qualitative analysis of fine sulfide grains was sometimes conducted to verify petrographic characterization as arsenopyrite or pyrite, particularly in fine relic grains. Semiquantitative analysis of pyrite was conducted in some instances to verify low or undetectable As.

A complete list of thin sections prepared and types of analyses completed is tabulated in Appendix C.

Pore water chemistry from sampled tailings was determined where sufficient water could be collected. Water samples were obtained by core squeezing or suction lysimeter methods comparable to those described by Rollo (2003). Arsenic was determined by hydride generation atomic absorption spectroscopy (AAS). Analytical results and methods are provided in Appendix D.

3.4 Results and Discussion

3.4.1 Characteristics of Mill Products and Giant Mine Tailings:

Bulk X-ray diffraction of the tailings samples is consistent with the ore host (chlorite-carbonate-sericite schist, Boyle 1960) and confirms the presence of quartz, dolomite, chlorite, muscovite and calcite in all samples including the calcine rich samples (M2M, CM1a AND CB1b S3). In some cases only a few major peaks of muscovite and calcite are observed suggesting a lower relative abundance in some samples. Arsenic-bearing phases including pyrite and roaster-derived maghemite are detected in only the calcine samples (M2M and CM1a) reflecting their low overall abundance in the other tailings. Arsenopyrite is not detected by conventional XRD in any samples, in fact the only As mineral detected by XRD is arsenolite in the ESP dust and possibly CM1a. The arsenolite in CM1a (if present) may be derived from weathering and reprecipitation in the stock-pile, but is more likely cross contamination from surface storage ponds of As trioxide sludge during 30+ years of storage. All subsequent micro-analysis of CM1a for this study was directed specifically at roaster-derived As-bearing Fe oxides.

3.4.1.1 Petrographic Analysis of As-bearing Phases

Petrographic characterization of the flotation tailings (M1M) in thin section confirmed the presence of pyrite and arsenopyrite as generally small (< 10 μm dia.) euhedral to subhedral grains typically enclosed or partly enclosed within silicate grains. Some free grains at a similarly fine scale were also noted along with a few larger pyrite grains up to 50 μm in diameter. These grains are essentially unaltered with no evidence of oxidation confirming the flotation process has little if any oxidative effect on the sulfides.

The main As-bearing tailings component at Giant is the calcine residue (M2M). It reportedly only constitutes about 10% of the tailings discharged by tonnage, but contains up to 80% of the As discharged to the tailings (Table 1-4, Fawcett *et al.* 2006). The main As-bearing phases identified in the Giant calcine residue sample (M2M) are nanocrystalline grains of maghemite containing <0.5 to 7 % As (w/w) as a mixture of As^{III} and As^{V} (Walker *et al.* 2005). The maghemite exhibits either concentric textures (lower temperature direct oxidation of sulfide to Fe oxide) or spongy texture grains (via a pyrrhotite intermediate formed at higher temperatures) (Walker *et al.* 2005, Chapter 2 and references therein). Some pyrite and very small amounts of arsenopyrite are present usually as unroasted relic cores within concentric grains, but occasionally as free grains and near pristine inclusions within silicates. Free grains in some cases may be partly reacted cores that were liberated during regrinding in preparation for cyanidation. Pyrrhotite intermediate particles are inferred to form under conditions where evolving SO_2 protects the sulfide surface from complete oxidation to magnetite or maghemite. However these are rarely preserved in the final calcine, probably because they are completely oxidized to Fe oxide by the end of the second stage roast. Their characteristic spongy texture is preserved in the resulting Fe oxide. Mineral associations observed in very low abundance are: spongy hematite-maghemite mixtures, spongy pyrrhotite enclosed by thin maghemite rims, coarsely porous pyrrhotite as discrete grains or rimming pyrite, more massive pyrrhotite relics within finely porous maghemite, and roaster Fe oxides within silicates. The latter indicates that silicate inclusion does not always protect pyrite and arsenopyrite from reaction in the roaster. One lower reflectivity spongy and rounded grain was also observed in sample M2M. The Con mine calcine (CM1a) is similar to Giant calcine except it contains much less concentric textured maghemite and a greater amount of spongy maghemite. Spongy hematite-maghemite mixtures (optically identified by bright red internal reflections) are also more abundant than in the Giant calcine. Petrographic interpretation of the ESP dust is limited by its fine grain size (fine silt and clay). It

contains a few coarse silt sized irregularly shaped brownish opaque oxide grains as well as fine maghemite grains similar to those observed in calcine. A single square unreacted pyrite grain was also observed. The ESP dust is matrix supported with coarse silt sized grains of silicates, carbonates and the opaque phases described above comprising at most a few percent in the thin section.

Tailings samples are interpreted to be mixtures of flotation tailings and calcine residue tailings in varying proportions, plus fine grained opaque material that may be either the finest size fractionated calcine or ESP dust. There is good qualitative correlation between elevated As content (>1500 ppm) and visual evidence of roaster-derived wastes (Table 3-1) including macroscopic (distinctive reddish-brown, dark brown and dark grey-brown colours) and microscopic (presence of roaster Fe oxides or fine brown semi-opaque matrix material). There is no evidence of sulfide mineral oxidation (Fe oxyhydroxide rims) due to weathering in samples from the tailings impounds (North Pond, North-West Pond) which is consistent with previous reports (Jambor 2000). Due to their fine grain-size, and on-going discharge of mine tailings and mine water, these tailings have probably remained largely saturated. Also, drilling and sampling by the mine in the mid-1980s (Halverson 1984) indicated that some older tailings layers at depth remained frozen (which is not unexpected given the cold climate and presence of discontinuous permafrost in the region). However, the shoreline tailings which were mounded above lake level for over 50 years do show Fe oxyhydroxide rims on sulfides characteristic of weathering (Chapter 2, Walker *et al.* 2005). EPMA analysis of several of these rims has confirmed them to be As-bearing at concentrations up 1 wt. %. The source of As in these rims may be due to weathering and remobilization of As within vadose zone (unsaturated) tailings. However significant atmospheric deposition of As and acidity has occurred in the area around the mine site due to operation of the roaster. Atmospheric deposition of As was very high in the first few years of

operation (1948 to 1951) since there was no gas treatment at the time (Hocking *et al.* 1978). Gas treatment for As vapour gradually decreased As emissions, but they probably remained significant until implementation of the ESP (operating at elevated temperature) and bag house in 1958 (Tait 1961). Therefore it is possible that some of the As in the Fe oxyhydroxides and (perhaps even the roaster Fe oxides if sorption sites were available) is from infiltration of As dissolved from the aerial dispersed source.

Sulfur dioxide emissions from the roaster have varied and overall increased over time in keeping with the level of production at the mine. Therefore, the weathering of the sulfides may have been promoted by local acid-deposition from roaster-stack sulfur dioxide emissions. It is likely that such acidity would be readily neutralized during transport through the carbonate-rich vadose zone of the tailings. However, a change in pore water chemistry (eg. increased Ca^{2+} and SO_4^{2-}) might be expected. The magnitude of such effects and importance on the weathering reactions (if any) is unknown. However, since the sulfur dioxide and As emissions ceased with the closure of the Giant Mill in 1999, minor changes in pore water chemistry could be occurring.

3.4.1.2 Characterization by Sequential Selective Extractions

Sequential selective extractions for the samples indicate variable proportions of As associated with the six operationally defined leaches (Figure 3-1a). The flotation tailings (M1M) have the lowest total As concentration (930 ppm) with more than 95% associated with the sulfide (aqua regia) and total digestion (hot tri-acid) extractions. This is consistent with petrographic observations presented above. Mill processing (flotation) removed much of the sulfide (thus the low As content) and remaining As-bearing sulfides showed no evidence of oxidation. Almost 40% of the As was returned in the total digestion suggesting almost half of the arsenopyrite and arsenical pyrite were included within silicates. The sulfide content of M1M was sufficiently low

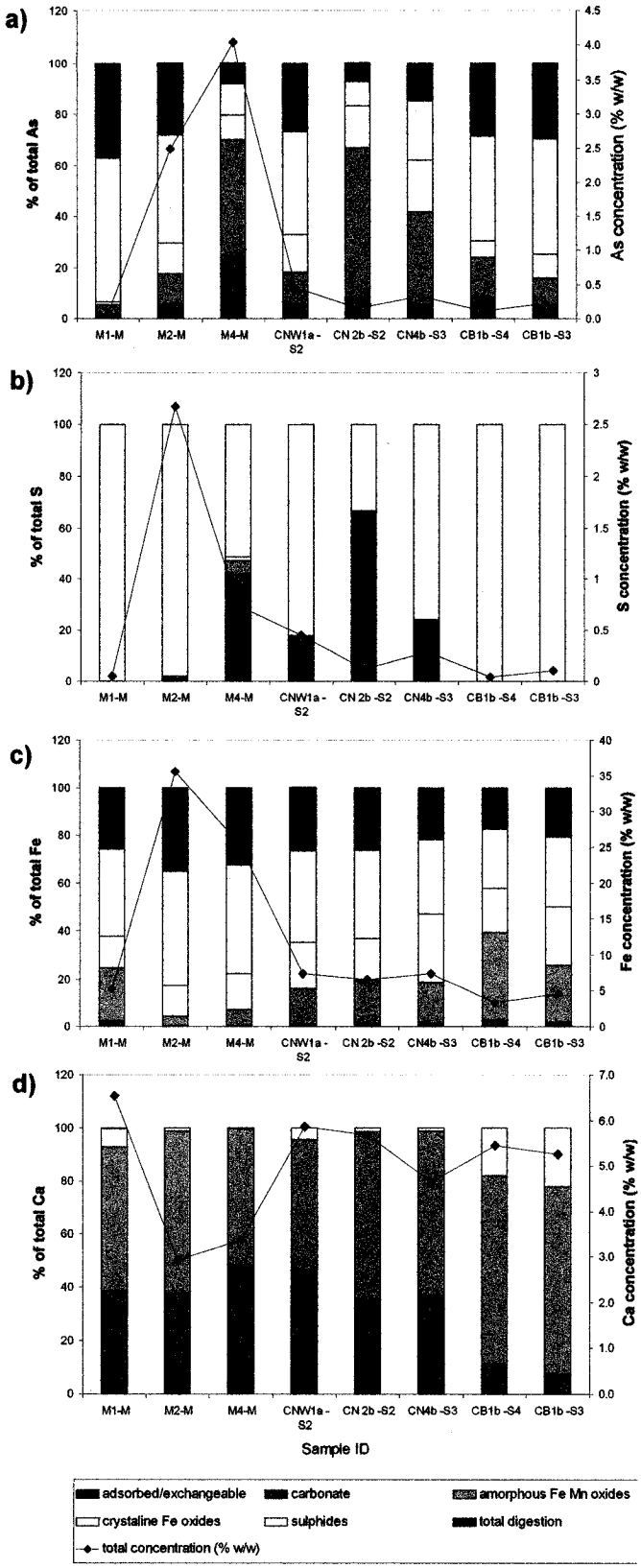

Figure 3-1. Sequential Selective Extraction Results for Mill Products and Tailings.

(<1%) that it is difficult to estimate modal amounts, but they were commonly observed included in silicates.

The As content is much higher in the calcine and ESP dust (roasted ore mill products M2M and M4M) and greater proportions of the As are associated with the less aggressive leaches especially the Fe oxide extractable fractions. The ESP dust contains more than 4 weight % As with only 20% of this in the combined sulfide and total digestion fractions, 55% in the combined Fe oxide extractable fractions and 25% in the combined exchangeable and carbonate fractions. The significant concentration of As in the exchangeable and carbonate extractions of the ESP dust (which amounts to almost 1% (w/w)) is probably due to the dissolution of arsenolite that was detected by XRD. The calcine contains approximately 2.5 weight % As with 70% in the combined sulfide and total digestion fractions, 24% in the combined Fe oxide fractions, and 6% in the combined exchangeable and carbonate fractions. The tailings samples contain substantially less As ranging from 4500 ppm at CNW1a-S2 to 1200 ppm at CB1b-S4 which reflects the dilution of the high As waste streams (calcine and ESP dust) in flotation tailings at time of deposition. The distribution of the As within the sequential extraction fractions varies for the samples with CN2b-S2 appearing similar in proportions to the ESP dust and CB1b-S4 and CB1b-S3 appearing similar in proportions to the calcine. CN4b-S3 has greater Fe oxide extractable fractions than the two CB1b samples, but less than CN2b-S2.

Sulfur behavior within the sequential extractions is less variable and indicates primarily an association with the sulfide fraction for most samples (Figure 3-1b), although almost 50% of the sulfur in M4M (the cyanided ESP dust) is associated with other extractions including 36% in the exchangeable fraction. In addition to M4M, a significant amount of soluble sulfur (probably sulfate) is observed for samples CNW1a-S2, CN2b-S2 and CN4b-S3. The other samples

(flotation tailings, calcine and the two CB1b samples) contain almost 100% sulfide associated sulfur. It is notable that the samples with the least As in the sulfide and total digestion fractions (M4M, CN2b-S2 and CN4b-S3) also contain the most sulfur in the exchangeable fraction. The two north-pond tailings samples contain laminae of fine-grained opaque material (fine silt and clay) which could be derived from distal preferential settling of ESP dust tailings.

The strong As association with Fe (arsenopyrite, arsenical pyrite, As-bearing Fe oxyhydroxides and As-bearing roaster-derived Fe oxides) would suggest that the Fe sequential extraction results could be key in determining solid-phase As speciation in these complex materials. In fact all samples do show a significant distribution of Fe among four of the six operationally defined fractions (amorphous Fe-Mn oxides, crystalline Fe oxides, sulfides and total digestion, Figure 3-1c). However, in addition to the aforementioned minor Fe phases, Fe is a major constituent within the bulk mineralogy of all of the samples (Fe rich dolomite and iron-bearing phyllosilicates, e.g. chlorite). Close inspection of the data has confirmed that the Fe concentrations in specific fractions show little relationship to the As-bearing Fe phases and instead respond largely to Fe in the As-free dolomite (Fe oxide extractions) and phyllosilicates (sulfide extraction). The refractory character of the Fe dolomite to the carbonate extraction and dissolution in the amorphous and crystalline Fe oxide fractions is confirmed by the presence of significant calcium (Figure 3-1d) and Mg (Appendix E) in the Fe oxide extractable fractions. This has also been confirmed by laboratory analysis of dolomite and ankerite (Fe dolomite) under the same sequential extraction procedure (Hall, unpublished data). Most of the calcium elutes in the amorphous Fe oxide fraction while the Fe elutes to an equal or greater extent in the crystalline Fe oxide fraction (Figure 3-1c,d). This may be due to the presence of crystalline Fe oxides, however some of this may also be due to incongruent dissolution of the Fe dolomite. The link between Fe originating from phyllosilicates in the sulfide fraction instead of sulfides is confirmed

by similar magnitude molar quantities of Mg, and Al (Appendix E). In addition, the Fe in the sulfide fraction exceeds stoichiometrically available sulfur by 10 to 100 times. The two samples with the highest Fe content (M2M and M4M) also warrant additional discussion. While major element concentrations (Mg and Al) in the sulfide extraction suggest similar phyllosilicate content in the ESP dust as other tailings and depleted phyllosilicate content in the calcine (by about 1/3), the Fe content for both samples is up to an order of magnitude higher than the other tailings. This suggests either the presence of an Fe phase resistant to the crystalline Fe oxide leach or inhibited (incomplete) dissolution of the Fe oxides in these leaches due to the high leachate Fe concentration (3 to 4 % w/w). The reported crystalline Fe oxide-associated As fraction in these two samples (M2M and M4M, Figure 3-1a) may also be underestimated, unless As dissociation is predominantly occurring through desorption rather than complete dissolution. The relatively small amount of As in the sulfide and residual fractions for M4M suggests any underestimation for this sample is small.

Other fine tailings located at the north end of Baker Pond (HC1b-S1&S2) show a similar SSE pattern for As as the cyanided ESP Dust (M4M) and fine laminae in the North Pond (CN2b-S2) (Figure 3-2). These tailings are very fine-grained and generally massive (unstratified), but otherwise similar in appearance to material within individual thin fine grained laminae of the North Pond. The tailings exist as a mound within the north-east corner of Baker Pond. The lack of coarse silt and sand, suggests these tailings are fines deposited down flow of the tailings containment system. Their mounded form may indicate that they were redeposited from their original location perhaps in preparation for open pit mining at B3 Pit (located between the polishing pond and Ingraham Trail).

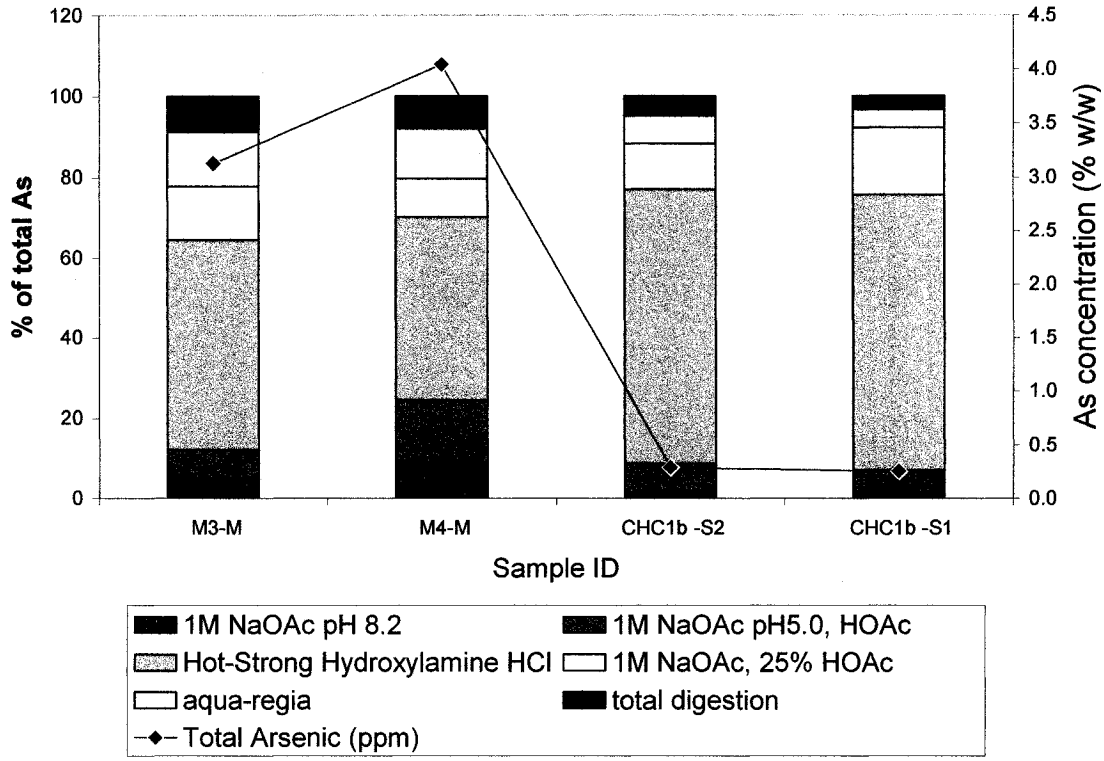

Figure 3-2. Comparison of SSE results of ESP dust and fine tailings at the edge of Baker Pond. M3M is uncyanided ESP dust and M4M is cyanided (carbon in pulp) ESP dust. CHC1b samples are from cores taken in apparent tailings at the north-east limit of Baker Pond. This area is downflow of the former tailings decant and more recent water treatment systems.

It is clear from the above results that the As associations within the mill products and tailings are complicated. It appears that the sequential extraction procedure is reasonably effective at determining the quantity of sulfide bound As (with the possible exception of the very high As and Fe content calcine). The aqua-regia extraction is interpreted to represent the extraction of sulfide associated As from liberated and partly liberated pyrite and arsenopyrite grains as well as some sulfides occluded within phyllosilicates. The residual fraction is expected to represent remaining sulfides occluded within phyllosilicates and those wholly occluded within other silicates (mostly quartz). The presence of mixed As oxidation states (As^{III} and As^{V}) and an incomplete understanding of the As mineral association in all but the flotation tailings sample precludes

meaningful interpretation of the less aggressive leaches. As^{III} and As^{V} may behave differently under the differing conditions of the SSE steps. For some of the tailings samples (CB1b S3 and CB1b S4) there is the additional complication that they contain mixtures of roaster derived Fe oxides (maghemite and mixed maghemite-hematite grains) as well has Fe oxyhydroxide weathering rims all of which contain significant As. Understanding the potential mobility and bioavailability of As in these materials as well as sediments and possibly soils that could contain roaster-derived wastes depends on an understanding of the form of As and binding mechanisms in the roaster Fe oxides. A micro-analytical approach that combines coincident synchrotron μXRD and μXANES, previously described (Walker *et al.* 2005), has been widely applied to a range of As and mineral associations in the mill products and recent tailings. This data combined with existing metallurgical and mineralogical studies in the literature allows us to propose a mechanism for the incorporation of the As in the Fe oxides. This data is also used to aid in interpreting the form of As in older tailings samples from the Giant mine.

3.4.2 Microanalytical Characterization of Roaster-derived Source Materials:

A wide range of roaster-derived Fe oxide morphologies and mineral associations were targeted for analysis in both the Giant calcine (M2M), Con Calcine (CM1a) and recent tailings CNW1aS2 in an attempt to understand the mechanisms that lead to the incorporation of As into the Fe oxides.

Incompletely reacted grains that contained relic or intermediate sulfides (arsenopyrite, pyrite and pyrrhotite) were felt to be particularly important for this purpose even though they tend to represent phases that are otherwise in low abundance.

A large concentric textured grain with relic pyrite (Figure 3-3) was subjected to a range of characterization techniques (EPMA, X-ray mapping, μXANES, μXRD, and uXRF mapping). At greater than 150 μm in diameter this grain is somewhat atypical since roaster Fe oxides are generally less than 50 μm in diameter due to a post-roasting wash and regrind. However, we expect the roaster-derived features of this grain are applicable to smaller grains or grain fragments. X-ray mapping of this grain (Figures 3-3b,c,d,e) confirms the strong association of As with the Fe oxide rim. A characteristic of this grain is the presence of a calcium rich rim surrounding the entire grain (Figure 3-3e). This rim is unlikely to be related to roasting, and may be due to post-roast liming for cyanide treatment. The As content of the Fe oxide rim on this grain ranges from 2.4-3.6% As with the higher concentrations on the inner-most rim in contact with the pyrite with trace As (<0.5%). This represents at least a seven fold increase in As concentration from the pyrite to the Fe oxide rim which cannot be accounted for simply by the reduction in molecular volume from pyrite to maghemite (~31%). We infer that the source of the As is largely from the vapor in the roaster and not the pyrite. This fits with the observation by Vian *et al.* 1963) that production of Fe oxides must be carefully avoided during roasting in order to prevent retention of As in the calcines. Synchrotron μXRF mapping of this grain (Figure 3-3f) is consistent with that of the EPMA showing the Fe-rich rim and faint calcium outer rim. The most As-rich spots (purple) in Figure 3-3f, correspond to small arsenopyrite grains either observed in thin section photos or inferred as buried grains. Arsenic response within the Fe oxide rim is too low to be clearly seen in this false colour image (Figure 3-3f). The different apparent dimensions of the grain in Figure 3-3f and Figures 3-3a,e are a result of the beamline configuration (sample is at 45° to the beam in the horizontal plane), coarser resolution, and greater penetrating power of the X-ray beam (depth averaged response).

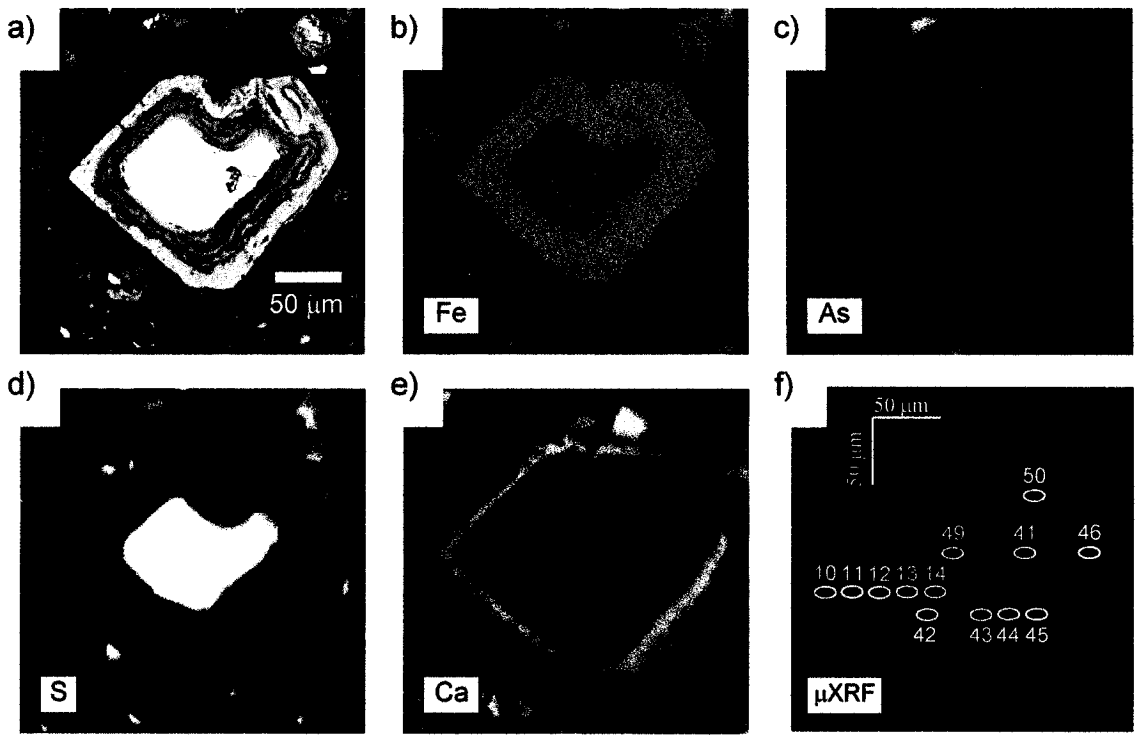

Figure 3-3. Large concentric roaster Fe oxide grain. a) Reflected light photo. Note bright thick outer rim and fine inner concentric layers. There is also a barely visible low reflectivity rim outside of the outer most Fe oxide rim. b) through e) X-ray maps of grain in a). There is clear differentiation of the low reflectivity outer Ca rim, the As-bearing Fe oxide and the pyrite core. f) False colour μXRF map of grain. Red is Fe, blue is As and green is Ca. The effect of depth averaged response, grain orientation (45° to the beam) and lower resolution is evident when compared to the X-ray maps. Numbered ellipses are locations of μXRD and μXANES. Spots 10 through 14 are XANES only, obtained prior to lifting section with acetone. Scale is X-Y stage coordinates.

Spot μXANES analyses for this grain (Figure 3-3f, Figure 3-4) show a wide range in the ratio of As^{III}/As^{V}. Interpretation of the variation is clearer when combined with coincident μXRD (Figure 3-3f, Table 3-2). The Fe oxide rimming the pyrite in this grain is maghemite (primitive cubic form) and this is the dominant μXRD pattern in all spots analyzed. Monohydrocalcite is also frequently observed as spotty rings with the best pattern observed at location 46 (Figure 3-5). Arsenic appears to be associated with the calcium rim, predominantly as arsenate. X-ray mapping (Figures 3-3c,e) indicates the width of the As band around the pyrite core coincides generally with the calcium limit and not that of iron. However, it is noted that the As response is relatively weak and the outer most limit rather diffuse. Micro-XANES analyses of spots that

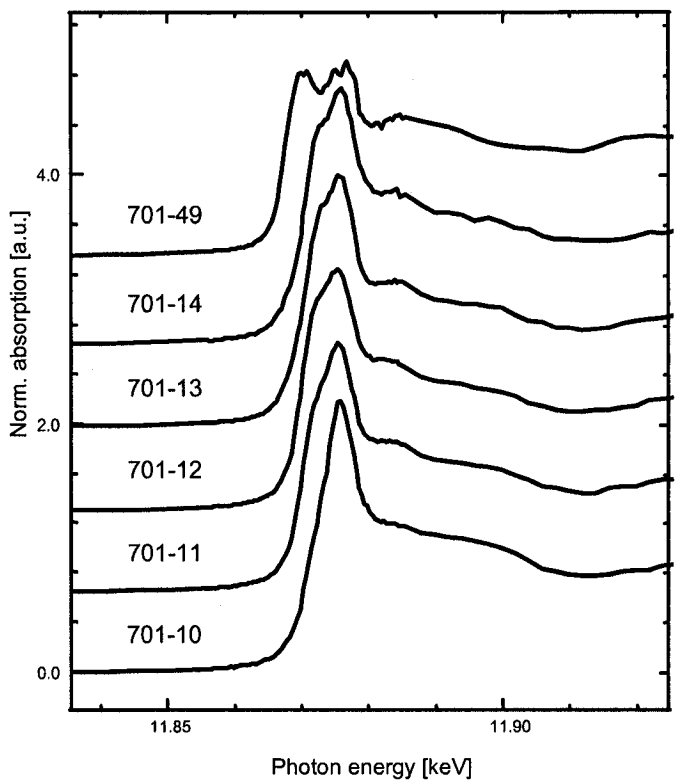

Figure 3-4. μXANES spectra of traverse across left hand side of grain in Figure 3-3. The compound spectra (mixed As^{III} and As^{V}) show a shift from As^{V} dominated to AsIII dominated toward the sulfide core. At the sulfide core (701-49) the spectra is dominated by the arsenical pyrite (As^{-I}).

Table 3-2 Spot μXRD and μXANES results for large rimmed roaster iron oxide in Figure 3-3

Location[1]	Phases by μXRD[2]	$mhCal_{101}/Mgh_{311}$[3]	As^{-I} (%)	As^{III} (%)	As^{V} (%)	As^{III}/As^{V}
10*/119	mhCal(†), Mgh	‡	5.93 / 0.00**	33.45 / 45.92	60.63 / 54.08	0.55 / 0.85
11*	n.a.	-	10.2	52.6	37.2	1.4
12*120	Mgh	‡	7.93 / 12.7	59.9 / 53.0	32.2 / 34.4	1.9 / 1.5
13*	n.a.	-	8.73	55.8	35.5	1.6
14*/121	Mgh	‡	10.1 / 11.9	54.4 / 57.7	35.46 / 30.34	1.5 / 1.9
42	mhCal (6), Mgh	0.03	4.12	56.3	39.6	1.4
43/122	mhCal (2), Mgh	0.01	0.50 / 14.3	64.6 / 56.2	34.9 / 29.5	1.8 / 1.9
44	mhCal (3), Mgh	0.04	1.74	54.0	44.2	1.2
45	mhCal (6), Mgh	0.08	3.21	43.2	53.6	0.80
41	mhCal (4), Mgh	0.04	1.65	39.8	58.6	0.68
46	mhCal (6), Mgh	0.05	4.85	33.2	61.9	0.54
49/123	Mgh (weak)	-	58.7 / 58.2	25.6 / 18.6	15.7 / 23.2	1.6 / 0.80
50	mhCal (6), Mgh	0.03	3.80	48.7	47.5	1.02

[1] Locations from Figure 3-3f. Second 100 series numbers (where given) are μXANES and μXRD analyses repeated over 1 year later after X-ray mapping and EPMA point analyses (rastering of electron beam on target for more than 8 hours). Targeting was by repeat μXRF mapping. Smaller d-spacing range was intersected for these μXRD analyses due to a fixed, but longer sample to detector distance (20 cm± instead of the previous standard 17 cm±).

[2] Pattern for mhCal is generally weak. Number in brackets is number of peaks identified.

[3] Ratio of 101 mhCal reflection to 311 Mgh reflection in integrated pattern.

* μXANES analysis only.

† Good pattern for mhCal. Four of four mhCal peaks observed within the d-spacing interval sampled, but interval differs from previous analyses (see note 1).

‡ mhCal 101 to Mgh 311 ratio cannot be calculated in the same manner as earlier analyses (41 through 50). See note 1.

** LC XANES fit gave small negative value for this component so fit was made with the other two components alone.

n.a. – not analysed.

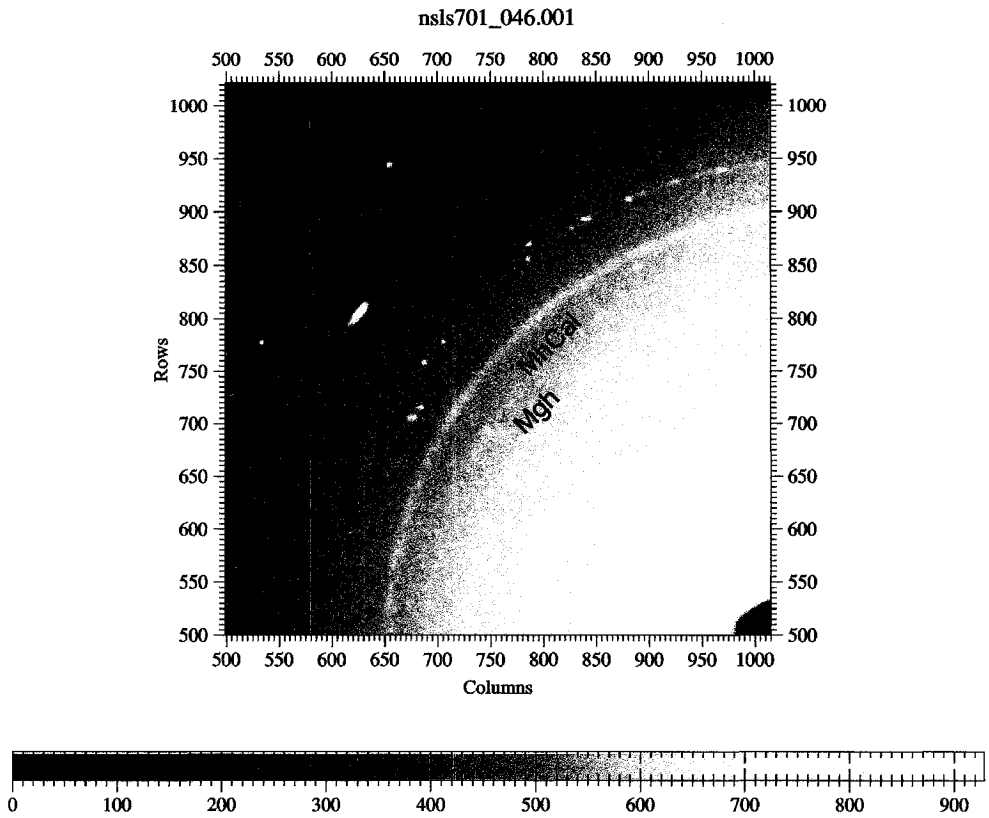

Figure 3-5. μXRD pattern for location 46 in Figure 3-3f. Smooth rings are maghemite (Mgh) including several weaker rings characteristic of the primitive cubic form and spotty rings are monohydrocalcite (MhCal).

show the greatest evidence of mhCal in coincident μXRD patterns show the lowest ratio of As^{III}/As^{V} in the range of 0.5 to 0.8. Conversely those that show little evidence of mhCal have As^{III}/As^{V} ratios in the 1.5 to 1.9 range. The low As^{III}/As^{V} ratio may also be related in whole or in part to the bright outer Fe oxide rim since it seems to be spatially related to the mhCal and contains less As than the interior rims. We interpret the scatter within the data to the beam to grain orientation (45° to the grain boundaries inferred to be approximately vertical into the section) and potential heterogeneity at depth within the section.

Another important group of partially-reacted grains in the Giant calcine is that containing relic pyrrhotite. Reaction of pyrite and arsenopyrite occurs via a pyrrhotite intermediate at more elevated temperatures than the concentric form or other conditions (eg. SO_2 enriched atmosphere) that may inhibit direct reaction of pyrite to Fe oxide (Grimsey & Aylmore 1990, Jha & Kramer 1984, Swash & Ellis 1986, Grimsey & Aylmore 1992, Dunn *et al.* 1995). Such conditions favor the partial removal of sulfur from pyrite and preferential removal of As from arsenopyrite (and presumably arsenical pyrite). Two small grains containing relic pyrrhotite and exhibiting different textural morphologies in the calcine residue sample (M2M) were specifically targeted for analysis (Figure 3-6a,b) with two spot analyses completed on each. The As^{III}/As^{V} ratios for the grain in Figure 3-6a were 2.8 and 2.0 for the center and rim respectively. The As^{III}/As^{V} ratios for the grain in Figure 3-6b were 1.8 and 0.98 for the relic sulfide portion and low reflectivity Fe oxide target respectively. Both grains show a predominant smooth ring maghemite pattern with spotty rings of pyrrhotite. The μXRD pattern for the microporous pyrrhotite (Figure 3-6c) is distinctive as nebulous spots and patchy arcs in contrast to the smooth rings of maghemite and fine spotty rings of pyrite. The nebulous nature of spots for pyrrhotite may indicate a mixture of hexagonal and monoclinic varieties, the presence of crystallite strain or both. The presence of relic pyrite in the μXRD pattern for the grain (which is not evident by reflected light microscopy) suggests the grain represents the rapid decrepitation of pyrite to pyrrhotite at the micron scale following a brief direct reaction of pyrite to nanocrystalline maghemite recorded by the thin outer rim. We interpret the presence of dominantly As^{III} in the core as the initial stages of oxidation of the pyrrhotite and incorporation of the As under elevated partial pressure of SO_2 (partial pressure of O_2 kept low due to reacting pyrrhotite). The lower As^{III}/As^{V} ratio toward the outer rim may indicate either a previously established lower As^{III}/As^{V} ratio in the outer rim (during direct oxidation of pyrite to magnetite/maghemite) or As oxidation state equilibration with higher partial pressure of O_2 at the outside of the grain. It is difficult to discern the primitive cubic maghemite

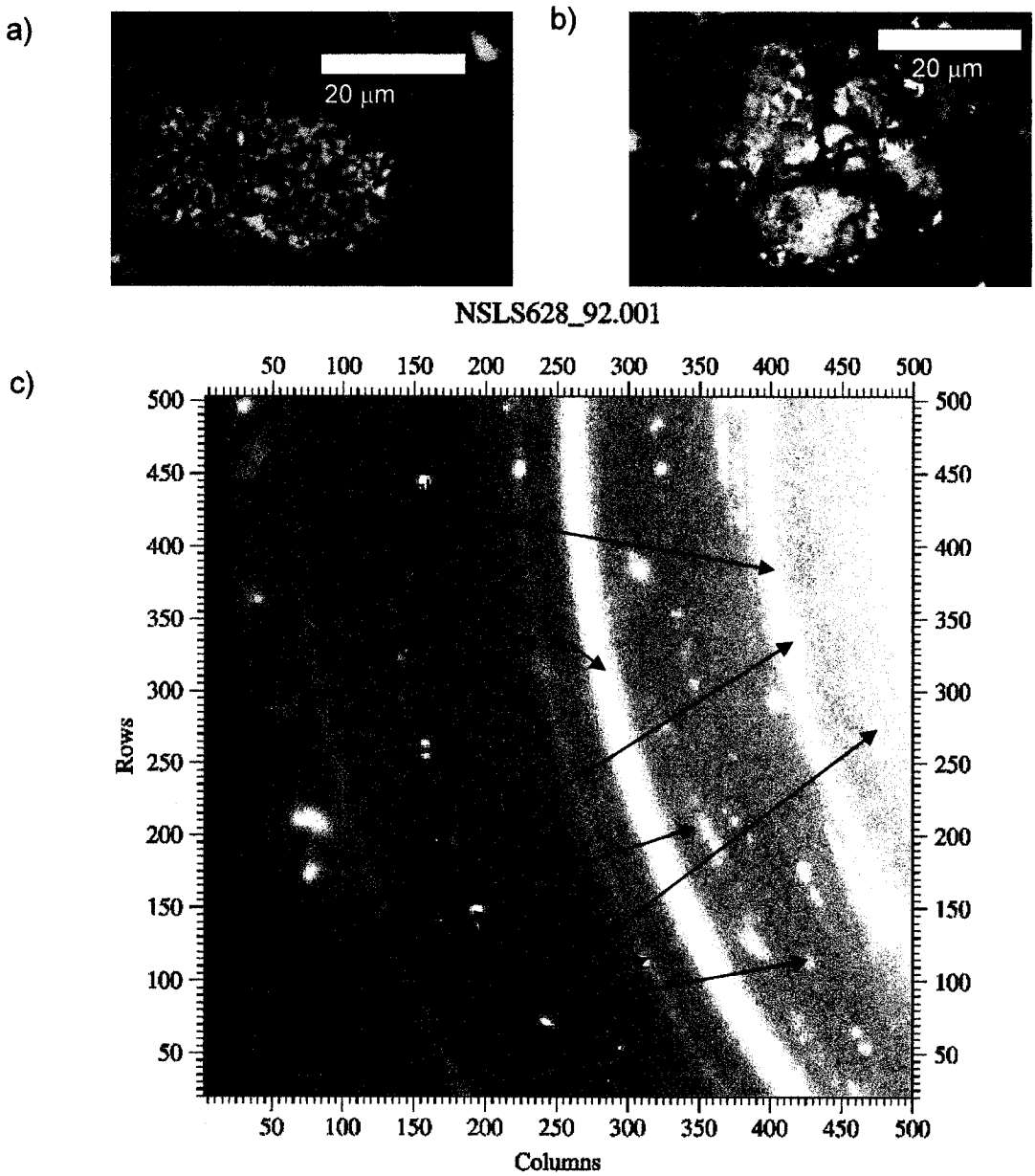

Figure 3-6. μXRD of Roaster-derived Pyrrhotite. a) Reflected light photo of microporous Po grain with outer rim of Mgh. b) Reflected light photo of finely microporous Mgh and relic Po. Less reflective microporous Fe oxide in upper left of this photo. c) μXRD image of microporous Po grain on left (target was centre of grain). Diffraction includes smooth rings for Mgh, nebulous spots and arcs for Po and fine spots for pyrite.

peaks in either of these patterns suggesting either magnetite (or very finely divided maghemite) is the Fe oxide formed (Cornell & Schwertmann 2003, Haneda & Morrish 1977). Both maghemite/magnetite XRD patterns are weak, but it is interesting that the weaker of the two patterns (rim) shows slight evidence of two of the primitive cubic peaks (5.95Å and 3.73Å), while the pattern from the core shows no evidence. Optically the outer rim appears to be maghemite. Another important observation is the coexistence of pyrite, pyrrhotite and magnetite/maghemite. It has been suggested (e.g. Grimsey & Aylmore 1992, and Dunn *et al.* 1995) that the oxidation of pyrrhotite will not commence until pyrite is exhausted. This data suggests this need not be the case. It may be that the shrinking core of pyrite gets so small that it does not generate sufficient SO_2 to prevent oxidation of the pyrrhotite to Fe oxide. A change in local gas atmosphere around the particle could also play a role. The XRD pattern for both targets in Figure 3-6b contain the primitive cubic lines for maghemite.

Table 3-3 lists observed mineralogy (confirmed by μXRD), μXANES and EPMA results for a range of roaster-derived grains from recent calcine (M2M, NW1aS2), old Edwards roaster calcine from Con Mill stockpile (CM1a) and analysis of cyanided ESP dust (M4M). Though the grains take many forms, in the absence of sulfide, ratios of As^{III}/As^{V} are typically less than 1.4. A number of grains analysed by EPMA suggest lower concentrations of As on particle surfaces (outer layers) than interior regions.

Three analyses of fine grained matrix of ESP dust indicates this material is dominated by As^{III} (Table 3-3). Bulk XRD has identified the probable presence of arsenolite in this material. However, we have yet to confirm that arsenolite this is responsible for the elevated As^{III} in these samples. Similarly high As^{III}/As^{V} ratios have been reported for some thin laminae in North Pond tailings (Fawcett *et al.* 2006). The ESP dust constitutes only a small volume fraction of the As

Table 3-3 Selected μXANES Analyses of Roaster-derived Phases in Mill Products

Sample Identification	Grain Description	Total As		Arsenic Speciation				
		% (w/w)[2]	N	As-I (%)	AsIII (%)	AsV (%)	AsIII/AsV	n
M4M[1]	Fine grained matrix	N.A.	-	22 - 6	60 - 76	16 - 20	3.0 - 4.2	3
M2M-CA3	Microporous Mgh with "dense" rim	1.3 to 1.6	2	2 - 0	34 - 35	63 - 66	0.50 - 0.55	2
M2M-CA5	Square concentric Mgh	4.2 (rim) to 5.6 (core)	2	2 - 0	30 - 32	67 - 68	0.45 - 0.47	2
M2M-AX2	Low reflectivity concentric Mgh rim with Py core	2.0	1	18 - 0	60 - 63	22 - 37	1.7 - 2.7	2
CM1a AX1a[1]	Microporous Mgh	n.a.	-	0	45	55	0.81	1
CM1a AX1b[1]	Mgh with "speckled" relic sulfide	n.a.	-	3	53	44	1.2	1
CM1a AX2[1]	Microporous Mgh-Hem	n.a.	-	0	29	72	0.40	1
NW-AX5	Large concentric Mgh with mhCal rim and Py core*	2.7 (rim) to 3.6 (near Py)	19	10 - 0.5	33 - 65	32 - 62	0.54 - 1.9	13
NW-AX8	Large low reflectivity microporous Mgh	2.7 to 3.0	4	6 - 0	39 - 41	53 - 59	0.65 - 0.77	4
NW-AX9b-1	Irregular "dense" high reflectivity Mgh	3.5 to 5.0	2	4	27	69	0.40	1
NW-AX9b-2	Microporous Mgh	1.4 to 2.0	3	5	45	50	0.9	1
NW-AX10	Concentric Mgh	2.2 (rim) to 3.9 (core)	5	2	58	40	1.4	1

[1] No μXRD available. [2] By EPMA. n= number of analyses.

* Analysis of Mgh Rim only. Analysis of Py core is 58% As^{-1} (see also Table 3-2 and Figure 3-4).

tailings discharged (Table 1-4), but its high As content, and fine grain-size are expected to increase its importance with increasing distance from the discharge point.

3.4.3 Arsenic incorporation in roaster iron oxides

In addition to the nanocrystalline nature of the roaster Fe oxides, there are a number of other factors that may be important in the incorporation or binding of As to these phases during roasting. The effect of roasting gold ores in the presence of water vapour has seldom been considered with the work of Grimsey & Aylmore (1990) being a notable exception. Their work indicates that water vapor primarily acts as a diluent in roasting and has little effect apparent effect on mineralogy. However, they consider only magnetite and hematite in their discussions and therefore the potential importance of maghemite and the stabilizing effect water may have in this type of environment has not been considered (Cornell & Schwertmann 2003 and especially data of Stanjek & Sabil in preceding reference). Of potentially more importance is the possible effect roasting in steam may have on the speciation of As vapour that we are proposing is interacting with the Fe oxide reaction products. Pokrovski *et al.* 2002 indicates $As(OH)_3$ is the dominant form of As in vapour under hydrothermal conditions (instead of the generally assumed As_4O_6) at atmospheric pressure and above 200 °C. H_2O gas may be a significant portion of gas phase in many roasters (including Giant) since the feed enters as a slurry and significant water is added to control roasting temperature (Halverson 1990).

Based on our preceding findings and discussion, we hypothesize that the As as either $As(OH)_3$ or As_4O_6 is carried along with oxygen to contact the newly formed or reacting Fe oxide surface where it chemisorbs probably in a manner similar to low temperature aqueous sorption processes (bidentate inner sphere complex) although As_4O_6 would have to dissociate in order to accomplish this. If the surface coverage of As reached sufficient site density the possibility of forming nanoclusters or fine crystallites of Fe arsenates or Fe arsenites also arises. An alternative could

be the incorporation of As^{III} as trigonal bridging complexes at defect sites in maghemite (Peterson 2005). Binding of As in such a manner (if it occurred) could account for the resistance of As^{III} to oxidation in the oxic subaerial tailings environment.

Another important observation that has been made is that the presence of hematite usually coincides with lower As content. We have previously reported a characteristic spotty texture on Debye-Scherrer rings from hematite (Chapter 2, Walker *et al.* 2005). A coarsening in grain-size (and corresponding decrease in As) upon transformation of maghemite to hematite is one explanation for the observed decrease in As content in hematite-rich grains. This spotty nature of the hematite μXRD pattern can also be observed in a pseudo-3D plot (Figure 3-7) where the

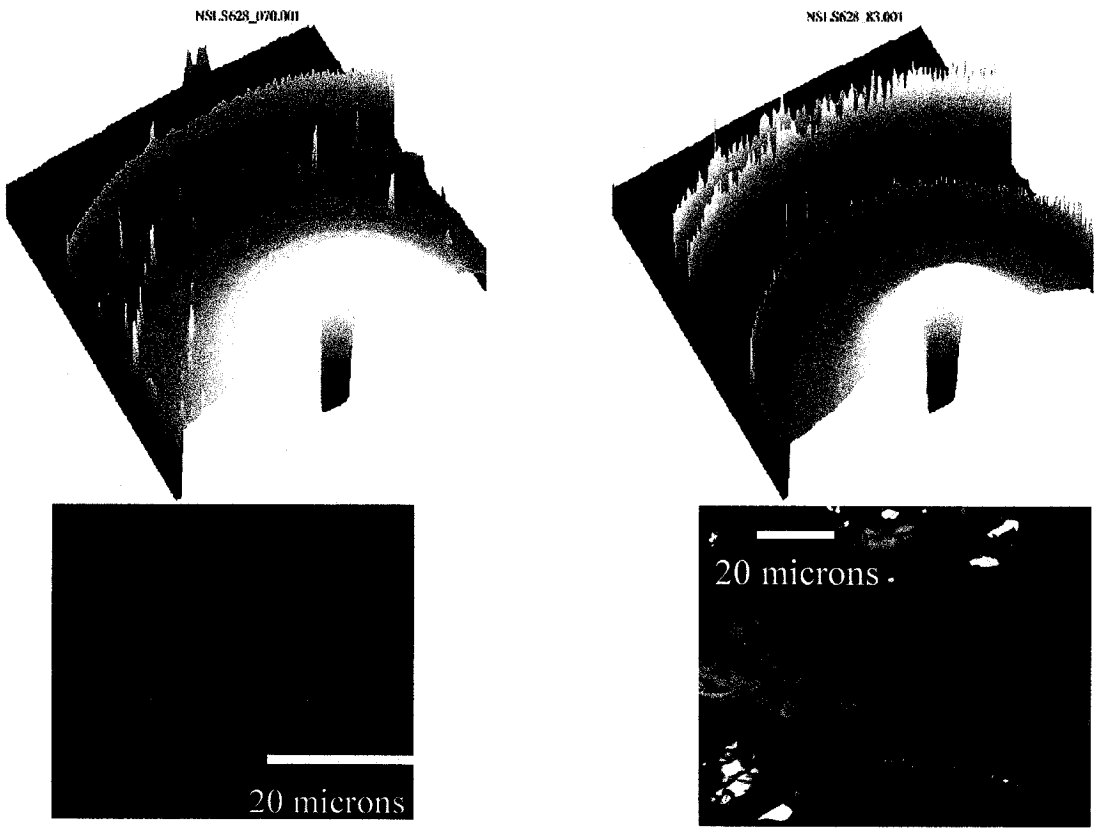

Figure 3-7. MicroXRD as qualitative evidence of increasing crystallite size upon transformation to hematite. The μXRD patterns for two grains are shown as a 3-D surface to highlight the saw-tooth nature of the Hem rings (right) in contrast to the smoother appearing Mgh rings on the left.

hematite exhibits a "saw-tooth" pattern in comparison to the smoother pattern for a typical maghemite grain.

3.4.4 Roaster Fe oxides in tailings at the Giant Mine

The roaster Fe oxides have been dispersed into the surrounding environment and some exposed to the atmosphere for as long as 58 years. Roaster Fe oxides generally appear similar in the tailings to those observed in the Mill products and recent tailings. Micro-XRD and μXANES also give similar results although the subaerial shoreline tailings at Yellowknife Bay seem to have less arsenic and lower As^{III}/As^{V} ratios (Walker *et al.* 2005, Table 3-4).

Even though As^{III} is considered mobile and should be readily oxidized to As^{V} in the oxic environments investigated in this study, it none the less persists in association with the roaster-derived maghemite. A possible exception is the subaerial shoreline tailings which exhibit lower As content in roaster Fe oxides as well as the lowest As^{III}/As^{V} ratios observed. The presence of weathering sulfides confirms exposure to more oxidizing environments. There is also the possibility that acid deposition from SO_2 emissions for over 50 years has led to preferential leaching of As and especially of As^{III} which is less strongly bound at lower pH (Pierce & Moore 1982). However, the water chemistry will be significantly buffered by carbonates and indeed the measured pH in the subaerial tailings in 1999 was neutral as were all other measured tailings pore waters (Appendix D). The limited number of analyses from this material and the unique roasting conditions at the time for which we have no "source" material to analyze make this a subject requiring further investigation. We attempted to analyze the Con Mine calcine for this purpose and this did confirm the more frequent presence of hematite in the hearth roaster calcine from Con which supports the greater apparent hematite component (and more red character) observed in the Giant Yellowknife Bay calcine. The Con calcine (CM1a) roaster Fe oxides also exhibited

Table 3-4 Selected μXANES Analyses of Roaster-derived Phases in Tailings

Sample Identification	Grain Description				
		As^{-I} (%)	As^{III} (%)	As^{V} (%)	As^{III}/As^{V}
CB1bS3r CA3	Bright concentric Mgh	6	36	58	0.62
CB1bS3r AX1	Microporous Mgh	2	12	86	0.14
CN2bS3r AX2	~ 20 μm diameter concentric Mgh grain	3	22	75	0.29
P7Stn5r CA3	Concentric Mgh	0	36	64	0.56
P8 Stn5r AX11	Microporous Mgh	19	27	54	0.50

the characteristic mixed $As^{III} - As^{V}$ oxidation state. However, the possible presence of arsenolite in this material may have a direct or indirect effect on the As^{III}/As^{V} ratios.

The application of grain-scale analysis using synchrotron μXRD and μXANES with mill products and tailings from the Giant mine, has led to a hypothesis that explains how As may be bound within the nanocrystalline composite roaster-derived Fe oxide grains. The processing of ore at Giant imprints the roaster derived phases with unique characteristics that have persisted in the subaerial environment for 20 to 50 years.

Chapter 4 – Characterization of Arsenic in Solid Phase Samples Collected on the Giant Mine Townsite, Yellowknife, NWT

4.1 INTRODUCTION

In the summer of 2000, the City of Yellowknife planned to build a new boat launch at the former Giant Mine Townsite. This raised concern that As contamination encountered during construction and future use of the launch could potentially affect human health or the environment. The City of Yellowknife excavated two test pits approximately one meter deep in the vicinity of the proposed dock. Soil results indicated As present at concentrations between 754 and 9580 ppm. These values significantly exceed the generic CCME guideline of 12 ppm and they also exceed the risk-based value (160 ppm) determined for Yellowknife (RiskLogic 2002).

Under the direction of INAC, the Environmental Sciences Group (ESG) at Royal Military College (RMC) sampled and analyzed 23 soils (Figure 4-1) at 16 locations across the Townsite (18 samples) and Great Slave Cruising Club (5 samples) in September 2000 (ESG 2000). Dr. Heather Jamieson's Research Group and ESG (at the direction of INAC) then conducted a joint study aimed at better understanding the mineral form of As in the Townsite soil samples (ESG & Queen's 2001). The joint ESG-Queen's work has since been supplemented by additional characterization work on the original ESG samples as part of this thesis, generally applying the methods developed and described in Chapter 2.

4.1.1 Background

The Giant Mine Townsite was built on the shore of Back Bay (around the mouth of Baker Creek) in the 1950's, although it probably arose from earlier exploration and construction camps. The Townsite provided accommodations for miners and their families as well as service and support

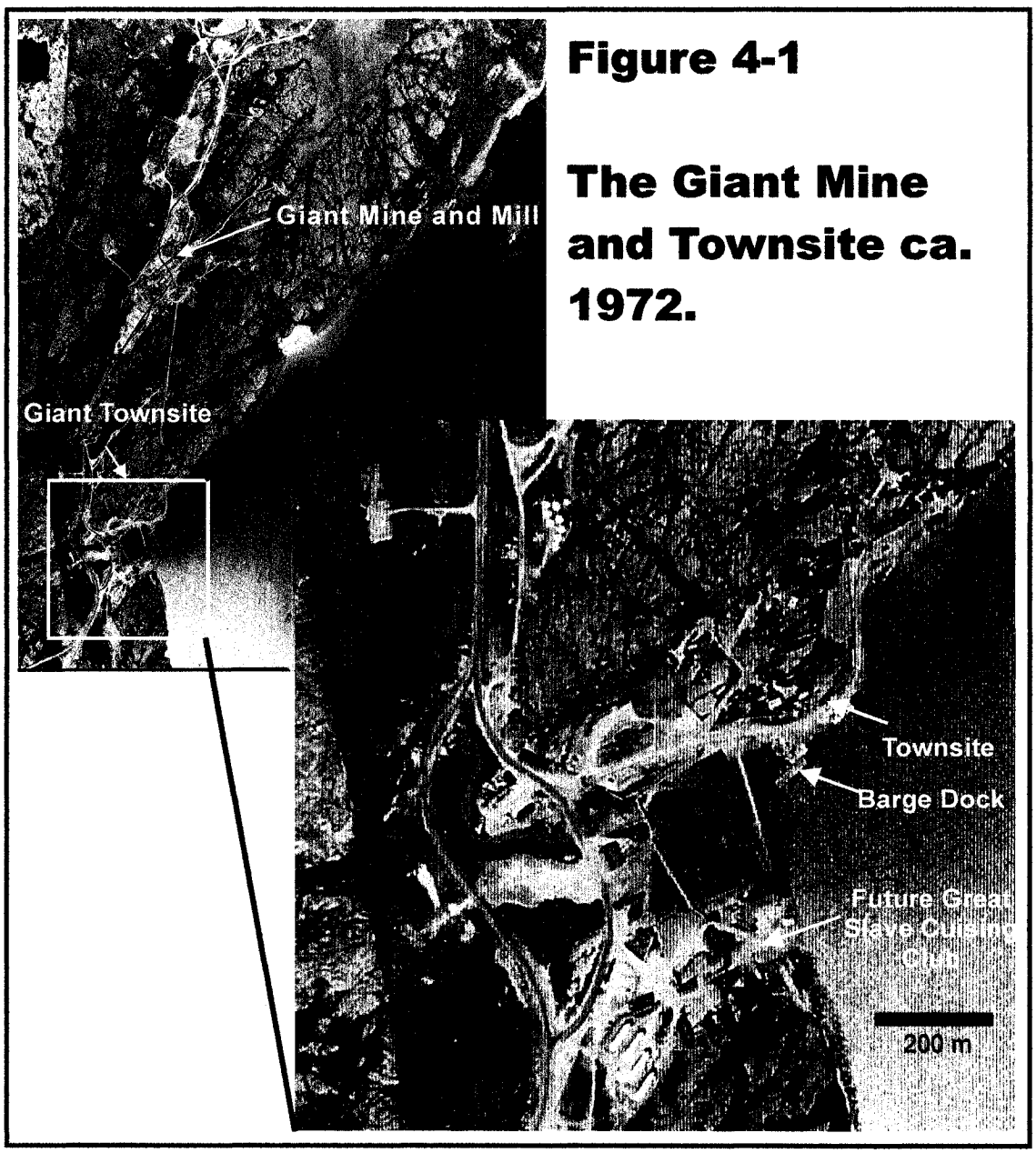

Figure 4-1

The Giant Mine and Townsite ca. 1972.

for the mine. The site is accessed from the Ingraham Trail. The property north of Baker Creek mouth seems to have seen mostly residential use from the earliest days of mining. The area to the west and south seems to have been mixed usage to service and support the mine (Pitcher 1953, Figure 4-1). Roadways are often (if not exclusively) constructed of crushed waste rock fill (hereafter referred to as crushed rock road-fill). It appears the breakwater and portions of the waterfront have been filled with similar crushed rock fill material (hereafter referred to as crushed rock lake-fill) including the area of the new boat launch. This area was constructed originally as a docking facility (Figure 4-1).

At the time of sampling by ESG in September 2000, there were 22 wooden residences on the northern portion of the Townsite property along with a playground built on sand (Figure 4-2). The Great Slave Cruising Club (Cruising Club) presently occupies the southern portion of the site and the NWT Mining Heritage Society (museum site) occupies the western portion of the site (Figures 4-1 and 4-2). To avoid confusion in this text, Townsite Subdivision will refer to the existing (largely unoccupied) residential area to the north of Baker Creek mouth. Cruising Club and museum site will refer to the areas to the south and west of Baker Creek mouth respectively.

4.1.2 Arsenic Sources

The fact that there are elevated concentrations of As in soils at the site is not surprising given its close proximity and relationship to historic mining activities. Gold has been mined and milled at the Giant mine site since 1948. Since gold in the Yellowknife area is intimately associated with As in the form of the mineral arsenopyrite (FeAsS), it can be expected that surficial soils in the area of the mine (and the entire Yellowknife area) may contain naturally elevated concentrations of As. In addition, activities at the mine over the past 50 years have resulted in the release of As to the surrounding environment (anthropogenic inputs). Regardless of the source, it is the form of

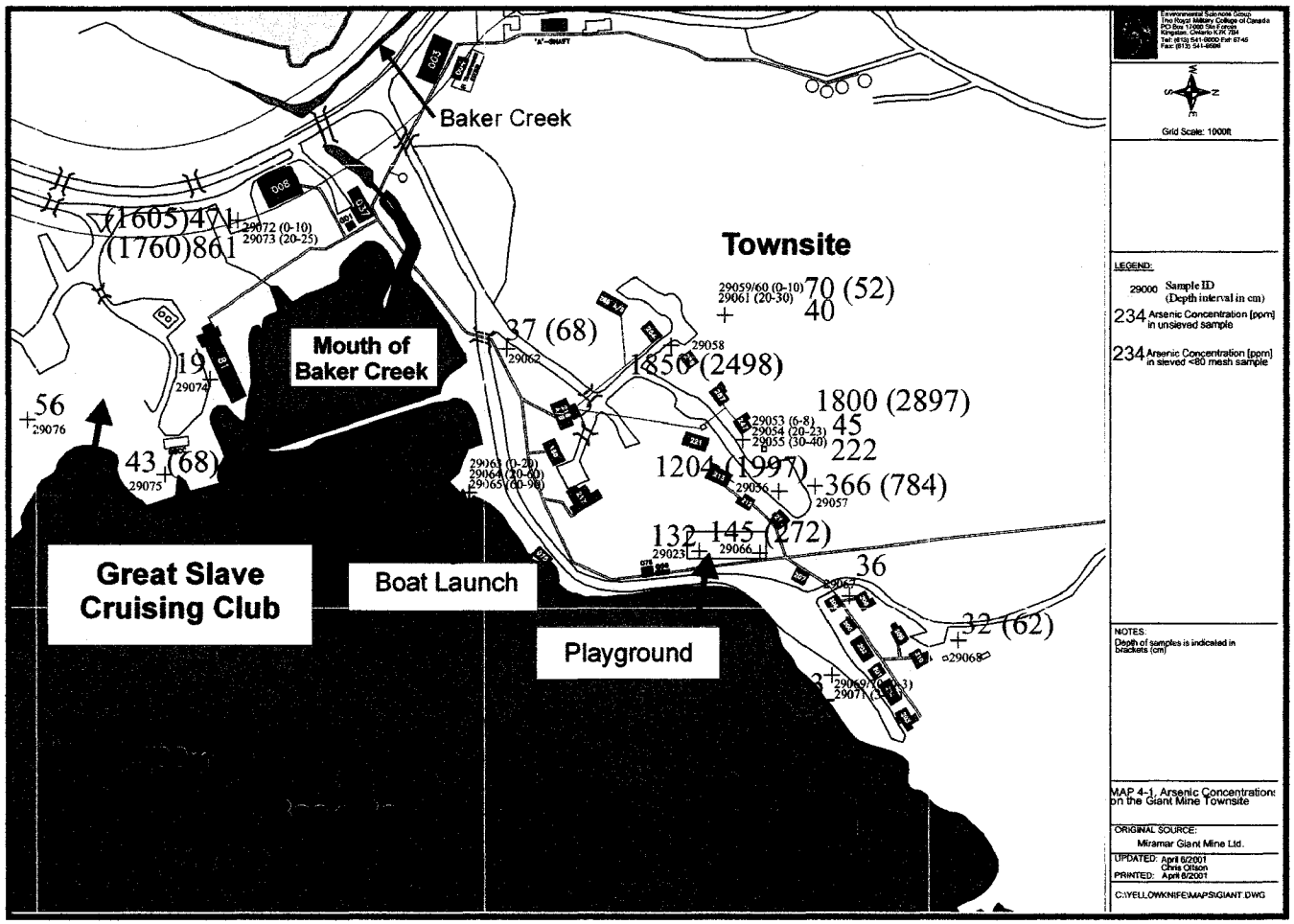

Figure 4-2 Townsite Soil Sample Locations and Distribution of Arsenic Concentrations in Soil and Crushed Rock Fill. Values in red are total arsenic (by NAA) in bulk soil. Values in blue are total arsenic (by NAA) for the sieved fraction (<0.18 mm diameter). Sequential selective extractions and mineralogy were carried out on the sieved portion. (Modified from Map 4-1, ESG-Queen's 2001).

the As and its physical and chemical associations in the environment that determines mobility and bioavailability (Bhumbla & Keefer 1994).

It can be inferred that historical mining and milling activities at Giant may have introduced As to the site in the following ways:

- Localized disposal, construction and lake-filling utilizing arsenopyrite-bearing waste rock (crushed rock fill) generated from mine workings,
- Site-wide aerially dispersed fallout from nearby (~1.5 km) roaster stack emissions (GNWT 1993, CPHA 1977), particularly in the first 10 years of roasting, and
- Shoreline deposition of fine-grained sediment carried from the Giant mine tailings discharge areas to the Townsite via Baker Creek with greatest impacts probably in the mid to late 1950s and 1960s (Andrade 2006).

The principal objective of the current work was to study the form of the As in the high As content crushed rock fill materials. However, it is important to consider the potential overprinting or mixing of As phases that may have occurred from other sources. The most important site wide factor is likely to be the aerially dispersed As from the roaster although the magnitude of this influence has not been quantified. A related aspect of the roaster emissions is the acid deposition that would have resulted from roaster SO_2 emissions. In addition, a limited review of early air-photos suggests that there was localized filling along the lakeshore including the eastern limit of the Cruising Club, the Breakwater and the region around the new boat launch. In places this crushed rock fill may be mixed with this sediment. The degree of impact to sediment quality at a given time and the time of placement of the fill would determine how important any mixing may be with respect to solid phase As.

The oldest crushed rock fill materials in the area probably originated following the sinking of A shaft in the fall of 1945 (Pitcher 1953). This establishes an upper limit of 61 years of exposure of the crushed rock fill in the environment.

4.2 PREVIOUS WORK

4.2.1 ESG Soil Sampling and Analysis (2000)

ESG collected 25[2] soil samples (including 2 field duplicates) which were analyzed for As and a suite of additional selected inorganic elements (Sb, Fe, Au, K, Na, Zn, Mn, Cu and Ni). Samples included a range of soil types that were generally separated into one of two categories (crushed rock fill, or other surficial materials comprising soil, clay and granular fill). The highest concentrations of As were associated with crushed rock fill samples, which had an average As concentration of 1174±519 ppm (range 471 to 1850 ppm). The average concentration of the other soil samples (including the two playground sand samples at 132 and 145 ppm As) was 87±95 ppm (range 19 to 366 ppm). The highest concentration (for this soil type) of 366 ppm was reported for a sample (29057) obtained from a rock crevice near one of the residences. The second highest concentration of As (222 ppm) for the non-crushed rock fill samples was reported for sample 29055. This sample was from a buried former topsoil horizon beneath sand fill that contained only 45 ppm As (Appendix B in ESG 2000).

4.2.2 Joint ESG-Queen's Characterization Work (2001)

It was concluded that knowledge of the total concentration of As from this area was not sufficient to determine the potential risk posed to ecological and human health by this material. Therefore, additional work was undertaken (ESG & Queen's 2001) to more completely characterize 17 of

---

[2] This work by ESG sometimes refers to only 24 samples. This discrepancy appears to be for sample 29023 (playground sand) which appears on maps provided in reports, but is not included in data Tables.

the 25 ESG soil samples (15 samples plus 2 duplicates). The scope of this work and responsibilities were:

- Compare the total As concentrations in different grain size fractions of soil samples (ESG);
- Compare analytical methods used to determine total As (ESG);
- Characterize, through sequential selective extractions (SSE), the phases to which As in the 15 selected soil samples (plus the two duplicates) is bound (Queen's / ESG);
- Detail initial findings of mineralogical work performed (optical microscopy, qualitative EPMA, and preliminary μXANES analyses on a subset of 4 samples) and relate this to the corresponding SSE results (Queen's); and
- Conduct gastric fluid extractions on all 15 soil samples (plus 2 duplicates) to attempt to elucidate the potential bioavailability of this material (ESG).

This joint work by ESG and Queen's culminated in a report of findings (ESG & Queen's 2001).

4.3 Additional Studies (2002 to present)

Time constraints for the preceding work only allowed for presentation of initial mineralogical results. Therefore, additional studies to more completely characterize the As-bearing Fe oxyhydroxide weathering products were completed as part of this thesis. This work was conducted on samples 29053, 29057, 29064, 29066 and 29072 using the methods detailed in Chapter 2 and included:

- Additional optical microscopy;
- Quantitative EPMA analysis of Fe oxyhydroxide weathering rims on sulfides;
- Additional μXANES analysis of selected targets on polished thin sections; and
- Combined μXANES and μXRD of selected targets on sample 29072.

Work on samples 29057 and 29064 was limited to optical microscopy only. As a point of clarification, sample 29064 was to be included (along with 29072) in the analysis by combined μXANES and μXRD. However, sieving of additional sample was required in preparation for this work, since the previous material from the SSE analysis had been completely used in subsequent ESG work. The material for the sieving came from small subsamples (~2 mL) retained at Queen's as a visual record of the samples. This material was not obtained to be a careful split of the original and apparently the sample for 29064 was not representative, since the resulting thin-section for 29064 (29064r) contained significantly fewer weathered sulfide targets than the original section. Since the new section for 29072 (29072r) did appear generally representative of the original section, 29072 is the only Townsite sample analyzed using combined μXANES and μXRD.

4.4 Work Within the Scope of this Thesis

This Chapter documents results of SSE and bulk XRD of the 15 soil samples (ESG & Queen's 2001), and final results of optical microscopy, EPMA, μXANES and μXRD conducted selectively on 3 of the samples (two crushed rock fill samples and one playground sand sample). The other representative sample types (fills and organic soils) are not represented in the detailed mineralogical work due to their low As content. Polished thin-section 29064 and polished section 29057 were inspected and photographed under petrographic microscope, but not subjected to any further analysis at this time.

4.5 SAMPLING AND ANALYSIS

4.5.1 Summary of ESG Field Sampling and Sample Handling

The fieldwork was carried out in September 2000 as part of a study being conducted by ESG in the Yellowknife area at that time. Samples were obtained using individual disposable plastic scoops and stored in a Whirl Pak™ bag. Each sample was given a number, which was the only identifier provided when submitted for analysis. Soil samples to be analyzed for inorganic elements were kept at a temperature of less than 0 °C, prior to and during shipping. Sampling locations and descriptions were recorded in field notebooks and/or on field maps, and a photographic record was made of each general area that was sampled. Sampling locations for this study were not surveyed but all locations are considered to be approximate within a few meters.

Each sample was clearly labeled and stored below 0 °C in a secure area before and after analysis. Neutron activation analysis (NAA) was used to determine total As concentration in the soil samples (including the <80 sieve size fraction), while inductively coupled plasma-mass spectrometry (ICP-MS) was used for measuring As concentrations in extracts of sequential selective extractions. Brief summaries of the methods carried out are detailed in the following sections. Detailed methods of the work completed by ESG are provided elsewhere (ESG & Queen's 2001).

4.5.2 Sample Selection and Preparation

A representative sub-set of samples (17 in total) of the original 25 soil samples (ESG 2000) were selected for the more detailed As characterization work. In order to facilitate the sequential selective extraction (SSE), mineralogical and gastric fluid work, and to increase homogeneity, the soil samples were air dried and sieved to <80 mesh (<0.18 mm).

The samples selected for mineralogical analysis were:

29053 Grey, crushed rock fill (surface material, roadside in Townsite Subdivision).

29057 Brown organic rich soil veneer from rock crevice with > 700 ppm As in the sieved fraction (elevated rock outcrop adjacent to House 211, Townsite Subdivision).

29064 Grey, crushed rock fill (subsurface material, possible lakefill at proposed boat launch area, Townsite Subdivision).

29066 Brown playground sand (Townsite Subdivision).

29072 Grey, crushed rock fill (surface material, parking lot near Ingraham Trail, presently Museum site.

The samples for mineralogical characterization were selected on the following basis.

1. Inspection of sequential extraction results for different characteristics.
2. Location, type and depth of sample.

Each of the samples also exhibits a distinctive pattern in the SSE As distribution (see Section 4.5.2). Sample selection was limited to inorganic fill materials with the exception of organic-rich soil 29057, which contained >700 ppm As in the sieved fraction.

4.5.3 Sequential Selective Extraction

Samples were submitted to ALS Chemex (Chemex) for sequential selective extraction using the methods as detailed by Hall *et al* (1996a,b,c). The <80 mesh sieved samples (<0.18 mm) were subjected to increasingly strong chemical extractions to aid in identifying how As is bound in the soil matrix. The decanted supernatant was analyzed at each stage for a standard analytical suite of parameters. The list of parameters varied somewhat depending on the specific analytical method employed for each extraction step, and whether reagents added precluded analysis of

certain elements (e.g. Na). The full set of SSE analytical data for the crushed rock fill samples as well as the rock-crevice sample (29057) are included in Appendix F.

4.5.4 Mineralogical Methods

A combination of analytical techniques was employed to identify As-bearing phases in the prepared (i.e. sieved) samples. Mineralogical methods carried out include the following and generally follow the methods previously described (Chapter 2), except as indicated.

- Powder X-ray diffraction of each sample to identify the major mineral phases present.
- Optical microscopy of four polished thin sections (samples 29053, 29064, 29066 and 29072) and one polished section (sample 29057).
- Electron micro-probe analysis (EPMA) of target grains in three of the four thin sections (29053, 29066 and 29072).
- Synchrotron μXANES analysis of selected targets on thin sections 29053, 29066 and 29072.
- Synchrotron μXANES and μXRD on selected targets on thin section 29072r (acetone slide removal technique).

Bulk XRD work utilized a powder diffractometer with a Philips PW1011 generator, with Cu Kα radiation (40Kv and 20 mA) with Ni filter and a thallium activated sodium iodide crystal detector with pulse height discrimination. Scans were run from 3 to 60 degrees 2θ with an edge filter in place to reduce background scatter at low angles.

4.6 RESULTS

4.6.1 Supporting findings by ESG

An average increase of 100±67% in total As concentration was seen in the <80 mesh (<0.18mm) soil fraction, over that of the unsieved portion (ESG 2000). This observation of increased As in the fine fraction of an environmental sample is consistent with findings of others (McBride 1994; Ruby *et al.* 1999). Total As concentrations in both fractions are shown in Figure 4-2. No apparent difference was found when the total As concentration (determined by NAA in the <80 mesh fraction) was compared to the total concentration determined in sum of the sequential selective extractions. In fact, the average percent difference was 8±5%, well within expected analytical error (ESG & Queen's 2001).

4.6.2 Sequential Selective Extraction (SSE)

Seventeen soil samples were subjected to the SSE analysis (Hall *et al* 1996a,b,c). The operationally-defined SSE can be viewed as an initial step in identifying the way in which the As is distributed in solid samples.

The following grouping of extractions provides an overall perspective on potential As availability based on the aggressiveness and type of extractions.

- Group 1 (Sum of Steps 1, 2 and 3) - Potentially environmentally available at ambient conditions: adsorbed/exchangeable, carbonates, organics. Step 3 was only completed for the organic-rich samples.
- Group 2 (Sum of Steps 4 & 5) - Potentially environmentally available under specific Eh-pH condition: amorphous Fe oxyhydroxides and crystalline Fe oxide.
- Group 3 (Sum of Steps 6 & 7) - Not environmentally available under most immediate

conditions: sulfides and residual.

Figure 4-3 compares the concentration of As extracted in each phase of the SSE analysis with the total concentration of As extracted for each sample. The concentrations determined for each extraction step have also been tabulated (Table 4-1). The majority of the As from the crushed rock fill as well as the playground sand and sample 29062 (light brown poorly sorted granular fill) is observed in the sulfide fraction (Step 6), suggesting that the As is predominately in its unweathered (sulfide) form. Samples 29064 and 29065 (crushed rock lake-fill) and 29057 (rock crevice sample) are exceptions where the majority of the As is found in the Fe oxide fractions (Group 2). These fractions (Group 2) are the second most prevalent in which the As is found in the rest of the samples. The only sample with the majority of As reporting to the most available fractions (Group 1) is the organic rich sample 29059/60 that was also the sample with the lowest total As content at 48 ppm.

The organic-rich samples with low As content (< 75 ppm) are the only samples that contain a significant percentage (51%, 31% and 20% for 29059, 29068 and 29075 respectively) of the As in the more environmentally available fraction (Group 1). However, the playground sand sample (29066) does contain 17% of the As in this more available fraction. The elevated total As content of this sample (287 ppm) and the fact that it is from a playground makes this an important observation. For this sample, the As concentration reported for the more available fraction (Group 1) is 48 ppm with more than half (25 ppm) in the weakly bound (adsorbed/exchangeable) fraction.

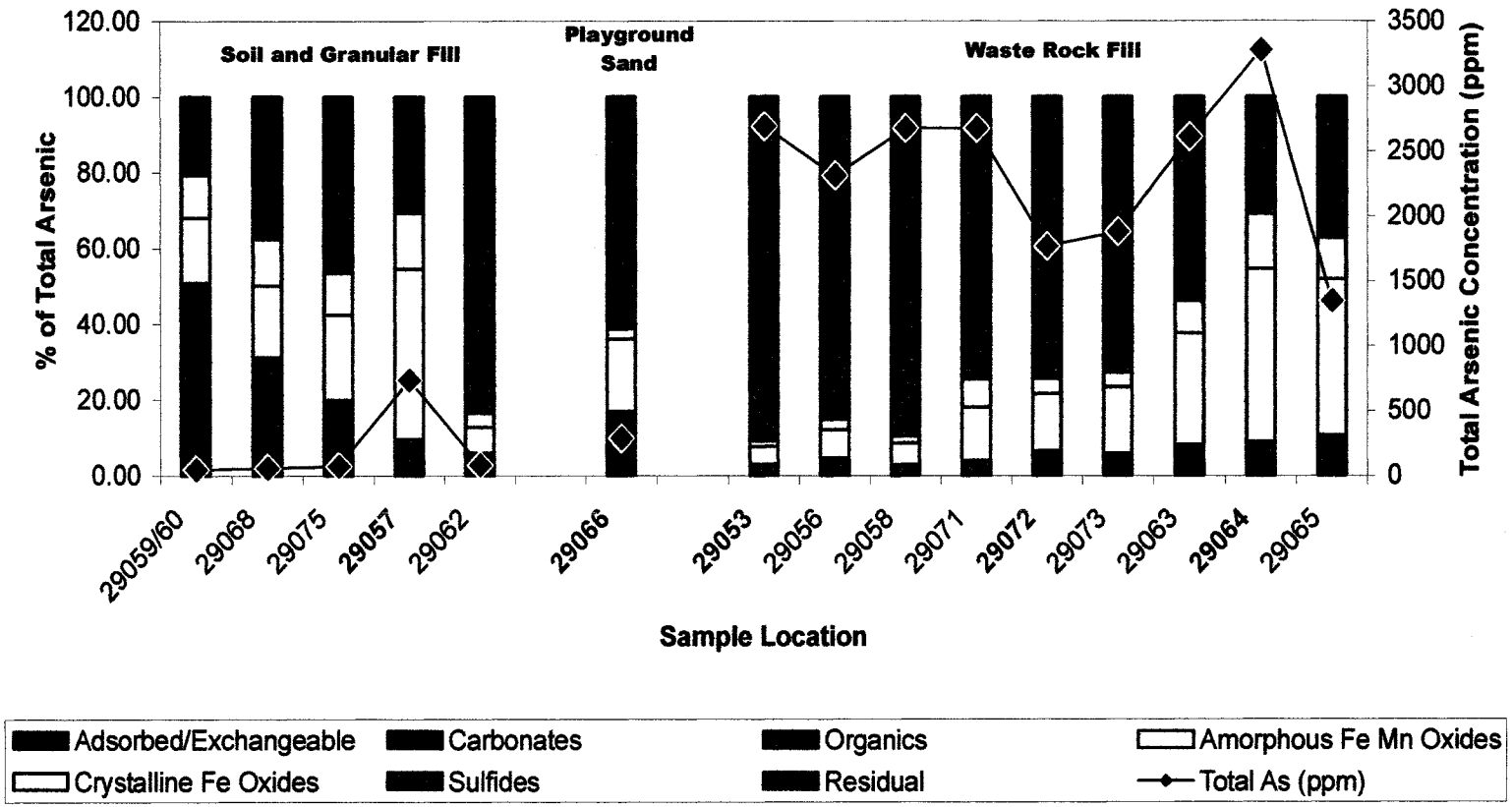

Figure 4-3 Arsenic Content in Sequential Selective Extraction Fractions (Townsite).

Sequential selective extraction results showing the percentage of arsenic associated with each extracted phase. The results are grouped by sample type and arsenic content (ie. low arsenic soil and granular fill materials on the left, and high arsenic crushed rock fill on the right). Results for a sample of playground sand are highlighted in the center. Lower arsenic content samples were analyzed using a 7 step extraction process that included a leach specific for organic material. The extraction completed on the waste rock fill materials was identical except it did not include the organic fraction since little or no organic material was expected in the waste rock fill. Samples numbered in red were further inspected by petrographic microscope.

Table 4-1 As Sequential Selective Extraction Results (Townsite)

Description	Sample Identification	Sieved Sample (< 0.18mm)									Unsieved
		Step 1 Adsorbed Exchangeable As (ppm)	Step 2 Carbonate As (ppm)	Step 3 Organic As (ppm)	Step 4 Amorphous Fe-Mn Ox As (ppm)	Step 5 Crystalline Fe Ox As (ppm)	Step 6 Sulfide As (ppm)	Step 7 Residual As (ppm)	SSE Total (Sieved) As (ppm)	NAA Total (Sieved) As (ppm)	NAA Total (Unseived) As (ppm)
Soil and Granular Fill	29059/60	11	2.6	11	8.2	5.5	4.9	5	48	52	70
	29068	7.3	3.5	7.6	11	7.3	17	5	59	32	32
	29075	4.8	0.7	9.0	16	8.1	29	5	73	68	43
	29057#	4.7	34	31	331	109	216	10	736	784	366
	29062	2.6	0.5	1.8	5.5	3.1	58	10	82	68	37
Playground Sand	29066	25	8.8	15	55	7.8	166	10	287	272	145
Crushed Rock Fill	29053	18	61	N/A	124	41	2350	95	2690	2897	1800
	29056	22	84	N/A	170	64	1895	75	2310	1997	1204
	29058	11	65	N/A	153	52	2300	95	2675	2498	1850
	29071	17	87	N/A	375	201	1925	70	2675	2650	845
	29072	23	91	N/A	266	71	1260	55	1766	1605	471
	29073	20	88	N/A	329	72	1320	50	1879	1760	861
	29063	35	177	N/A	766	227	1350	55	2610	2630	1500
	29064	52	238	N/A	1500	476	966	45	3277	3705	1490
	29065	32	111	N/A	555	147	482	20	1347	1345	544
Replicate and Duplicate Analyses	29057# *	4.7	34	31	331	109	216	10	736	N/A	N/A
	29057# *	4.7	31	N/A	333	137	205	5	716	N/A	N/A
	29059	10.1	2.6	9.6	7.7	5.6	4.4	5	45	N/A	N/A
	29060†	11.1	2.6	12.8	8.7	5.3	5.4	<5	46	N/A	N/A
	29063*	38	162	126	614	280	1340	55	2615	N/A	N/A
	29063*	35	177	N/A	766	227	1350	55	2610	N/A	N/A
	29080‡	36	169	N/A	996**	226	1370	55	2853	N/A	N/A

Organic-rich soil veneer from rock crevice. * Split Sample (Chemex) run in parallel through both 7 step and 6 step extraction schemes. † Blind duplicate sample of 29059 (Split in the Field). ‡ Blind duplicate sample of 29063 (Split at RMC Lab). ** All other analytes in this aliquot also show similar (5% to 30 %) increase in comparison to 29063.
N/A = not analysed. SSE = sequential selecteive extraction. NAA=neutron activation analysis.

Other potentially significant observations when considering As concentration (instead of the proportion representation within each sample) include up to 52 ppm and 238 ppm As in the Adsorbed/Exchangeable fraction (Step 1) and carbonate fraction (Step 2) respectively for the crushed rock fill materials.

Overall, the low As content samples have a high percentage of As in potentially environmentally available extractions (Group 1), while the crushed rock fill materials have a high percentage of As in the potentially less available extractions (Group 3). Several samples including 29057 (rock crevice sample) and 29064 (crushed rock lake-fill) have the highest percentage in the Fe oxide fraction (Group 2). However, the As content of the crushed rock fill samples in the weakest extractions (Group 1) are generally more than an order of magnitude greater than the corresponding extractions for the low As content samples. This feature is further highlighted by the fact that the As content of the crushed rock fill samples in the carbonate extraction (61 to 238 ppm) alone is often greater than the total As of low As content samples (48 to 82 ppm). This is important since the carbonate extraction is essentially a weak acid extraction suggesting this As is readily available. Significant concentrations of As are present in the Fe oxide fractions of the crushed rock fill samples (range of 124 to 1500 ppm for the amorphous Fe oxide fraction (Step 4) and 41 to 476 ppm for the crystalline Fe oxide fraction (Step 5)). The typical total Fe oxide extractable fraction (Group 2) is in the order of 500 ppm.

4.6.3 Powder X-ray Diffraction (XRD) Analyses

Results of the XRD analyses have identified the major mineral phases present in the crushed rock fill samples consistent with known mineralogy of local geological units. As expected, the minor mineral phases responsible for the elevated As in the samples were not detected by XRD. The major mineral components include quartz, chlorite, and muscovite. Calcite is also identified in all crushed rock fill samples although it appears as weaker and fewer peaks, suggesting lower

relative abundance in samples 29065 and 29071. Plagioclase is also always present, but can be either an abundant or apparently minor phase. Quartz and lesser amounts of plagioclase dominate the sample of playground sand. The organic soils exhibit similar apparent mineralogy characterized by the presence of quartz, chlorite, muscovite and plagioclase. However, the patterns are considerably weaker and exhibit lower peak heights in contrast to the crushed rock fill materials which originated from the nearby mine. Some or all of these materials may have been imported or influenced by imported material. Therefore, there may be some ambiguity in identification of phases just above background.

4.6.4 Petrography

Petrographic work concentrated on mineral identification of minor and trace phases that may contain As (As-bearing sulfides and their weathering products).

Assessment and discussion of the mineral phases of interest is made in the context of primary and secondary minerals (Jambor 1994). Primary minerals are those found in the host material (in this case presumably waste rock mined and crushed from past mine workings). Secondary minerals are those that have formed since placement of the fill material.

As expected, the playground sand exhibits a narrow grain size range dominated by sand-sized particles, while the crushed rock fill materials show a broad grain size variation which is predominantly silt-sized with some sand and trace clay. It is likely that the playground sand is imported sand mixed over the years with crushed rock fill from adjacent areas.

4.6.4.1 Arsenic-bearing Primary Phases

Microscopic identification methods confirmed the following As-bearing or potentially As-bearing primary phases in all sections examined.

- arsenopyrite (FeAsS)
- pyrite (FeS_2)

By far the greatest quantity of primary As on a single grain basis will be contained in arsenopyrite (46% w/w). However, some of the primary As may have been present in pyrite with a lower concentration per grain, but with greater volumetric representation in the fill material. Some of the pyrite at Giant is arsenical (up to a few percent As) (Armstrong 1997, Chryssoulis 1990). However, on the basis of mineralogical reports of arsenopyrite at sub-equal quantities to pyrite in the ore (Coleman 1957, Boyle 1960) and frequent observations of arsenopyrite in thin sections in this study, it should be expected that arsenopyrite is the main source of As in the crushed rock fill. Other potential primary As sources include solid solution in tetrahedrite-tennantite ($(Cu,Fe)_{12}Sb_4S_{13}$)-($(Cu,Fe)_{12}As_4S_{13}$)) and Pb-Sb sulfosalts. These relatively rare minerals are present in the ore, but may have much less significance in mine waste-rock (the crushed rock fill) which is usually derived from more barren "non-ore" sources. However, one large Sb-Pb sulfosalt was identified in thin-section 29053. Antimony and Pb concentrations will be an indicator of the magnitude of their potential presence. The total Sb concentration reported in the crushed rock fills (sum of SSE, Appendix F) range from 30 ppm (29071) to 130 ppm (29063). It should be noted that Sb and Pb may also be present as stibnite (Sb_2S_3) and galena (PbS). In addition to their potential association with As, both Pb and Sb are elements of environmental concern in their own right.

In addition to the As-bearing sulfides (arsenopyrite and pyrite), pyrrhotite ($Fe_{1-x}S$, $x<0.2$) was frequently observed in all sections examined (polished section of the organic-rich 29057 being an exception). Pyrrhotite is not common in the ore or mine tailings; however it is present in many of the rock units adjacent to the ore zone (Boyle 1979). While pyrrhotite is unlikely to contain As

itself, oxidation products of the pyrrhotite could be important in scavenging dissolved As from pore-water as identified in tailings at the Delnite Mine in Ontario (Alpers *et al.* 1994).

4.6.4.2 Weathering Products of Sulfide Minerals

The primary sulfide minerals are present as both free grains (apparent diameter in section typically between 10 and 100 um) and as fine (usually <10 um diameter) grains or grain assemblages included within larger silicate grains (Figure 4-4). The free grains are often present as a sulfide core with an oxidized reaction rim, while those included within silicates appear pristine (unweathered) presumably due to their effective isolation from pore fluids. No sulfides were specifically identified as being included within carbonates although this association seems probable as well. Free pyrite and arsenopyrite grains with oxidized reaction rims are the dominant form observed in all thin sections. The reaction (or replacement) rims are evidence of weathering in situ.

In some cases, the arsenopyrite and pyrite appear as free unrimmed grains (Figure 4-4). This suggests that weathering in the crushed rock fill has been slower to initiate in some sulfides or that there has been a graduated physical release of free sulfides in the material over time. It may be that fresh material has been periodically added for regrading, or that fresh sulfides are periodically liberated from larger lithic fragments over time (freeze-thaw or mechanical breakdown by grading equipment and vehicular traffic).

Like pyrite and arsenopyrite, pyrrhotite exhibits weathering characteristics. In contrast to the rimmed appearance of the weathered pyrite and arsenopyrite, pyrrhotite commonly exhibits a characteristic banded weathering texture (Figure 4-4 and 4-5) (Jamieson *et al.* 1995, Alpers *et al.* 1994). Unique weathering characteristics are also observed in a few pyrite and arsenopyrite grains where weathered rims cut through grains along fractures.

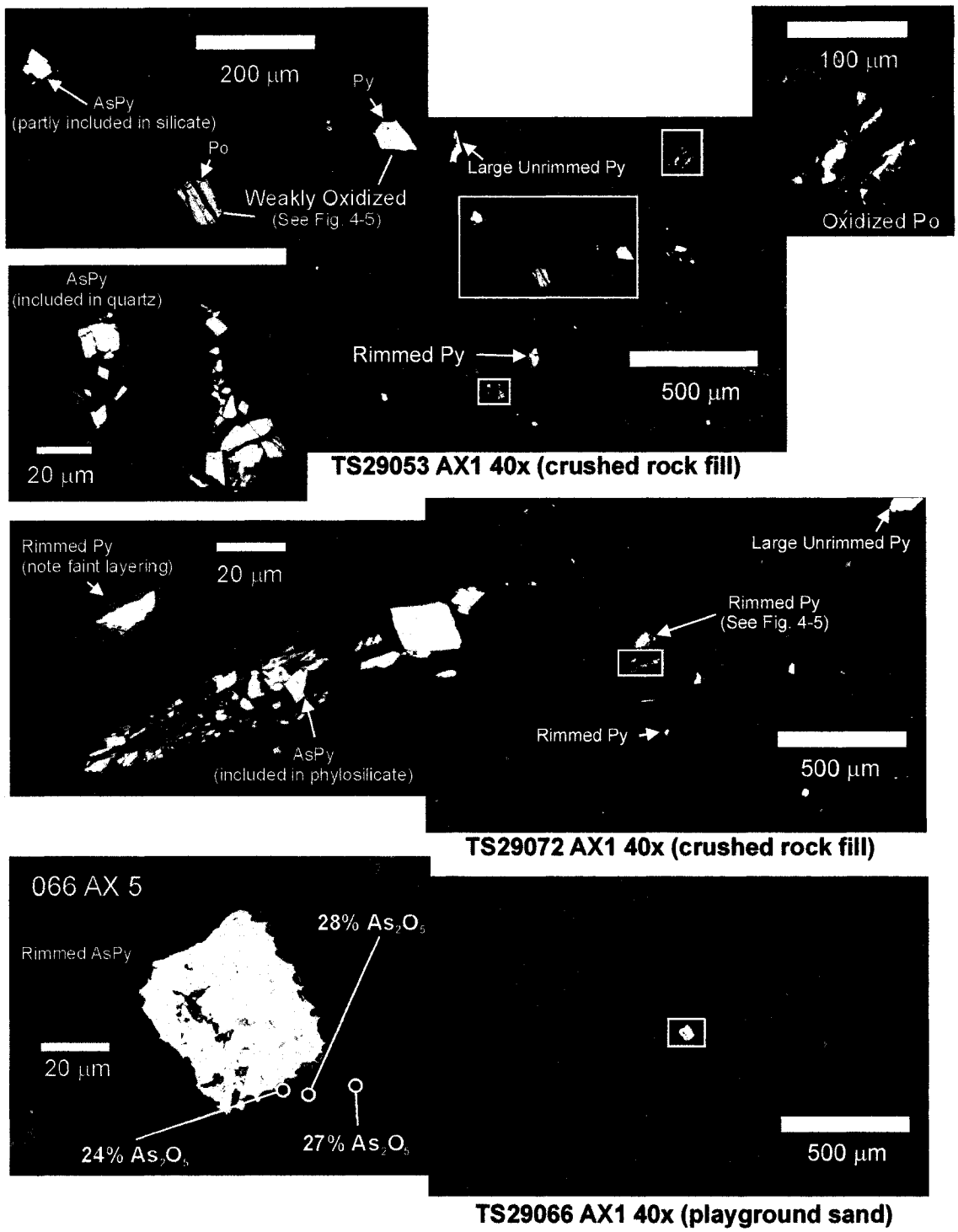

Figure 4-4 Sulfides in Crushed Rock Fill and Playground Sand at Townsite.

Reflected light photos of typical views of thin sections at low magnification (large images on the right). Selected sulfides (Aspy, Py and Po) are identified and some areas expanded at higher magnification to show detail. EPMA results are indicated for an Fe oxide weathering rim on Aspy in playground sand.

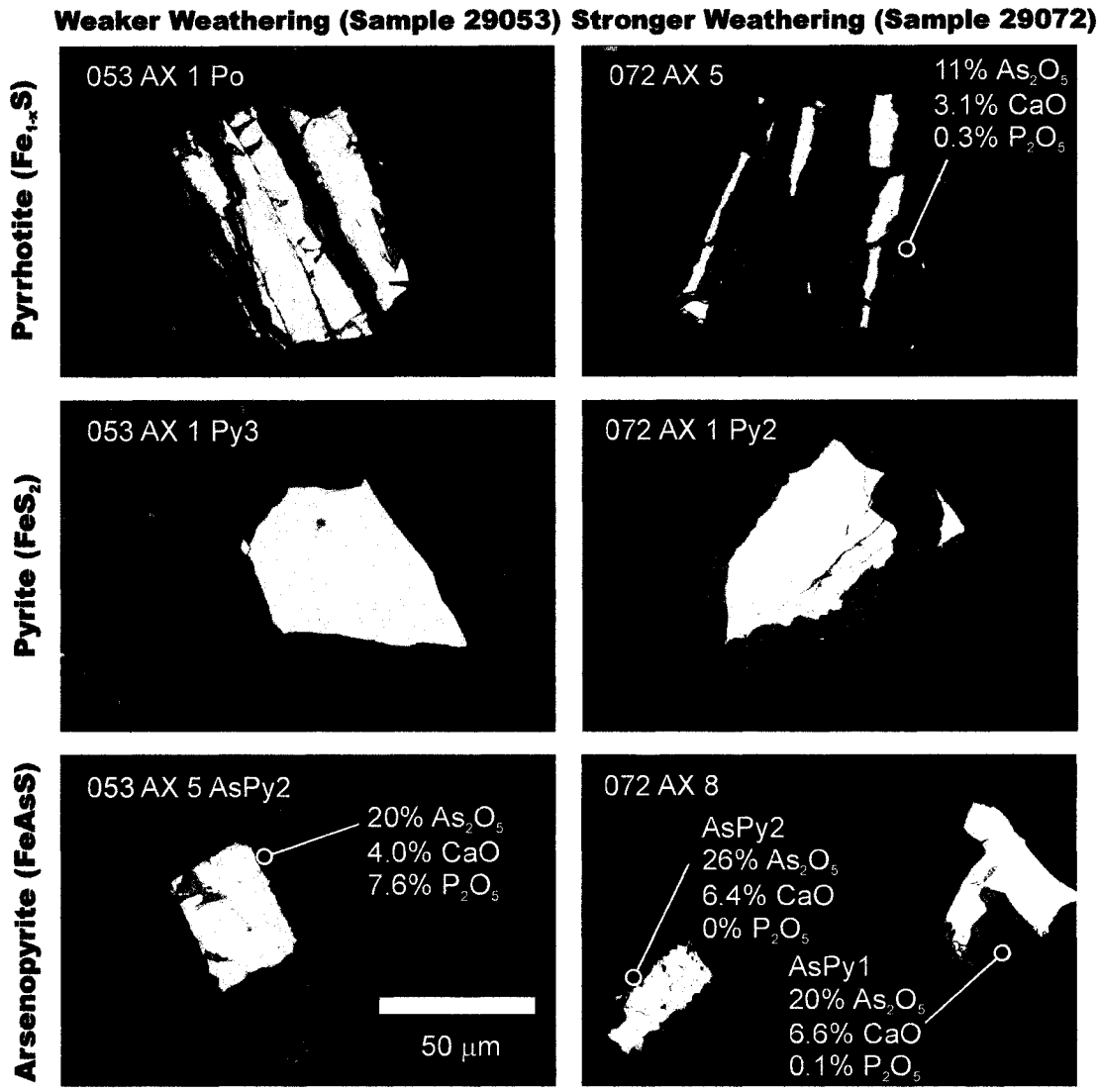

Figure 4-5 Variation in the Degree of Sulfide Weathering.

Reflected light photos of oxidized rims (grey) replacing sulfides (white). The rim thickness is a measure of the degree of weathering (oxidation). Photos on the left represent typical rims observed in sample TS29053 and those on the right typical of TS29072. Examples of each of the principal sulfides is represented for each section with Po at the top, Py in the middle and Aspy at the bottom. There is a range of apparent oxidation within each sample ranging from unrimmed grains to more deeply oxidized ones and Po always exhibits the greatest evidence of oxidation. EPMA data for As, Ca and P is shown where available. Note brownish internal reflections in rim on pyrite (middle left hand photo, TS29053 AX1 Py3) and arsenopyrite (lower right hand photo, 29072Ax8AsPy1). All photos are the same scale.

In general, pyrite is the most abundant weathered sulfide, followed by arsenopyrite and then pyrrhotite. In total, sulfides make up only a small fraction of each thin section (1 to 3 % for the crushed rock fill, and much less for the playground sand and rock crevice sample). In a given thin section pyrrhotite is always the most weathered sulfide with pyrite and arsenopyrite showing little difference in the degree of weathering. This is consistent with relative sulfide reactivities observed by others (Jambor 1994; Jamieson *et al.* 1995).

4.6.4.3 Detailed Description of Thin Sections

As noted above, the overall sulfide content is low in all thin sections (<3%), however when compared to each other, 29053 appears to contain greater sulfide abundance than 29064 and 29072 (Figure 4-4). Sections 29057 and 29066 contain much lower sulfide content. The apparent degree of weathering (based on observed rim thickness) is noticeably less in sample 29053 (Figure 4-5). The other two samples of crushed rock fill (29064 at the proposed boat launch area and 29072 from parking lot at the Cruising Club) show more extensive weathering. The rock-crevice sample (29057) and playground sand (29066) also shows significant weathering of sulfides though the sulfides are in low abundance and in the case of 29057 generally < 40 μm in diameter.

In short, the overall sulfide content by visual estimation qualitatively correlates to relative As content in the SSE sulfide fraction for As-rich samples 29053, 29064 and 29072. When the degree of oxidation is considered, SSE results (i.e. total As content, sulfide fraction (Step 6) and Fe oxide fractions (Group 2)) can be visually reconciled to observations of the principal As-bearing phases (Fe oxyhydroxides and sulfides) observed in these sections (Figure 4-3, 4-4 and 4-5).

Another characteristic difference between the less weathered sample (29053) and more weathered samples (29064 and 29072) is the presence of more fine (1 to 10 um diameter) Fe oxide/oxyhydroxide grains in the latter. Based on optical observation and EPMA analysis (Section 4.5.5 below) these small oxide grains appear to be fine weathered sulfides similar to the rims of the larger oxidized sulfide grains. If they contain similar As concentrations to other Fe oxide weathering product and they are present in sufficient abundance these will add to the As extracted in the Fe oxide fraction (Step 4 and possibly Step 5).

Inspection of a polished section of the organic-rich rock crevice sample (29057) revealed small weathered sulfide grains, unweathered sulfides and a few small grains resembling fine roaster Fe oxides (Figure 4-6). Cellular structured reflective coatings may point to the presence of precipitates on organic material, but it is not known if these are As-bearing. Other As-bearing phases may exist but were not observed due to the fine grain size and dark, obscuring organic

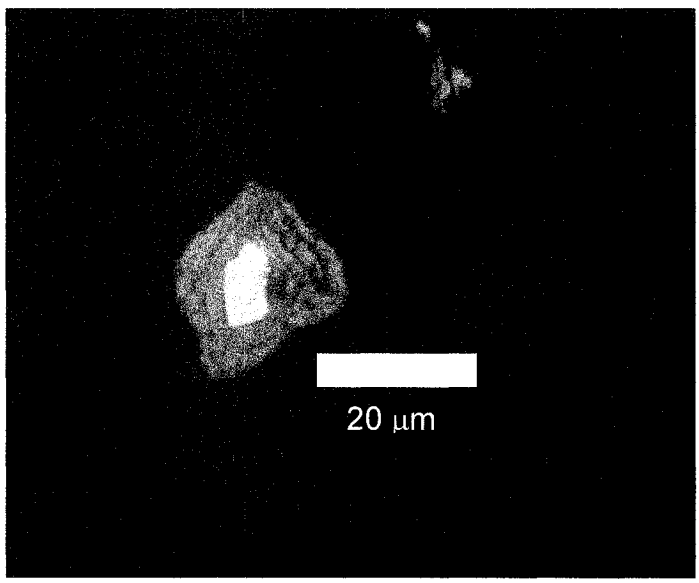

Figure 4-6. Possible Roaster Fe Oxide From Rock Crevice Sample (TS29057)

component. The observation of possible roaster Fe oxides is intriguing and suggests the potential presence of a relatively recalcitrant As phase in some soils proximal to the Giant roaster.

4.6.5 EPMA Results

EPMA of targeted Fe oxyhydroxides within the three selected thin sections (29053, 29066 and 29072) has confirmed As concentrations from trace to almost 30 % As_2O_5 (w/w). The highest As concentrations (20.1 to 29.3 % As_2O_5) are found in rims adjacent to arsenopyrite (Table 4-2).

Arsenic concentrations in oxidized rims of pyrite and pyrrhotite are lower and range from <0.5 to 10.9% As_2O_5). Considering that pyrite contains much less As than the surrounding Fe oxyhydroxide rims and pyrrhotite may contain no As at all, the Fe oxyhydroxides must be scavenging As from the surrounding environment as previously reported by Alpers *et al.* (1994).

Due to the apparent layered and radial nature of the weathering rims on pyrite and arsenopyrite, profiling of the As concentration across several of the rims in section 29066 was attempted. Totals decrease near grain edges, which may indicate a partly heterogeneous analytical volume and lower quality results. However, while both Fe and As decrease toward the edge on the As-rich oxyhydroxide rim on arsenopyrite (29066 AX5, Table 4-2), similar decreases in Fe and totals for two rims on pyrite are accompanied by doubling of the As concentrations (29066 AX1 and 29066 AX3, Table 4-2). This suggests that not only is the source of As external to the pyrite and pyrrhotite grains, but that there is a concentration gradient within the layered oxyhydroxide rims on pyrite. The source of the As in these rims is presently unknown since aerially dispersed As inputs over time have not been reconciled with the age of weathered sulfides in the playground sand, and with the timing and loading of As derived from weathering within the crushed rock fill itself. Regardless of the reason for increased As on outer rims, its presence has implications from

Table 4-2 Townsite EPMA Data

Sulfide*	Thin Section	File No.	Description	Fe_2O_3	As_2O_5	CaO	P_2O_5	SO_3	MnO	Al_2O_3	SiO_2	Total
Arsenopyrite	29053	259	AX3	50.1	25.1	3.21	3.32	0.93	0.28	0	3.1	86.1
		260	AX5 Aspy2	41.1	20.1	4.05	7.63	0.63	0.14	1.29	3.42	78.4
		261	AX6	45.7	23.1	4.34	7.88	0.8	0.12	0.24	2.86	85.1
	29066	276	AX4	44.5	29.3	5.62	0	0.56	0	0.17	1.28	81.4
		277	AX5 Edge	40.8	26.9	6.70	0	0.22	0	0.51	1.15	76.3
		279	AX5 Mid	48.7	28.3	6.69	0	0.31	0	0.47	1.37	85.9
		278	AX5 Adjacent to Sulfide	48.7	24.4	6.18	0	0.42	0	0	1.29	81.0
	29072	287	AX8 Aspy1	53.9	20.1	5.61	0.14	0.25	0	0.45	5.48	86.0
		288	AX8 Aspy2	44.8	25.9	6.37	0.86	1.12	0	0.3	3.05	82.4
Pyrite	29053	252	AX1 wPy	79.7	1.37	1.52	1.45	2.4	0.16	0.52	3.41	90.5
	29066	269	AX1 Edge	79.6	1.63	2.27	0	1.04	0.26	0.46	3.46	88.7
		268	AX1 Mid	83.6	0.76	2.53	0.1	1.47	0.2	0.59	2.34	91.6
		271	AX3 Edge	71.7	6.55	2.66	0	0.97	0	0.65	2.7	85.2
		270	AX3 Mid	80.6	2.85	2.10	0	0.75	0.15	0.74	3.1	90.3
		272	AX3 Mid	78.8	2.47	2.26	0	0.72	0.11	0.75	3.25	88.3
		275	AX4	78.0	5.21	2.46	0.37	0.57	0	1.26	3.11	91.0
		280	AX7 Small Fe Ox.**	76.2	5.29	3.58	0.27	0.42	0.1	0.74	5.92	92.5
	29072	283	AX1 Py1	72.0	3.51	2.22	0.22	2.3	0	0.69	3.17	84.1
		284	AX3 Small Fe Ox**	68.3	0.89	2.04	0.1	0.83	0.16	0.54	5.7	78.6
Pyrrhotite	29053	251	AX1	62.9	2.20	1.39	4.96	10.3	0.11	0.48	2.14	84.5
		263	AX6 Po	60.9	4.91	1.96	6.82	7.42	0	0.48	3.93	86.5
		264	AX6 Po2	70.1	1.94	1.53	5.14	8.51	0.19	0.69	3.41	91.5
	29072	286	AX5	69.4	10.9	3.12	0.32	3.48	0.24	0.38	2.32	90.2

* Associated weathering sulfide. ** Small Fe oxyhydroxide without associated sulfide. Elemental composition most similar to pyrite associated Fe oxyhydroxides.

a bioavailability perspective, since it places higher As concentrations at the most accessible portion of the grains. The concentrations are still likely to be lower than those observed on weathered arsenopyrite grains. Similar processes may be at work within the pyrrhotite grains, however a comparable profiling has not been attempted for them.

In addition to As, a number of other elements have been detected in these oxidized rims. Calcium and Si are detected in all rims analysed at several wt. %, while S and Al are detected in most analyses at variable, but generally low concentrations (< 1 wt.%). Fe oxyhydroxides on pyrrhotite are the exception for S where concentrations of 3.5 to 10.3 % SO_3 (w/w) have been determined. Some of the pyrrhotite grains show fine relic pyrrhotite disseminated through the oxidized rim so it is possible that the elevated S is a result of very fine remnant sulfide not discerned in the backscatter electron image at the time of analysis. The relatively consistent totals with other iron-oxyhydroxide analyses however, suggest this may indicate significant sulfate in the oxyhydroxide weathering products of pyrrhotite unique to weathered pyrrhotite. Phosphorus is present at low to undetected concentrations in analyses from 29066 and 29072, but at much higher concentrations (up to 7.9 % w/w P_2O_5) in sample 29053. The source of P at 29053 is not known at this time, but further discussion and potential implications of P are provided below.

Probing of two small (10 μm diameter or so) Fe oxyhydroxide grains has confirmed similar chemical makeup to the larger oxyhydroxide rims on the sulfide grains. Of the two analyses, one had an elevated As concentration (5.3 % As_2O_5), while the second had less As (0.9 % As_2O_5). The two analyses of these small grains most resemble analyses of Fe oxyhydroxide rims on pyrite.

A single Pb-Sb (minor Fe) mineral was also identified and confirmed by qualitative EPMA. The mineral shows a weathering rim similar to sulfides and like pyrrhotite incorporates As in the rim (Figure 4-7a,b). However, this weathering rim contains Pb, S, Sb, As^{V} (Figure 4-7b,c) and Fe presumably in an oxidized form.

4.6.6 μXANES and μXRD

Micro-XANES was successful at confirming the presence of only As^{V} on several pyrite and pyrrhotite weathering rims (eg. Figure 4-8a,b). Rims on arsenopyrite were not thick enough to avoid self-absorption and overlap with the As^{-I} peak. Micro-XRD was successful at determining the presence of goethite as the Fe oxyhydroxide weathering product on pyrrhotite (Figure 4-8c). Attempts at identification of weathering rims on pyrite and arsenopyrite by μXRD were unsuccessful. Clay peaks interfered in all attempts.

4.7 Discussion

4.7.1 Arsenic and chemistry of sulfide weathering

Arsenic may have been coprecipitated with Fe(III) oxyhydroxides in the final stage of sulfide oxidation (As content derived from localized As concentrations at time of Fe oxyhydroxide formation) or it may be adsorbed from solution at a later time. It is likely that both mechanisms play a role in the Giant crushed rock fill. It has been shown in numerous studies that the coordination with Fe is primarily as a tightly bound bidentate binuclear inner sphere complex regardless of whether it is coprecipitated or adsorbed (Waychunas *et al.* 1993, Paktunc *et al.* 2004). However, some monodentate coordination may be favoured at higher surface coverage. The arsenopyrite appears to be the As source for the weathering rims on those grains. Even though weathering of the arsenopyrite occurs via the same basic oxidation mechanism as the other sulfides, As availability is much greater for reaction with the freshly-forming oxide rim

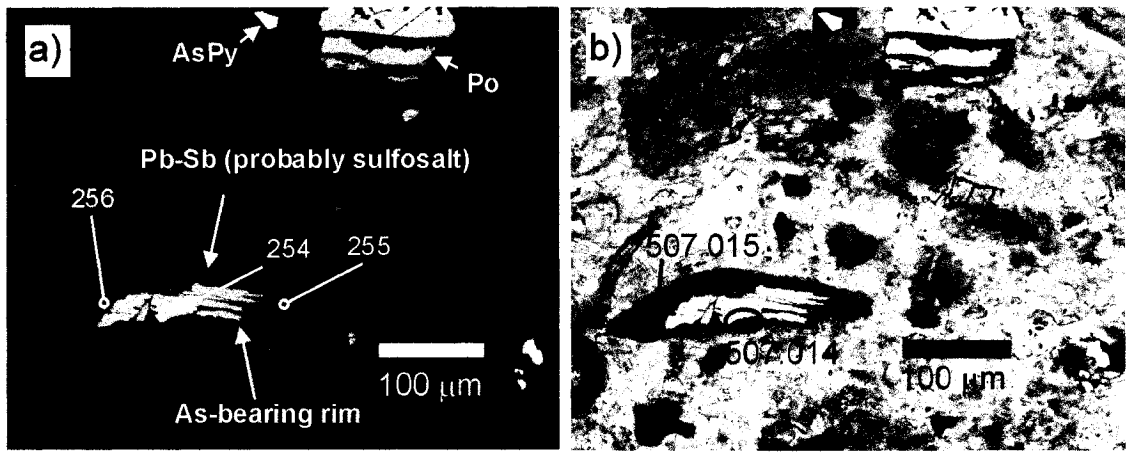

TS29053 Ax2

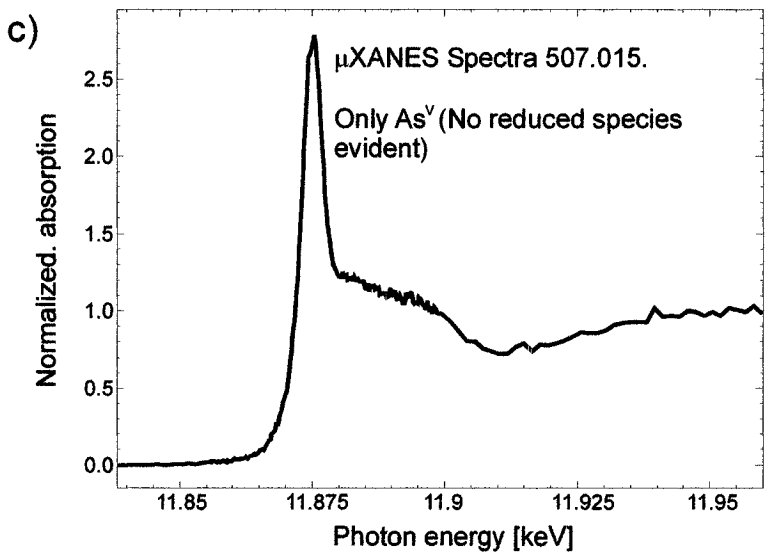

Figure 4-7 Weathered Pb-Sb mineral.

Photographs of Pb-Sb mineral and other sulfides in crushed rock fill (TS29053). a) reflected light photo showing bright grey Pb-Sb sulfosalt with low reflectivity weathering rim. Rim appears to be As-bearing, but sulfosalt is not. Numbered points are locations of qualitative EPMA. Pb, Sb, S and minor Fe were identified at spot 254. Pb, Sb, S, As and Fe were identified at spots 255 and 256. b) Transmitted and reflected light photo of the same region as a). Numbered spots are locations of μXANES analyses. c) μXANES of spot 507_15 in b). As edge position matches As^{V}. Linear combination fits with standard spectra show no improvement by including reduced species (As^{III} and As^{-I}).

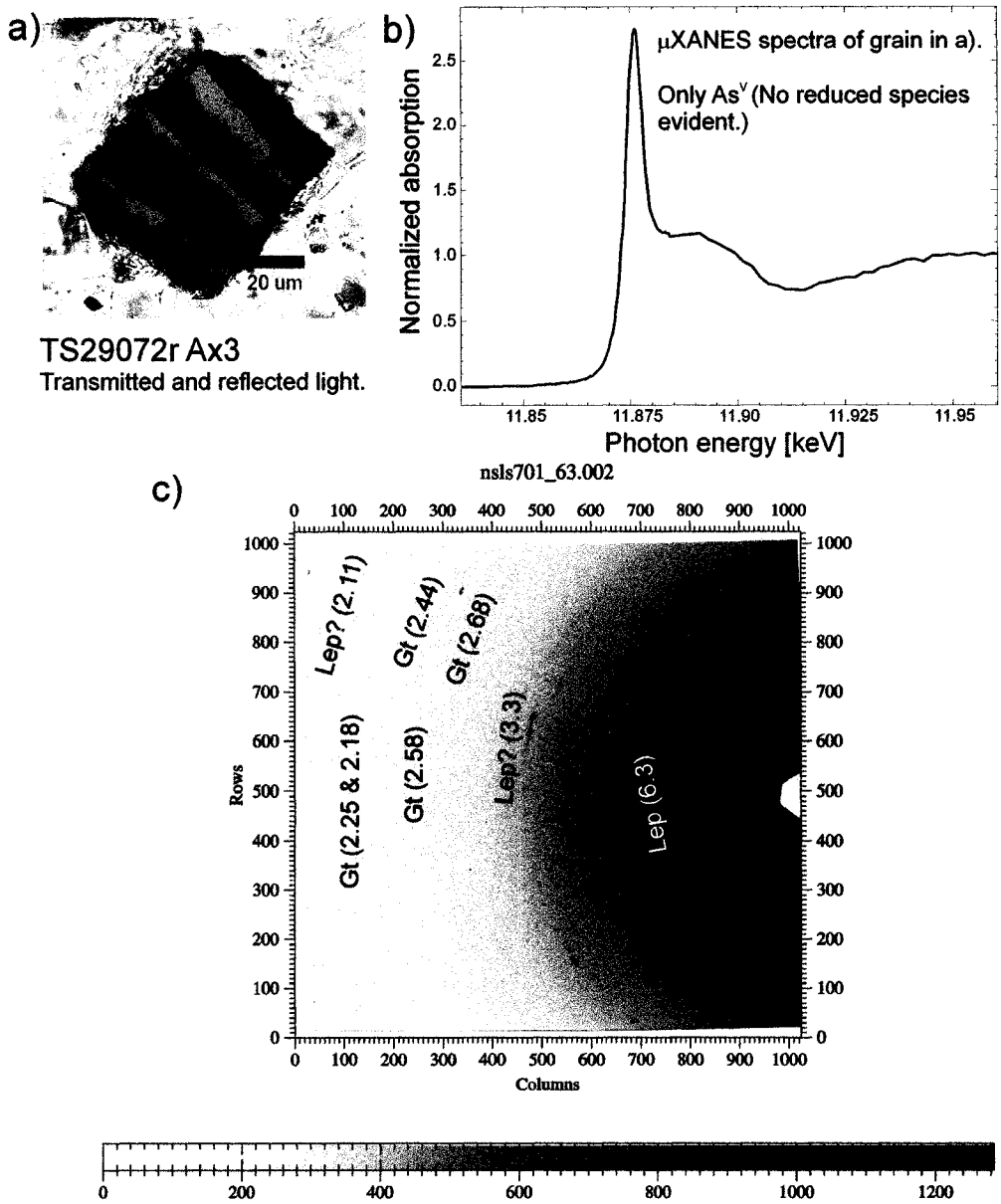

Figure 4-8 μXANES and μXRD of Fe oxyhydroxide on pyrrhotite in crushed rock fill.

a) Photograph of weathered pyrrhotite grain from crushed rock fill TS29072r. XANES spectrum of grain in a) showing no evidence of reduced As, only AsV. This is consistent with As adsorbed or coprecipitated with iron oxyhydroxide weathering product and confirms that there is no As associated with the pyrrhotite as expected. c) XRD pattern of grain in a) showing weak diffraction pattern of goethite (Gt) and lepidocrocite (Lep). Values indicated are d-spacings in angstroms. The very weak Gt ring at 2.58 Å is observed in the original data, but is too weak to be viewed in the Figure. Gt is very fine to nano-crystalline, while lepidocrocite shows preferred orientation and may be coarser crystallites. Given the preferred orientation and limited number of peaks definitive identification of Lep is not possible. The relatively bright point reflections at approximately 3.3 Å may be discrete Lep crystallites or more likely small quartz or muscovite crystallites.

leading to coprecipitation and fairly low Fe/As molar ratios (2 to 3). The rims on pyrite and pyrrhotite have Fe/As molar ratios >9.

Thus, on the Fe_2O_3 vs. As_2O_5 plot (Figure 4-9), Fe oxyhydroxides and the Ca-As rich Fe-rims from the Giant townsite samples plot in two distinct regions. Those associated with pyrite and pyrrhotite plot below the Fe/As molar ratio of 9. Those associated with arsenopyrite plot midway between Fe/As molar ratios of 4 and 1.5. The analyses seem to follow a trend from goethite and ferrihydrite toward the Fe and Fe-Ca arsenates. This is consistent with data of Paktunc *et al.* 2004 and Corriveau (2006) that show a similar trend.

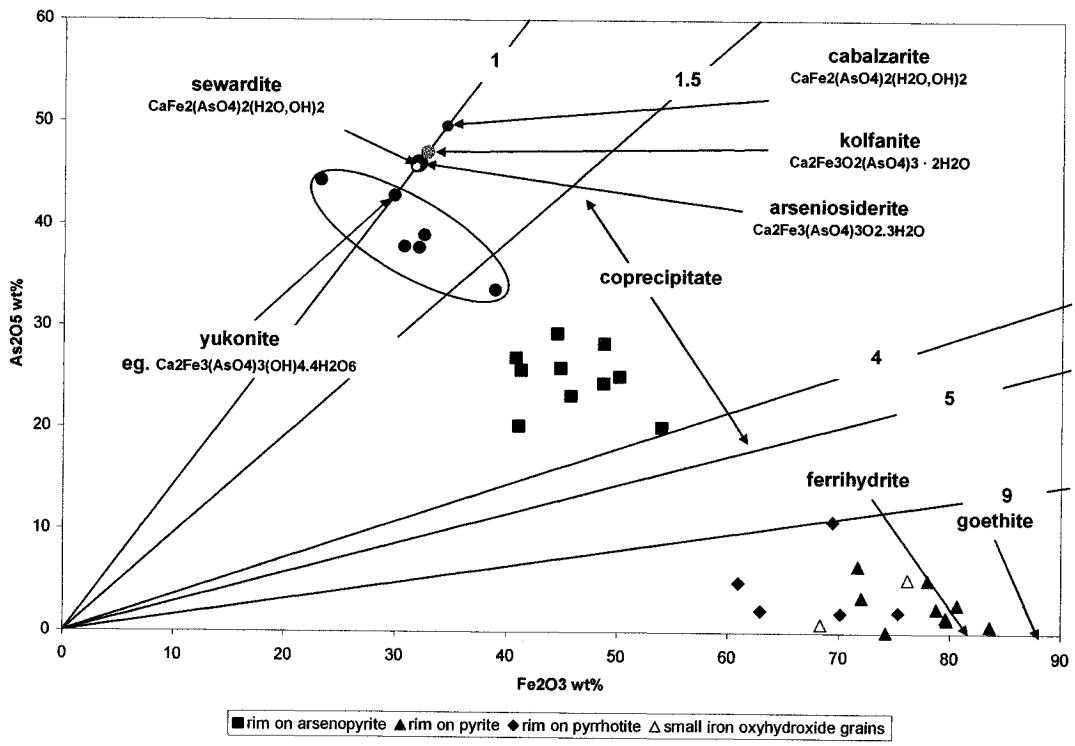

Figure 4-9 Plot of Fe_2O_3 vs. As_2O_5 for EPMA data. Diagonal lines with values are Fe/As ratios. (After Paktunc *et al.* 2004)

On the CaO vs. Fe_2O_3 plot (Figure 4-10), the analyses again are distributed in two distinct regions. Oxidized rims on arsenopyrite are once again distinct (based on the high As_2O_5) from those of pyrite and pyrrhotite. The Fe-Ca rims on arsenopyrite would appear to be trending toward yukonite or perhaps an iron-rich end member of a rare mineral, cabalzarite. It should be noted that there is no trend toward cabalzarite in the preceding plot of Fe_2O_3 vs. As_2O_5 (Figure 4-9). The trend toward yukonite is similar to that of Corriveau (2006). However, the data of Paktunc (2004) suggests a trend toward the more Ca, Fe and As rich arseniosiderite.

For the high Fe/As phases (pyrite and pyrrhotite associated) this data appears similar to Corriveau (2006), but different from Paktunc (2004). All Ca/As molar ratios are above 0.67 whereas in Paktunc's case they were all approaching but not exceeding 0.67. This could suggest greater

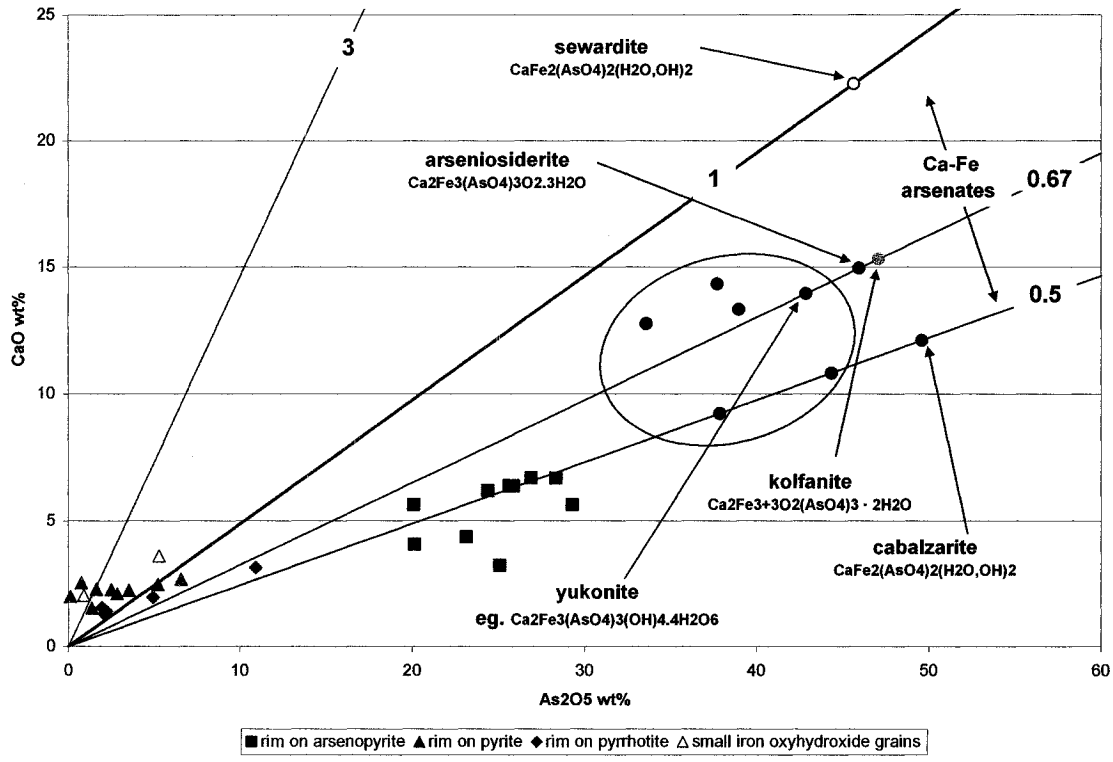

Figure 4-10 Plot of CaO vs. As_2O_5 for EPMA data. Diagonal lines are molar Ca/As ratios. (After Paktunc *et al.* 2004)

sorption or precipitation of Ca in our system, (Kasama & Murakami 2001). It might be expected that the Giant Townsite crushed rock fill and the Nova Scotia tailings studied by Corriveau (2006) would show more similarity than the Ketza River site of Paktunc (2004) which is an orebody that has weathered in-situ. However, site specific conditions are probably unique at all three sites.

According to Krause & Ettel (1989), Ca-Fe arsenates and Fe arsenate precipitates with Fe/As molar ratios less than 4 are more soluble than their higher Fe-As molar ratio counterparts. This would suggest that the Ca-As rich rims on arsenopyrite are less stable than the Fe oxyhydroxides that have Fe/As molar ratios greater than 9. However, the significant amount of calcium in the Fe oxyhydroxides may or may not be a factor in the stability of As in these phases.

4.7.2 Mineralogical Interpretation of Sequential Selective Extraction Results

The results discussed above show the presence of three distinct As-bearing phases that are readily interpreted in the context of the SSE results. The three phases are: 1) oxidized sulfides, 2) free grains of arsenopyrite and pyrite and 3) silicate-locked arsenopyrite and pyrite.

We expect the oxidized sulfides are intimately associated with the As liberated by the two Fe oxide extraction procedures (amorphous and crystalline). However, the significance of the amorphous vs. crystalline fractions remains poorly understood in the context of the mineral form of the two or more Fe oxide replacement phases present. We expect that the free grains of pyrite and arsenopyrite are interpreted to be directly associated with the sulfide extraction procedure.

The best evidence to confirm the effectiveness of the SSE for the selectivity of As in the Fe oxide and sulfide extractions is observed in the specific weathering characteristics of two of the thin sections scrutinized closely, namely 29053 and 29064. Sample 29053, which exhibits the least

amount of weathering observed petrographically (proportion of sulfide to Fe oxyhydroxide is greatest), also has very little Fe oxide bound As and mostly sulfide bound As in the SSE results (7% in oxides vs. 87% in sulfides). In contrast, sample 29064, which contains visual evidence of more extensive weathering (increased ratio of Fe oxyhydroxide(s) to sulfides), has a much greater proportion of Fe oxide bound As than sulfide bound As in the SSE results (60% in oxides vs. 30% in sulfides).

In the case of the silicate-locked arsenopyrite and pyrite phases, only some, if any, of the As would be available to the aqua-regia (sulfide) extraction procedure. This suggests that the remainder of the sulfide As would show up in the tri-acid leach when the silicates are actually broken down. Therefore, the As concentration in the tri-acid leach should give some indication of the amount of sulfide-bound As unavailable to weathering due to the presence of resistant silicates. Since there is a possibility of As loss due to volatilization in the tri-acid leach these concentrations should be interpreted as minimums. However, we note that the total As concentrations as determined by NAA agree very well with the SSE totals suggesting little loss in the tri-acid leach (see Section 4.6.1).

The reason for the variation in the extent of weathering may be a physical one where the ages of the materials have varied. Regrading would add fresh material in some areas, but not others. Alternatively, the reason could be chemical where moisture contents in certain areas are more favourable for weathering than in other dryer or very wet regions.

One potentially important aspect of the mineralogy and SSE data that has yet to be adequately explained is the source of exchangeable and carbonate-extractable As. Even though the sum of these two extractable amounts constitute only a small percentage of the total As extracted

(maximum of 290 ppm out of 3280 ppm for sample 29064), these fractions are potentially the most important from an environmental impact and human health point of view. It is possible that these fractions are related to small quantities of an as yet unidentified soluble phase or phases containing As. Alternatively, these fractions may be related to weak sorption processes, which may or may not involve the complex Fe oxyhydroxides and Ca-Fe arsenate-like phases.

4.7.2.1 Phosphorus relationship to Fe oxyhydroxides based on the SSE analyses

Phosphorus has been identified at elevated concentrations in all Fe oxyhydroxide weathering rims for sample 29053. The SSE data (Appendix F) was evaluated to determine how wide-spread P may be and what relationship(s) may exist with the Fe oxyhydroxide weathering rims. Only sample 29053 contains detectable phosphorus (40 ppm) in the exchangeable fraction (Step 1) of the SSE (Table 4-3). The other eight samples of crushed rock fill report < 5ppm. Only samples 29053 and 29071 contain P in the carbonate extraction (Step 2) at elevated concentrations (180 and 195 ppm respectively compared to 50 ppm or less for the remaining samples). Both of these samples contain total P at over twice the concentration of the other crushed rock fill samples. This may suggest that sample 29053 and possibly 29071 are unique with respect to phosphorus for the larger set of samples analyzed by SSE. However, inspection of the P/As ratios in the SSE analyses for the Fe oxide extractable fractions shows a similar, but more systematic pattern.

Sample 29053 contains the highest P/As at 3.9 and 2.4 in the amorphous Fe and crystalline Fe extractions (Steps 4 & 5) respectively (Table 4-3). The next highest P/As ratios are observed for 29058 (2.5 and 1.5 for Steps 4 & 5 respectively), 29056 (1.8 and 1.4 respectively) and 29071 (1.2 and 0.6 respectively). All of these samples are from shallow roadway fill material in the Townsite and they all show the same trend with greater P/As in the amorphous Fe oxide fraction than the crystalline Fe oxide fraction. This suggests a unique association of P with the Fe

Table 4-3 Phosphorus in SSE Analyses

SAMPLE ID	Step 1	Step 2	Step 4			Step 5			Step 6	Step 7	Total
	P	P	P	As	P/As	P	As	P/As	P	No Data	
	ppm	ppm	ppm	ppm		ppm	ppm		ppm		ppm
29053	40	180	485	124	3.90	100	41.1	2.43	120	-	925
29056	<5	25	310	170	1.82	90	64.2	1.40	120	-	545
29058	<5	5	375	153	2.46	80	51.9	1.54	140	-	600
29063	<5	10	270	766	0.35	60	227	0.26	90	-	430
29064	<5	<5	225	1500	0.15	60	476	0.13	30	-	315
29065	<5	<5	205	555	0.37	70	147	0.48	40	-	315
29071	<5	195	465	375	1.24	125	201	0.62	130	-	915
29072	<5	<5	255	266	0.96	75	71.4	1.05	100	-	430
29073	<5	<5	330	329	1.00	70	71.8	0.98	80	-	480

oxyhydroxides in shallow crushed rock fill in the roadways. The P/As ratios for the only two samples of crushed rock fill from the Great Slave Cruising Club are comparable to the lowest observed for the Townsite roadway in the amorphous Fe oxide fraction (P/As = 1). However, the ratio in crystalline Fe oxide fractions is the same as the amorphous fraction (P/As =1) rather than being lower as observed in the Townsite roadway fills. The P/As ratios for the three lake-fill samples (29063, 29064 and 29065) is much lower at < 0.4 in both the amorphous and crystalline Fe oxide fractions. This is largely due to the greater As content in these fractions for these samples, but they also tend to contain relatively low P compared to the roadway fill materials. A representative number of grains have not been analysed by EPMA to properly compare P/As ratios observed at the grain scale with the operationally defined leaches.

The presence and behavior of P in the sample suite seems to show predictability even based on the relatively small sample suite. The source of the P and the reason for the apparent relationship to the Fe oxyhydroxides is not understood at this time. However, the presence of P has other potentially important implications with respect to As mobility since phosphate may compete with arsenate for sorption sites.

4.8 CONCLUSIONS

The following are the principal conclusions of the Townsite investigations. Conclusions are provided first for the effectiveness of key methods employed in this study and second for interpretations of the stability, mobility and potential bioavailability of As at the Townsite.

4.8.1 Effectiveness of Methods

- The SSE method appears to be quite selective for As and responds predictably to the As-bearing weathered sulfides present in the samples. However, the presence of dolomite and possibly Fe-dolomite produces interference with key major elements of interest (especially Ca and Fe) in the Fe oxide fractions.

  Understanding of the behavior of the Ca associated with the As-bearing Fe oxyhydroxides in the SSE is prevented by the dolomite interference in the Fe oxide extractions. Similarly, the unambiguous interpretation of the As response in association with Ca and Fe in the adsorbed/exchangeable and carbonate fractions (Steps 1 & 2) is hindered by the multiplicity of phases and reactions (e.g. cation exchange with clay minerals in Step 1 and dissolution of carbonates in Step 2). In this latter case, the SSE is doing what it is designed to do and the limitation is due to the low abundance, but complex phases of interest in our samples.

- Micro-XRD was applied with mixed success for these samples. The results obtained for the weathered pyrrhotite shows the effectiveness of the technique and its ability to resolve diffraction from weakly diffracting samples. Results for pyrite and arsenopyrite rims suggest improvements in sample preparation may be required to minimize coagulation of clay minerals around grains during thin section preparation. Careful target selection where the phase of interest can be maximized with the analytical volume (i.e. selection of rims greater than 20 um in diameter or so (which are not always present in these sample) may also be a requirement. Synchrotron μXRD shows great promise with its small spot size and ability to combine μXRF and μXANES results.

4.8.2 Arsenic Availability at the Townsite

- Arsenic is present at elevated concentrations (1000s of ppm) in the crushed rock fill. The largest source of As in the fills appears to be arsenopyrite which is a minor mineral component. The concentrations of As increase significantly in the sieved (< 180 μm) fractions.

- Weathering has replaced sulfide with As-bearing Fe oxyhydroxide forming rims (on pyrite and arsenopyrite) and layers (within pyrrhotite) on these grains. The As content is greatest on arsenopyrite grains (up to 28% As_2O_5), but high concentrations are also reported on grains formed from non-As-bearing sulfides (up to 11% As_2O_5 on pyrrhotite). There is also some evidence that the As content increases in the outer-most layers of weathering rims on pyrite.

- Observation of sulfide weathering is consistent with sulfide oxidation in a neutral pH, oxygenated environment. In such environments the oxidation is often assumed to be abiotic, but microbially mediated processes may also exist. In these conditions, moisture content of the soil is important in determining reactions rates with most rapid oxidation occurring at intermediate saturations. The process is essentially oxygen-limited in the presence of significant soil moisture, leading to decreased reaction rates under saturated conditions. At very low water contents the process is water limited and reactions are slowed.

  The unsaturated conditions, the resulting wetting and drying, and annual freeze-up of the material may also be important in the aging and speciation of the As associated with the Fe oxyhydroxides since drying (and freezing) will lead to increased ionic strength in the soil pore water. This needs further consideration and investigation.

- The weathering arsenopyrite and historic deposition of soluble As from roaster emissions leads to two inferred sources of arsenic in crushed rock fill pore waters. Therefore the interaction of arsenic with actively weathering sulfides is complex.

- The goethite detected on weathered pyrrhotite is finely crystalline with a high surface area given the weak Debye-Scherrer rings from the monochromatic synchrotron XRD source.

- The As in the Fe oxides is probably tightly bound as inner-sphere complexes (a common form of arsenate binding in Fe oxides). However, the presence of associated calcium may suggest the presence of more soluble Ca-Fe arsenate like coordination (especially in the rims on arsenopyrite).

- The identification of a possible roaster Fe oxide in the rock crevice sample is important since it may prove to be confirmation of an As source significantly different than the more soluble As trioxide that is known to have been dispersed in the region by operation of the roaster.

Chapter 5 – Discussion

This chapter brings together the overall study findings, summarizing some broad views and important observations regarding As in the Yellowknife environment, discussing the application of combined synchrotron μXANES and μXRD in the study of solid-phase As speciation, and exploring common links between the tailings and soil/crushed rock fill studies (Chapters 2, 3 and 4).

5.1 Arsenic Sources and Behaviour in the Yellowknife Environment

5.1.1 Arsenic management at the Giant and Con mines

Both the Giant and Con mines are presently involved in extensive programs working toward closure and reclamation for alternative uses. Based on the knowledge gained on comparing and contrasting the Giant and Con operations as part of the background to this work, it is clear that both operations have some similarities, but also distinct differences in terms of the way As was handled and deposited in the environment. Both mines probably have roaster-derived (oxidized) As emplaced in potentially reducing environments at the base of their tailings ponds, the implication being that reductive dissolution of the Fe oxides may release As whose down-flow mobility will be determined by the site-specific hydrogeological and hydrogeochemical conditions. Both mines also have arsenopyrite present in oxidizing environments that, given the right conditions, will weather with the potential to release a portion of the As to groundwater. There is a challenge at both sites then to manage the co-disposal of wastes where neither can be placed in an ideal disposal environment. Both mines also implemented effluent water treatment

systems later on in mine life, requiring the management of As-bearing ferric oxyhydroxide sludge. Prior to implementing effluent treatment, excess tailings water carried soluble and fine particulate As to down flow regions (Baker Creek to Back Bay at Giant and Meg, Keg, Peg Lake and Yellowknife Bay as well as Kam Lake at Con). Both sites also have large quantities of surface soils containing elevated As concentrations that will require disposal, or risk-characterization and management.

The preceding issues provide the basis for much similarity. In contrast, when it comes to the As trioxide produced at both mines the resulting fate of the As is completely different. The operations at Giant have essentially resulted in the containment of a large portion of the of As in relatively soluble form underground, that has proved problematic to manage. At Con, more of the As may be in the original arsenopyrite form due to the greater quantity of free-milling ore which still contains some arsenopyrite. Con was also able to ship a significant portion of the As trioxide off-site in the 1980s through their refining operation. However, the need to treat the remaining As trioxide in the storage ponds toward the end of mining has placed a large portion of the As in processed form (autoclave tailings from processing As trioxide sludge with ore and stockpiled calcine) in near surface tailings storage. The complex mineralogy of these solids, their unique character and the conditions in which they have been deposited will determine the stability of this material and the associated future management costs. Arsenic-bearing autoclave processed wastes are relatively common; however, those that included reaction of a supplemental Fe source (in the form of the roaster calcine) and As trioxide are rare and their long-term stability is unknown.

5.1.2 Arsenic in Yellowknife soils

After more than 60 years since the initial studies of the influence of As in the environment around Yellowknife, there remains only a limited understanding of the distribution and fate of As as it

relates to natural background processes (glacial scouring of the mineralized shear-zones) and the overprinting, and cycling of anthropogenic As especially as it relates to soils. The recent research completed by Andrade (2006) and continuing with the work of Fawcett *et al.* (2006) directed toward Sb, indicate that progress has been made in understanding the anthropogenic influences of As and Sb in the sediments downstream of the Giant mine. However, the source (anthropogenic or natural), distribution and form of As in soils remains poorly understood. In this context, the soils referred to are not derived from mine waste rock or tailings, but are influenced only by atmospheric deposition of As, naturally occurring As or both. These materials were not the principal focus of this thesis, but some potentially significant observations have been made in this work that may aid in future investigations of aerially influenced soil materials in the region.

The following observations concern As in the Yellowknife area soils. These views are based on the background information reviewed in Chapter 1 and the studies completed as part of this thesis.

- It appears that the main aerially dispersed As source in the region was emplaced over a relatively short time span (Con 8 months in 1942 and then 1946 to 1949, possibly Negus between 1947 and 1952 but little is known, and Giant 1949 to 1958 and most before 1951).

- The large expanses of exposed bedrock in the region (estimated to be 1/3 of the area by Hocking *et al.* 1978) may lead to a concentration of aerial dispersed As in soils down-slope from these outcrops. Runoff of precipitation probably carried much of the aerial As fall-out to adjacent low lying regions in dissolved or particulate form.

- The As deposition monitoring and snow surveys of the 1970s clearly indicate continuing input of As to the environment at that time (from the Giant roaster), but they only give a partial idea of the magnitude of the residual As inputs from two decades earlier.

- Giant is the largest overall source of As deposition. The inputs pre- and post 1951 may be different in extent due to construction of the larger roaster stack and the implementation of partially effective gas treatment system in 1951.

- Before 1951 at Giant the dust may also have been different in form with a significant portion of emitted particulate similar to the Hot ESP dust phase collected after 1958 (sample M3M in this study). The Hearth roaster of the day (1948 to 1951) may not have generated as much dust as the later fluosolids roasters, and roasting probably extended to higher temperatures than later roasters. Therefore, the character of the dust could be subtly different than the ESP dust produced at Giant some 50 years later (M3M).

  The importance of this observation is that there may exist a complex As source (host) in the environment that is very different than the soluble As trioxide particulate that is known to have been dispersed into the surrounding area. Some fine particles present in the rock crevice sample from the Giant mine Townsite studied here, may be derived from the roaster and may represent such an As host.

- The early inputs by Con and Negus (if any) would probably have been similar to the early Giant inputs, but the quantity of refractory ores treated and resulting As emissions appears to have been smaller.

- Most of the soil sampling conducted in the Yellowknife area to date has been criteria focused, meaning that the analytical results were compared to some specified value (eg. CCME guideline, an estimate of background concentration or a human health risk derived criteria). Even the SSE and GFE approaches employed in this and related studies are essentially the same although they strive to assess the environmentally most important fraction of the As present. What is systematically lacking (for a complex system such as Yellowknife that has multiple solid-phase sources and routes of entry) is the development of working models of the behaviour and fate of anthropogenic and natural As in undisturbed soil strata.

- The concentration of As at 700 ppm and the 50% bioavailability as determined by a simulated GFE method (Reimer *et al.* 2003) for the sieved rock-crevice sample highlights the importance of reconsidering As in Yellowknife soils from the above perspective.

It is the view of the author that form of the As, where it resides in the environment and its eventual fate under prevailing or changing geochemical or biogeochemical conditions is fundamental to understanding the human health and ecological risk from As exposure. Continued studies on determining bioavailability from the various routes of exposure are beneficial, but these and more ecologically focused studies would benefit from a better understanding of the soil As cycle in the Yellowknife region as it relates to the natural and anthropogenic As sources.

5.2 THE GRAIN SCALE ANALYTICAL APPROACH WITH *μ*XANES AND *μ*XRD

A combination of optical microscopy, EPMA and synchrotron μXANES and μXRD has been applied to polished petrographic thin sections. The the form of As and mineral associations at the grain scale (silt sizes) have been elucidated using both powders and intact specimens mounted in epoxy.

5.2.1 Thin Section Preparation - Intact and Powder Mount Thin Sections

Intact specimens offer some distinct advantages for analysis if small quantities of secondary minerals are expected or if analysis of discrete strata is useful. Analysis of fine matrix, fragile grain coatings or pore-fillings may be just as useful as discrete grain analyses. Essentially the intact preparation minimizes dispersal of fine material or fragile phases through the section (see also Section 5.2.2) and keeps discrete strata together. Intact sections offer the potential to analyse size fractionated or mineral concentrated strata without external sample manipulation. Intact sections also allow the mounting and polishing of the sections in preferred orientations which can be used to advantage with μXRD. Intact thin sections will also preserve the spatial chemical distribution within the section which can be recorded by the μXRF mapping capability of hard X-ray synchrotron microprobes.

Powder material mounts will often be the preferred or necessary preparation technique. Examples of secondary sample preparation that may dictate this type of sample preparation include: sieving to specific grain-size fractions, analysis of homogenized split samples for comparison with other analytical techniques and analysis of magnetic separate fractions.

5.2.2 μXANES and μXRD

The μXANES and μXRD work in this thesis has been completed concurrently with continual improvements at NSLS Beamline X26A. It is not useful to list all of specific improvements, but in brief, XANES energy stability and spectral quality was improved significantly allowing for less frequent standard analyses (more target grain analyses) and quieter spectra at the same data collection rates. Overall, a significant improvement in productivity was observed. However, the single greatest advancement for this project was the implementation of transmission mode μXRD

with the CCD detector. Rapid collection of X-ray diffraction patterns (minutes) on <10 μm spot sizes is a powerful tool. Due to the speed of data collection, there is a strong link between petrographic characterization and μXRD. Many potential targets can be analyzed based on prior optical microscopy allowing a more selective approach for the more time intensive analyses μXANES, μEXAFS and μXRF.

For finely crystalline to nanocrystalline materials, the use of the monochromatic X-ray beam is ideal since it immediately provides qualitative data on the scale of crystallites under the beam and relegates diffraction from macroscopic crystals (usually gangue minerals of lesser interest in our case) to individual points or none at all. However, in cases where no diffraction is observed, only petrographic evidence is available to resolve the ambiguity between amorphous material and macro-crystalline phases not meeting the Bragg condition for diffraction.

The μXRD technique as applied here is extremely well suited to the strongly diffracting roaster Fe oxides. Work with the generally larger weathered sulfide grains from the crushed rock fill from the Giant mine Townsite was more problematic. Good diffraction patterns were obtained for goethite on a few well-weathered pyrrhotite grains, but the diffraction was much weaker than that of the maghemite and hematite from the roaster. This weaker diffraction and the frequent presence of clay mineral reflections often led to poor results. This was especially true for weathered arsenopyrite and pyrite grains where it seems a combination of factors led to inconclusive results for all attempts. It appears that the relatively thin rims and beam orientation to the grains was limiting in being able to get sufficient weathered material under the beam and ensure a good chance of diffraction. The ubiquitous presence of clay mineral reflections and, in some cases, petrographic observation of fine clay matrix around the boundaries of the target pyrite and arsenopyrite grains seems to suggest that clay mineral interferences may originate

during thin section preparation. It seems probable that during mixing of the sample with the epoxy there is a tendency for fine clay particles to end up fixed to the surfaces of other grains (either from general contact in the dry state, interaction during sieving or by agglomeration during mixing in the epoxy). If this is true then intact thin sections would not be as likely to show this effect. However, many samples will not be amenable to intact thin section preparation (Section 5.2.1).

Arsenic oxidation state is heterogeneous in both the crushed rock fill and tailings being present as As^{-I} and As^{V} in the former and As^{-I}, As^{III} and As^{V} in the latter. For tailings containing roaster Fe oxides the bulk results would have been ambiguous and may have erroneously been interpreted as two separate hosts for As^{III} and As^{V} In the case of the crushed rock fill a combination of petrography and bulk XANES would probably have been sufficient to arrive at the same conclusion about the presence or absence of As^{III}. Of course bulk XANES doesn't offer the option of μXRD and the potential sensitivity for detection of other oxidation states is much improved for μXANES over bulk XANES which will respond to the most concentrated form(s) of As. In fact, bulk XANES may often complement micro-methods, since it can quantify or semiquantify the relative amounts of multiple oxidation states. Beamlines operating at macroscopic spot sizes are best suited for this type of analysis. Unfortunately, this means analysis at multiple beamlines and XANES of this sort may not be viewed as the best use of beamtime. A compromise is to broaden the micro-beam, but this is not ideal. Critical time is lost in changeover and there is probably a practical limitation on the spot area that can readily be achieved (say 400um x 400um for X26A). In most cases at this scale averaging multiple analyses may still be required to ensure representative results.

5.3 Solid-phase Arsenic Speciation in Giant Mill Products, Tailings and Waste Rock

The grain scale analysis of solid-phase As in the mill products, tailings and mine waste rock conducted as part of this thesis are a start in developing a comprehensive understanding of the complex distribution and behaviour of As in the environment. In this thesis, it has been shown that sulfide weathering through oxidation is occurring in unsaturated tailings and waste rock in carbonate-rich environments. Two fundamental results of this work are the identification of As-bearing roaster derived Fe oxides that need additional study to determine their limits of As stability in anoxic environments and the observation of sulfide weathering in unsaturated materials (both tailings and waste rock). The sulfide weathering products have been particularly elusive in characterization attempts by μXRD. In some cases these phases may be amorphous, however, the rimming nature of the phases and their fine grain size often leads to significant interference from surrounding fine grained material (clay minerals).

The South pond and deeper portions of the North-west pond tailings were not accessible for sampling as part of this project. However, both represent unique regions within the Giant tailings impounds. The South pond, due to its age, will contain little if any backfill separated tailings. This means it will contain a greater proportion of flotation tailings probably characterized with a lower As content, but greater permeability due to the larger sand component. The deeper portions of the Northwest pond will contain layers of reprocessed tailings from the North pond. The layering is expected since the reprocessing plant did not operate during the winter months. If the reprocessed tailings included organic material from the base of North pond then geochemistry of these layers may be significantly different and more reducing than the rest of the tailings.

Chapter 6 – Summary and Conclusions

The principal conclusions of this thesis and recommendations for further work are provided below.

6.1 Solid Phase Arsenic and Mine Waste

- The Giant Mine case highlights the importance of understanding ore processing history and products when studying solid-phase speciation for the purpose of risk assessment and remediation.
- Examination of mill products proved critical for this study in order to (1) recognize the difference between the products of processing and the products of weathering and (2) understand that a volumetrically small component of discharged waste (ESP dust) is a significant source of available As.

6.2 Solid Phase Arsenic in the Yellowknife Environment

- A complex mix of As sources are responsible for elevated As in soils in the Yellowknife area. The sources have included (1) aerially dispersed As as soluble As trioxide particulate and a complex lower solubility particulate component probably similar to the ESP dust, and (2) weathered arsenopyrite and arsenical pyrite (and lesser As-bearing sulfosalts) derived by glacial scouring of As enriched bedrock including mineralized shear zones in the region. Windblown tailings and waste-rock used for fill and road construction are additional localized As sources.
- Down stream sediments at both mines have probably been impacted with both dissolved As and fine-grained particulate (silt and clay). The specifics of the milling process at each mine may be important in determining the nature of the particulate As. In the case of Giant fine

grained calcine and ESP dust residue may be a particularly important component of As bearing fines.

6.3 The Grain Scale Analytical Approach Applying μXANES and μXRD

- Micro-XRD combined with multi-element μXRF and μXANES/EXAFS is a powerful and flexible analytical tool especially for redox sensitive elements. For As, combining bulk methods such as XANES/XRD/total element analysis with μXANES, μXRF, μXRD, SEM, EPMA and other micro-analytical tools provides detailed solid-phase speciation of complex soils and sediments.
- Specifically, μXRD can aid in targeting for μXANES (and potentially quantitative μXRF as that technique matures) by identifying target spots on the basis of XRD patterns.
- Intact thin sections provide superior information because spatial mineral relationships are preserved and fine matrix material in thin strata can be analysed.
- Synchrotron-based monochromatic μXRD operated in transmission mode (as at NSLS X26A) in conjunction with prior petrographic characterization allows for rapid identification (minutes per spot) of finely crystalline minerals. It also provides qualitative information on crystallite size.
- Interference from clay minerals in μXRD is a common complicating factor arising from heterogeneity at depth within the thin section. This complication increases with decreasing target grain-size (or rim thickness) and appears to be more of a problem with powder mounted specimens than intact specimens.

6.4 Solid Phase Arsenic Speciation at the Giant mine

- Ore processing at the Giant mine has produced multiple As-bearing hosts within the solid tailings produced. The arsenopyrite largely coming from flotation tailings and calcine residue

tailings will be unstable under oxidizing and especially unsaturated conditions. The mixed oxidation state As in roaster-derived Fe oxides will be unstable under reducing conditions. Therefore, ideal long-term storage conditions for both of these As hosts cannot be achieved, rather a strategy to maintain sub-oxic conditions would seem to be most appropriate.

- As-bearing roaster-derived Fe oxides are expected to comprise the largest portion of the As mass within the tailings. The roaster Fe oxide As hosts are nanocrystalline composite grains of maghemite and sometimes hematite.
- Roaster-derived hematite generally contains less As than roaster-derived maghemite. This may be due to increasing crystallite size (less surface area) or a greater affinity of As for maghemite.
- The mixed oxidation state of As in the roaster-derived wastes appears to be established by reactions occurring at the time of roasting and this mixed oxidation state persists in the environment. In unweathered calcines, it can be seen that roaster-derived Fe oxide grains with relic sulfide cores contain the highest As^{III}/As^{V} ratios.
- The ESP dust constitutes a relatively small portion of the Giant tailings, but may be the largest source of more soluble As solid phases. It is often present as thin laminae in tailings due to differential settling, intermittent discharges or both. The ESP dust may represent a source of more soluble As phases in the tailings than its otherwise small amount (1 % of total tailings) suggests.
- Sulfides deposited in unsaturated conditions (subaerial Yellowknife Bay tailings and Townsite waste-rock) have weathered leaving a replacement rim of As-bearing Fe oxyhydroxide or in the case of arsenopyrite a Ca-Fe arsenate and Fe oxyhydroxide coprecipitate. Arsenic-bearing Fe oxyhydroxide on pyrrhotite in waste-rock has been determined by μXRD to be finely to nanocrystalline goethite.

6.5 RECOMMENDATIONS FOR FURTHER WORK

The outcome of this research has also identified a number of key areas where additional work is recommended to further the understanding of As-speciation and behaviour in the environment.

- Magnetic separation of selected tailings samples is recommended to increase the number of particles available for analysis in weathered tailings. Through analysis of these magnetic separates attempt to establish the effect of weathering on the high As^{III} content Fe ox-sulfide grains in impounds, subaerial and subaqueous tailings. Consider quantitative micro-probe analysis of a large number of roaster Fe oxide grains from subaerial, reworked subaqueous and distal subaqueous tailings to determine whether the As content is more elevated or depleted in any of the environments. Bulk XANES analysis can also be conducted on these samples to see if there is a systematic shift in the ratio of As^{III} to As^{V} in response to deposition in the different geochemical environments.
- Carry out μEXAFS on concentric and micro-porous roaster-derived maghemite, with and without the presence of hematite, and with low and high As content in an attempt to elucidate the local structure of As^{III} and As^{V} in these complex materials.
- Conduct followup pore-water sampling and geochemical modeling of subaerial tailings at Yellowknife Bay to compare with the sampling conducted in 1999 prior to closure of the Giant roaster.
- Conduct μEXAFS on Townsite Fe oxyhydroxides and Ca-Fe arsenate coprecipitates to test similarities and differences to the work of Paktunc *et al.* (2004).
- Evaluate the feasibility of conducting pore water sampling and geochemical modeling of the weathering waste-rock fill at the Giant mine townsite to provide additional data on the mobility of As and the stability of the solid As-bearing phases present.

- Combined hydrogeological and hydrogeochemical investigation of targeted regions within the tailings impounds are recommended to provide data on concentrations of dissolved As in the tailings impounds. This is particularly important for the base of impounds in contact with buried lake sediment and peaty organic materials. These regions may represent a significant source of dissolved As due to potential destabilization of As-bearing roaster Fe oxides and to a lesser extent the large pulse of As released by stack emissions in the first decade of milling at Giant.
- Conduct a targeted soil sampling program with the aim of identifying the fate, form and importance of aerially dispersed As in local undisturbed soils.
- Carry out a similar process focused evaluation and sampling program at the Con mine to aid in understanding the long-term stability of As in tailings at that site and contrast this with Giant.

References

Alpers, C.N., Blowes, D.W., Nordstrom, D.K., and Jambor, J.L. (1994): Secondary Minerals and Acid Mine-Water Chemistry. *In* Environmental Geochemistry of Sulfide Mine Wastes (J.L. Jambor & D.W. Blowes, eds.). *Mineral Assoc. Can., Short Course Vol.* **22,** 247-270.

Amasa, S.K. (1975): Arsenic pollution at Obuasi goldmine, town and surrounding countryside. *Environ. Health Perspect.* **12**,131-135.

Andrade, C.F. (2006): Arsenic cycling and speciation in mining-impacted sediments and pore-waters from Yellowknife Bay, Great Slave Lake, NWT. M.Sc. Thesis, Queen's University, January 2006.

Armstrong, J.P. (1997): Variations in silicate and sulphide mineral chemistry between free-milling "metallic" and refractory "invisible" gold ores, Con mine, Yellowknife, N.W.T. Ph.D. Thesis, University of Western Ontario, April 1997.

Arriagada, F.J. & Osseo-Asare, K. (1984): Gold extraction from refractory ores: Roasting behavior of pyrite and arsenopyrite. *In* Precious Metals: Mining, Extraction, and Processing (V. Kudryk, D.A. Corrigan & J. Liang eds.). TMS-AIME, New York, N.Y. (367-385).

Azcue, J.M. & Nriagu, J.O. (1994): Arsenic: historical perspectives. *In* Arsenic in the Environment, Part1: Cycling and Characterization (J.O. Nriagu, ed.). *Advances in Environmental Science and Technology*, **26**, 1-15.

Bamford, S., Osae, A.E., Aboh, I., Biney, C.A. & Antwi, L. (1990): Environmental impact of the gold mining industry in Ghana. *Biol. Trace Elem. Res.* **26-27**, 279-285.

Banfield, J.F. & Zhang, H. (2001): Nanoparticles in the environment. *In* Nanoparticles and the Environment (J.F. Banfield & A. Navrotsky, eds.). *Rev. Mineral.Geochem.* **44,** 1-58.

Bartlet, D. (1989): TRP Metallurgical Drill Hole Requirements. Internal Memo for Giant Yellowknife Mines, December 12, 1989.

Baur, W.H., Onishi, B.M.H. (1969): Arsenic. *In* Handbook of Geochemistry (K.H. Wedepohl, ed.). Springer-Verlag., Berlin. (33-A-1–33-0-5).

Berube, Y., Frenette, M., Gilbert, R. & Anctil, C. (1974): Studies of mine waste containment at two mines near Yellowknife, N.W.T. *Indian Affairs and Northern Development Canada*, Publ. **QS-3038-000-EE-A1, ALUR 72-73-32**.

Bhumbla, D.K. & Keefer, R.F. (1994): Arsenic mobilization and bioavailability in soils. *In* Arsenic in the Environment, Part1: Cycling and Characterization (J.O. Nriagu, ed.). *Advances in Environmental Science and Technology*, **26**, 51-82.

Bigham, J.M. (1994): Mineralogy of Ochre Deposits Formed by Sulphide Oxidation. *In* Environmental Geochemistry of Sulfide Mine-Wastes (J.L. Jambor & D.W. Blowes eds.). *Mineral. Assoc. Can., Short Course Vol.* **22**, 103-132.

Bonazzi, P., Menchetti, S., Pratesi, G., Muniz-Miranda, M. & Sbrana, G. (1996): Light-induced variations in realgar and β-As_4S_4: X-ray diffraction and Raman studies. *Am. Mineral.* **81**, 874-880.

Bostick, B.C. & Fendorf, S. (2003): Arsenite sorption on troillite (FeS) and pyrite (FeS_2). *Geochim. Cosmochim. Acta,* **67**, 909-921.

Boyle, R.W. (1960): The geology, geochemistry, and origin of the gold deposits of the Yellowknife district. *Geol. Surv. Can., Mem.* **310.**

Boyle, R.W. (1979): The Geochemistry of Gold and its Deposits. *Geol. Surv. Can, Bull.* **280.**

Brooks, W.E. (2005): Arsenic. *In* U.S. Geological Survey Minerals Yearbook 2005. U.S. Department of the Interior and U.S. Geological Suvey.

Camm, G.S. Camm, Powell, N., Glass, H.J. Cressey, G. & Kirk, C. (2003). Soil geochemical signature of a calciner site, Cornwall, SW England. Applied Earth Science: IMM Transactions B, **112**(3), 268-278.

Campbell, N. (1947): The West Bay Fault, Yellowknife. *Can. Inst. Mining Metall., Trans.* **50**, 509-526.

Canadian Council of Ministers of the Environment (1999): Recommended Canadian Soil Quality Guidelines. Chapter 6. Canadian Environmental Quality Guidelines.

Canam, T.W. (2005): Discovery, Mine Production, and Geology of the Giant Mine. *In* Gold in the Yellowknife Greenstone Belt, Northwest Territories: Results of the EXTECH III Multidisciplinary Research Project (C.D. Anglin, H. Falck, D.F. Wright & E.J. Ambrose, eds.). *Geol. Assoc. Can. Spec. Pub.* **3**.

Carter, R. & Samis, C.S. (1952): The influence of roasting temperature upon gold extraction by cyanidation from refractory gold ores. *Can. Inst. Mining. Metall., Trans.* **55**, 120-126.

Chakraborti, N. & Lynch, D.C. (1983): Thermodynamics of roasting arsenopyrite. *Metall. Trans. B* **14B,** 239-251.

Chakraborti, N. & Lynch, D. C. (1985). Thermodynamic Analysis of the As--S--O Vapor System. Can. Metall. Q. **24**(1), 39-45.

Charles, J.A. (1980): The coming copper and copper-base alloys and iron: A metallurgical sequence. *In* The coming of age of iron. (T.A. Wertime and J.D. Muhley (eds.). Yale University Press, New Haven, CT, pp. 151-180.

Chryssoulis, S.L. (1990). Process mineralogical study of Au in concentrator and calcine samples from Giant Yellowknife, N.W.T. Unpublished report for Giant Yellowknife Mines Ltd.

Coleman, L.C. (1957): Mineralogy of the Giant Yellowknife Gold Mine, Yellowknife, NWT. *Econ. Geol.,* **52**, 400-425.

Cornell, R.M. & Schwertmann, U. (2003): *The Iron Oxides, Structure, Properties, Reactions Occurrences and Uses* (2nd ed.). Wiley-VCH, Weinheim.

Cornell, R.M. & Schwertmann, U. (1996): *The Iron Oxides, Structure, Properties, Reactions Occurrences and Uses.* VCH, Weinheim.

Corriveau, M.C. (2006): Characterization of arsenic-bearing near-surface and airborne particulates from gold-mine tailings in Nova Scotia, Canada. M.Sc. Thesis, Queen's University, February, 2006.

CPHA (1977). Final Report, Canadian Public Health Association Task Force on Arsenic, Yellowknife, Northwest Territories. Canadian Public Health Association, Ottawa, December 1977.

Cross, B.C. (1987): Waterboard information request of October 1, 1987 on Giant Yellowknife Tailings Retreatment Project. (Items relating to Hg in Tailings). Unpublished Internal Report, Giant Yellowknife Mines.

Cullen, W.R. & Reimer, K.J. (1989): Arsenic Speciation in the Environment. *Chem. Rev.* **89**, 713-764.

Cullen, W.R., McBride, B.C. & Reglinski, J. (1984): The reaction of methylarsenicals with thiols: Some biological implications. *J. Inorg. Biochem.* **21**,179-194.

Cummings, D.E., Caccavo, F., Fendorf, S. & Rosenzweig, R.F. (1999): Arsenic mobilization by the dissimilatory Fe(III)-reducing bacterium *Shewanella alga* BrY. *Environ. Sci. Technol.* **33**, 723-729.

Davis, A., Ruby, M.V., Bloom, M., Schoof, R., Freeman, G. & Bergstrom, P.D. (1996): Mineralogical constraints on the bioavailability of arsenic in smelter-impacted soils. *Environ. Sci. Technol.* **30**, 392-399.

Deb, P., Basumallick, A., Chatterjee, P. & Sengupta, S.P. (2001): Preparation of α-Fe2O3 nanoparticles from a nonaqueous precursor medium. *Scripta Mater.* **45**, 341-346.

Dunn, J.G., Graham, J. & Nguyen, G.H. (1995): Textures of roasted pyritic concentrates and some modes of gold loss by cyanidation. *Aust. Inst. Mining Metall., Proc.* **1995** (1), 69-77.

Dutrizac, J.E. & Jambor, J.L. (2000): Jarosites and their application in hydrometallurgy. *In* Sulfate Minerals, Crystallography, Geochemistry, and Environmental Significance (C.N. Alpers, J.L. Jambor, D.K. Nordstrom, eds.). *Rev. Mineral. Geochem.* **40.** 405-452.

EBA Engineering Consultants Ltd. (1998): Surface Contaminant Study Giant Mine Site, Yellowknife, NWT. Unpublished Report to Royal Oak Mines Ltd.

EBA Engineering Consultants Ltd. (2001): Assessment of Back Bay tailings deposit, Giant mine, Yellowknife, NT. Unpublished report to Royal Oak Project Team, Indian and Northern Affairs Canada, January, 2001.

Egli, D.H. & MacPhail, A.D. (1978): Cominco Ltd. – Con Operations. *In* Milling Practice in Canada (D.E. Pickett, ed.). *Can. Inst. Mining. Metall., Spec. Vol.* **16**, 56-58.

Ellis, C.E. & Hearn, K. (1990): Operating Mines. *In* Mineral Industry Report 1986-87 Northwest Territories (C.E. Ellis, ed.). NWT Geology Division, Department of Indian Affairs and Northern Development, Ottawa, Ontario (11-32).

Eneroth, E. & Koch, C.B. (2003): Crystallite size of haematite from the thermal oxidation of pyrite and marcasite effects of grain size and iron disulphide polymorph. *Minerals Eng.* **16**, 1257-1267.

Eng, P.J., Rivers, M., Yang, B.X. & Schildkamp, W. (1995): Micro-focusing 4keV to 65keV x-rays with bent Kirkpatrick-Baez mirrors. *In* X-ray microbeam technology and applications (W.Yun, ed.). *Proc. SPIE* **2516,** (41-51).

Environment Canada (2006). National Pollutant Release Inventory (NPRI), On-line data search, 1994 Facility On-Site Releases, Royal Oak Mines Inc., Giant Mine, <http://www.ec.gc.ca/pdb/querysite/query_e.cfm> Accessed August 14, 2006.

ESG (Environmental Sciences Group, RMC) (2000). Environmental Study of Arsenic Contamination from the Giant Mine, Yellowknife, Northwest Territories Part I. Unpublished report to Indian and Northern Affairs Canada. RMC-CCE-ES-00-024.

ESG (Environmental Sciences Group, RMC) & Queen's (2001): Characterization of arsenic in solid phase samples collected on the Giant mine townsite, Yellowknife, NWT. Unpublished report to Indian and Northern Affairs Canada.

Fawcett, S.E. (2005). Personal communication.

Fawcett, S.E., Andrade, C.F., Walker, S.R. & Jamieson, H.E. (2006). Understanding the environmental legace of the Giant gold mine, Yellowknife, NWT: Lessons from recent research. *In* Proceeding of CLRA/ACRSD 2006 annual meeting, Reclamation and Remediation: Policy to Practice, August 20-23, 2006, Ottawa, ON. (In Press).

Fendorf, S.E. & Sparks, D.L. (1996): X-Ray absorption fine structure spectroscopy. *In* Methods of soil analysis. 3. Chemical Methods. (J.M. Bartels, ed.). Soil Science Society of America, Inc. and American Society of Agronomy Inc., Madison, Wisconsin, USA (377-416).

Foster, A.L., Brown, G.E., Jr., Tingle, T.N. & Parks, G.A. (1998): Quantitative arsenic speciation in mine tailings using X-ray absorption spectroscopy. *Am. Mineral.* **83**, 553-568.

Foster, E.O. (1963): The collection and recovery of gold from roaster exit gases at Giant Yellowknife Mines Limited, *Can. Inst. Mining Metall., Trans.* **66**, 245-251.

Fowler, B. (2000): Iceman, Uncovering the life and times of a prehistoric man found in an alpine glacier. Random House, New York.

Frankenberger, W.T., Jr. & Arshad, M. (2002): Volatilization of Arsenic. *In* Environmental Chemistry of Arsenic. (W.T., Jr. Frankenberger, ed.). Marcel Dekker, Inc., New York, N.Y. (363-380).

Freeman, G.B., Schoof, R.A., Ruby, M.V., Davis, A.O., Dill., J.A., Liao, S.C., Lapin, C.A. & Bergstrom, P.D. (1995): Bioavailability of Arsenic in Soil and House Dust Impacted by Smelter Activities Following Oral Administration in Cynomolgus Monkeys. *Fundam. Appl. Toxicol.* **28**, 215-222.

Frost, D.V. (1967): Arsenicals in biology – retrospect and prospect. *Federation Proceedings, Trace Elements in Nutrition.* **26**(1), 194-208.

Fuller, C.C., Davis, J.A. & Waychunas, G.A. (1993): Surface chemistry of ferrihydrite: Part 2. Kinetics of arsenate adsorption and coprecipitation. *Geochim. Cosmochim. Acta,* **57** (10), 2271-2282.

Geldart, J., Williamson, R. & Maltby, P. (1992): Aqueous pressure oxidation as a waste treatment process--stabilizing roaster wastes. *Hydrometallurgy.* **30**, 29-44.

Giant Yellowknife Mines (1981): Submission to the Northwest Territories Water Board by Giant Yellowknife Mines Limited, Yellowknife, NWT. Unpublished report supporting water license renewal, dated, January 16, 1981.

GNWT (1993): An Investigation of Atmospheric Emissions from the Royal Oak Giant Yellowknife Mine, Environmental Protection Division, Department of Renewable Resources, Government of the Northwest Territories, Yellowknife, NWT, June, 1993.

Golder Associates (2002). Environmental Assessment, Yellowknife Bay Tailings, Giant Mine, Yellowknife, NT. Unpublished report to Miramar Giant Mine Limited, March 2002.

Gong, Z., Lu, X., Cullen, W.R. & Le, X.C. (2001): Unstable trivalent arsenic metabolites, monomethylarsonous acid and dimethylarsinous acid. *J. Anal. At. Spectrom.* **16**, 1409-1413.

Goodfellow, M.E. (1987): Estimated Tonnage to Tailings. Internal memo, Giant Yellowknife Mines Limited, dated June 26, 1987.

Gossler, W., Schlagenhaufen, C, Irgolic, K.J., Teschler-Nicola, M., Wilfing, H. & Seidler, H. (1995): Priest, hunter, alpine shepard, or smelter worker? *In* Der Mann im Eis: Neue Funde und Ergebnisse, Vol. 2. (K. Spindler, E. Rastbichler-Zissernig, H. Wilfing, D. zur Nedden & H. Nothdurfter (eds.). Springer-Verlag., New York, 269-273.

Gossman, G.I. (1987): Pyrometallurgy of gold. *In* The Extractive Metallurgy of Gold in South Africa, 1 (G.G.Stanley, ed.). *S. Afr. Inst. Mining Metall., Monogr.* M7, 345-377.

Grainge, J.W. (1963): Water Pollution, Yellowknife Bay, Northwest Territories. Canadian Department of National Health & Welfare, Public Health Engineering Division, Edmonton, Alberta, December 1963.

Greenwood, N.N. & Earnshaw, A. (1998): *Chemistry of the elements* (2nd ed.). Butterworth-Heineman, Oxford, U.K.

Grimsey, E.J. & Aylmore, M.G. (1990): Roasting of arsenopyrite. *In* Gold '90, Proceedings of the Gold '90 symposium, Salt Lake City, Utah, February 26 to March 1, 1990 (D.M. Hausen, D.N. Halbe, E.U. Petersen & W.J. Tafuri, eds.). SME, 1990.

Grimsey, E.J. & Aylmore, M.G. (1992): Mineralogical and chemical profile of a gold roaster. *Aust. Inst. Mining Metall., Proc.* **1992** (1), 43-49.

Grogan, K.C. (1953): Treatment plant operation at Giant Yellowknife. *Can. Inst. Mining Metall., Trans.* **61**, 88-99.

Hall, G.E.M., Gauthier, G., Pelchat, J.C., Pelchat, P. & Vaive, J.E. (1996a): Application of a Sequential Extraction Scheme to Ten Geological Certified Reference Materials for the Determination of 20 Elements. *J. Anal. At. Spectrom.* **11**, 87-96.

Hall, G.E.M., Vaive, J.E., Beer, R. & Hoashi, M. (1996b): Selective leaches revisted, with emphasis on the amorphous Fe oxyhydroxide phase extraction. *J. Geochem. Explor.* **56**, 59-78.

Hall, G.E.M., Vaive, J.E. & MacLaurin, A.I. (1996c): Analytical aspects of the application of sodium pyrophosphate reagent in the specific extraction of the labile organic component of humus and soils. *J. Geochem. Explor.* **56**, 23-36.

Halverson, G. (1984): Tailings Dam Drilling Project – 1984 Results and Conclusions. Internal memo, to K. Morton, Giant Yellowknife Mines Limited, February 22, 1984.

Halverson, G.B. (1990): Fluosolids roasting practice at Giant Yellowknife Mines Limited. *In* Proceedings of the 96th annual Northwest Mining Association Convention, Spokane Washington, December 5 – 7, 1990. NWMA, Spokane WA.

Halverson, G. & Raponi, T.R. (1987): Treatment of and gold recovery from effluent at Giant Yellowknife Mines Limited. *Water Polut.Res J. Can.* **22**(4), pp. 570-583.

Hamel, S.C., Buckley, B. & Lioy, P.J. (1998): Bioaccessibility of Metals in Soils for Different Liquid to Solid Ratios in Synthetic Gastric Fluid. Environ. Sci. Technol. **32**(3), 358-362.

Hammersley, A.P. (1998): FIT2D V10.3 Reference Manual V4.0, European Synchrotron Research Facility, Paper ESRF98-HA01T (program and manual available at http://www.esrf.fr/computing/expg/subgroups/data_analysis/FIT2D/).

Han, F.X., Su, Y., Monts, L., Plodinec, M.J., Banin, A. & Triplett, G.E. (2003): Assessment of global industrial-age anthropogenic arsenic contamination. *Naturwissenschaften* **90**(9), 395-401.

Haneda, K. & Morrish, A.H. (1977): Vacancy ordering in γ-Fe_2O_3 small particles. *Solid State Communications,* **22**(12), 779-782.

Harvey, C.F., Swartz, C.H., Badruzzaman, A.B.M., Keon-Blute, N., Yu, W., Ali, M.A., Jay, J., Beckle, R., Niedan, V., Brabander, D., Oates, P.M., Ashfaque, K.N., Islam, S., Hemond, H.F. & Ahmed, M.F. (2002): Arsenic mobility and groundwater extraction in Bangladesh. *Science,* **298**, 1602-1606.

He, B.B. (2003): Introduction to two-dimensional X-ray diffraction. *Powder Diffraction,* **18**, 71-85.

Health Canada (2003). Fact Sheet on Chromated Copper Arsenate (CCA) Treated Wood. Pest Management Regulatory Agency, Ottawa. June 2003. <http://www.hc-sc.gc.ca/pmra-arla/english/consum/consum-e.html> Accessed April 30, 2004.

Henderson, P.J., McMartin, I., Hall, G.E., Percival, J.B. & Walker, D.A. (1998): The chemical and physical characteristics of heavy metals in humus and till in the vicinity of the base metal smelter at Flin Flon, Manitoba, Canada. *Env. Geol.*, **34**(1), 39-58.

Hering, J.G. & Kneebone, P.E. (2002): Biogeochemical controls on arsenic occurrence and mobility in water supplies. *In* Environmental Chemistry of Arsenic (W.T. Frankenberger, Jr., ed.). Marcel Dekker, Inc., New York, N.Y. (155-181).

Hochella, M.F., Jr. (2002): There's plenty of room at the bottom: Nanoscience in geochemistry. *Geochim. Cosmochim. Acta* **66**, 735-743.

Hocking, D., Kuchar, P., Plambeck, J.A. & Smith, R.A. (1978): The impact of gold smelter emissions on vegetation and soils of a sub-arctic forest-tundra transition ecosystem. *J. Air Pollut. Control Assoc.* **28**(2), 133-137.

Huang, P.M. & Fujii, R. (1996): Selenium and arsenic. *In* Methods of Soil Analysis. 3. Chemical Methods. (J.M.Bartels, ed). Soil Science Society of America, Inc. and American Society of Agronomy Inc., Madison, Wisconsin, USA (793-831).

Hubbard, L., Marshall, D., Anglin, C.D., Thorkelson, D. & Robinson, M.H. (2005): Giant mine: Alteration, mineralization, and ore-zone structures with an emphasis on the Supercrest zone; Chapter 17. *In* Gold in the Yellowknife Greenstone Belt, Northwest Territories: Results of the EXTECH III Multidisciplinary Research Project, (C.D. Anglin, H. Falck, D.F. Wright & E.J. Ambrose, eds.). *Geol. Assoc. Can. Spec. Pub.* **3**.

ICDD (2003). Powder Diffraction File (PDF 2), Release 2003. International Centre for Diffraction Data, Newtown Square, Pennsylvania.

Inskeep, W.P., McDermott, T.R. & Fendorf, S. (2002): Arsenic (V)/(III) cycling in soils and natural waters: chemical and microbiological processes. *In* Environmental Chemistry of Arsenic (W.T. Frankenberger, Jr., ed). Marcel Dekker, Inc., New York, N.Y. (183-215).

Jackson, F.J., Lafontaine, C.N. & Klaverkamp, J. (1996): Yellowknife – Back Bay study on metal and trace element contamination of water, sediment and fish. Department of Indian and Northern Affairs Canada, Department of Fisheries and Oceans, and Freshwater Institute. November, 1996.

Jambor, J.L. (2000): Mineralogy of waste-rock and tailings samples from the Giant Mine, Yellowknife, Northwest Territories. Unpublished report to Golder Associates Ltd., Burnaby, B.C., December, 2000.

Jambor, J.L. (1994): Mineralogy of sulfide-rich tailings and their oxidation products. *In* Environmental Geochemistry of Sulfide Mine-Wastes (J.L. Jambor, & D.W. Blowes, eds.). *Mineral Assoc. Can., Short Course Vol.* **22**, 59-102.

Jambor, J.L. & Blowes, D.W. (1998): Theory and applications of mineralogy in environmental studies of sulfide-bearing mine wastes. *In* Modern Approaches to Ore and Environmental Mineralogy (L.J. Cabri & D.J. Vaughan, eds.). *Mineral. Assoc. Can., Short Course Vol.* **27**, 367-401.

Jamieson, H.E., Shaw, S.C. & Clark, A.H. (1995): Mineralogical factors controlling metal release at GECO, Manitouwadge, Ontario. *In* Mining and the Environment. (T.P. Hynes & M.C. Blanchette, eds.). **1**, 405-415.

Jha, M.C. & Kramer, M.J. (1984): Recovery of gold from arsenical ores. *In* Precious Metals: Mining, Extraction, and Processing (V. Kudryk, D.A. Corrigan, & J. Liang, eds.). TMS-AIME, New York, N.Y. (337-365).

Jorgensen, F.R.A. & Moyle, F.J. (1981): Periodic thermal instability during the isothermal oxidation of pyrite. *Metall. Trans.* **12B**, 769-770.

Kasama, T. & Murakami, T. (2001): The effect of microorganisms on Fe precipitation rates at neutral pH. Chemical Geology **180**, 117 – 128.

Kim, M-J., Nriagu, J.O. & Haack, S. (2000): Carbonate Ions and Arsenic Dissolution by Groundwater. *Environ. Sci. Technol.* **34**, 3094-3100.

Koch, I., Wang, C., Reimer, K.J. & Cullen, W.R. (2000): Arsenic Species in Terrestrial Fungi and Lichens from Yellowknife, NWT, Canada. *Appl. Organomet. Chem.* **14**, 245-252.

Krause, E. & Ettel, V.A. (1989). Solubilities and stabililities of ferric arsenates. *Hydrometrics,***22**, 311-337.

La Force, M.J. and Fendorf, S. (2000): Solid-Phase Iron Characterization During Common Selective Sequential Extractions. *Soil Sci. Soc. Am. J.*, **64**, 1608-1615.

Le, X.C. (2002): Arsenic Speciation in the Environment and Humans. *In* Environmental Chemistry of Arsenic. (W.T., Jr. Frankenberger, ed.). Marcel Dekker, Inc., New York, N.Y. (95-116).

Le, X.C., Yalcin, S. & Ma, M. (2000): Speciation of submicrogram per litre levels of arsenic in water: On-site species separation integrated with sample collection. *Environ. Sci. Technol.* **34**, 2342-2347.

Leblanc M., Morales, J.A. Borrego, J. & Elbaz-Poulichet, F. (2000): 4,500-year-old mining pollution in southwestern Spain: long-term implications for modern mining pollution. *Econ. Geol.* **95**(3), 655-662.

Lee, J.S. & Nriagu, J.O. (2003): Arsenic carbonate complexes in aqueous systems. *In* Biogeochemistry of Environmentally Important Trace Elements. (Y. Cai & O.C. Braids, eds.). *ACS Symposium Series* **835**, 33-41.

Lewis, D.W.T. (1985): The Giant Yellowknife Gold Mine: The geology of an archean epithermal precious metal system. Unpublished report for Giant Yellowknife Mines Limited.

Li, X., & Thornton, I. (1993): Arsenic, antimony and bismuth in soil and pasture herbage in some old metalliferous mining areas in England. *Environ. Geochem. Health.* **15**, 135-144.

Lindkvist, G. & Holmstrom, A. (1983). Roasting of complex concentrates with high arsenic content. Advances in Sulfide Smelting. *In* Advances in sulfide smelting: proceedings of the 1983 International Sulfide Smelting Symposium and the 1983 Extractive and Process Metallurgy Meeting, 1983 (H.Y. Sohn, D.B. George, & A.D. Zunkel eds.). Metallurgical Society AIME, 451-472.

Lord, C.S. (1951): Mineral Industry of District of MacKenzie, Northwest Territories. *Geol. Surv. Can., Mem.* **261.**

Majzlan, J., Grevel, K.-D. & Navrotsky, A. (2003): Thermodynamics of Fe oxides: part II. Enthalpies of formation and relative stability of goethite (α-FeOOH), lepidocrocite (γ-FeOOH), and maghemite (γ-Fe_2O_3). *Am. Min.* **88**, 855-859.

Manceau, A., Marcus, M.A. & Tamura, N. (2002): Quantitative speciation of heavy metals in soils and sediments by synchrotron X-ray Techniques. *In* Applications of Synchrotron Radiation in Low-Temperature Geochemistry and Environmental Science. (P.A. Fenter, M.L. Rivers, N.C. Sturchio, & S.R. Sutton, eds.). *Rev. Mineral. Geochem* **49**, 341-428.

Martin, A.J., and Pedersen, T.F. (2002): Seasonal and interannual mobility of arsenic in a lake impacted by metal mining. *Environ. Sci. Technol.* **36**, 1516-1523.

Martin, C. (1990): Nerco Con Mine Ltd, Metallurgical Development. Update including 1989 Metallurgical Development Program and CONMEX Critical Studies Program. Unpublished report to Nerco Con Mine, Ltd., February, 1990.

Masscheleyn, P.H., Delaune, R.D. & Patrick, W.H.(Jr.) (1991): Effect of redox potential and pH on arsenic speciation and solubility in a contaminated soil. *Environ. Sci. Technol.* **25**, 1414-1419.

McBride, M. B. (1994): Environmental Chemistry of Soils. Oxford University Press. New York.

McCreadie, H., Blowes, D.W., Ptacek, C.J. & Jambor, J.L. (2000): Influence of reduction reactions and solid-phase composition on porewater concentrations of arsenic. *Environ. Sci. Technol.* **34**, 3159-3166.

McCreadie, H., Jambor, J.L., Blowes, D.W., Ptacek, C. & Hiller, D. (1998): Geochemical behavior of autoclave-produced ferric arsenates: Jarosite in a gold-mine tailings impoundment. *In* Waste Characterization and Treatment (W. Petruk, ed.). Society for Mining, Metallurgy, and Exploration, Inc., Littleton, Colorado (61-78).

Mitchell, P. & Barr, D. (1995): The nature and significance of public exposure to arsenic: a review of its relevance to South West England. *Environ. Geochem. Health*, **17**, 57-82.

Moir, I., Falck, H., Hauser, B. & Robb, M. (2005): The history of mining and its impact on the development of Yellowknife. *In* Gold in the Yellowknife Greenstone Belt, Northwest Territories: Results of the EXTECH III Multidisciplinary Research Project. (C.D. Anglin, H. Falck, D.F. Wright, & E.J. Ambrose, eds.). *Geol. Assoc. Can. Spec. Pub.* **3**,(2).

Mok, W-M. & Wai C.M. (1990): Distribution and mobilization of arsenic and antimony species in the Coeur D'Alene River, Idaho. *Environ. Sci. Technol.* **24**, 102-108.

Moore, J.N. & Luoma, S.N. (1990): Hazardous wastes from large-scale metal extraction. *Environ. Sci. Technol.* **24**, 1278-1285.

More, M.A. & Pawson, H.E. (1978): Giant Yellowknife Mines Limited. *In* Milling Practice in Canada (D.E. Pickett, ed.). *Can. Inst. Mining. Metall., Spec. Vol.* **16**, 63-65.

Morin, G., Juillot, F., Casiot, C., Bruneel, O., Personne, J-C., Elbaz-Poulichet, F., LeBlanc, M., Ildefonse, P. & Calas, G. (2003): Bacterial Formation of Tooeleite and Mixed

Arsenic(III) or Arsenic(V)-Iron(III) Gels in the Carnoules Acid Mine Drainage, France. A XANES, XRD, and SEM Study, *Environ. Sci. Technol.* **37**, 1705-1712.

Morin, G., Lecocq, D., Juillot, F., Calas, G., Ildefonse, P., Belin, S., Brios, V., Dillmann, P., Chevallier, P., Gauthier, C., Sole, A., Petit, P-E. & Borensztajn, S. (2002): EXAFS evidence of sorbed arsenic(V) and pharmacosiderite in a soil overlying the Echassieres geochemical anomaly, Allier, France. *Bull. Soc. Geol. France*, **173**, 281-291.

Morjan, I., Alexandrescu, R., Soare, I., Dumitrache, F., Sandu, I., Voicu, I., Crunteanu, A., Vasile, E., Ciupina, V. & Martelli, S. (2003): Nanoscale powders of different iron oxide phases prepared by continuous laser irradiation of iron pentacarbonyl-containing gas precursors. *Mater. Sci. Eng. C* **23**, 211-216.

Mudroch, A., Joshi, S.R., Sutherland, D., Mudroch P. & Dickson, K.M. (1989). Geochemistry of sediments in the Back Bay and Yellowknife Bay of the Great Slave Lake. *Environ. Geol. Water Sci.*, **14**(1), 35-42.

Nakazawa, S., Yazawa, A., & Jorgensen, F.R.A. (2003a). Engineering Simulation of Sulfation Roasting Reactions. *Mater. Trans. JIM* **40**(10), 1166-1173.

Nakazawa, S., Yazawa, A., & Jorgensen, F.R.A. (2003b). Simulation of the removal of arsenic during the roasting of copper concentrate. *Metall.Mater. Trans. B* **30B**(3), 393-401.

Naqvi, S.M., Vaishnavi C., & Singh H. (1994): Toxicity and metabolism of arsenic in vertebrates. *In*: Arsenic in the Environment. II: Human Health and Ecosystem Effects. (J.O. Nriagu, ed.). John Wiley and Sons, Inc., New York (55-91).

National Research Council (1977). Medical and biological effects of environmental pollutants, arsenic. National Academy Press, Washington, D.C.

National Research Council (1999). Arsenic in drinking water. National Academy Press, Washington, D.C.

National Research Council (2001). Arsenic in drinking water, 2001 Update. National Academy Press, Washington, D.C.

Navrotsky, A. (2001): Thermochemistry of nanomaterials. *In* Nanoparticles and the Environment (J.F. Banfield,& A. Navrotsky, eds.). *Rev. Mineral. Geochem.* **44**, 73-103.

Nickson, R.T., McArthur, J.M., Ravenscroft, P., Burgess, W.G. & Ahmed, K.M. (2000): Mechanism of arsenic release to groundwater, Bangladesh and West Bengal. *App. Geochem.* **15**, 403-413.

Nishikawa, O., Okrugin, V., Belkova, N., Saji, I., Shiraki, K. & Tazaki, K. (2006): Crystal symmetry and chemical composition of yukonite: TEM study of specimens collected from Nalychevskie hot springs, Kamchatka, Russia and from Venus Mine, Yukon Territory, Canada. *Min. Mag.* **70**(1), 73-81.

Nordstrom, D.K. (2002): Worldwide occurrences of arsenic in ground water. *Science,* **296**, 2143-2145.

Nordstrom, D.K. & Archer, D.G. (2003): Arsenic thermodynamic data and environmental geochemistry. *In* Arsenic in Ground Water. (A.H. Welch, & K.G. Stollenwerk, eds.). 1-26.

Norwood, A.F.B. (1939): Roasting and treatment of auriferous flotation concentrates. *Aust. I.M.M. Proc.* **116**, 391-412.

Nriagu, J.O. (2002). Arsenic poisoning through the ages. *In* Environmental Chemistry of Arsenic. (W.T., Jr. Frankenberger, ed.). Marcel Dekker, Inc., New York, N.Y. (1-26).

Paktunc, D. & Dutrizac, J. E. (2003): Characterization of arsenate-for-sulfate substitution in synthetic jarosite using X-ray diffraction and X-ray absorption spectroscopy, *Can. Min.*, **41**, 905-919.

Paktunc, D., Foster, A. & Laflamme, G. (2003): Speciation and characterization of arsenic in Ketza River mine tailings using X-ray absorption spectroscopy. *Environ. Sci. Technol.*, **37**, 2067-2074.

Paktunc, D., Foster, A., Heald, S. & Laflamme, G. (2004): Speciation and characterization of arsenic in gold ores and cyanidation tailings using X-ray absorption spectroscopy. *Geochim. Cosmochim. Acta,* **68**, 969-983.

Pawson, H.E. (1973): Giant's Milling Operation. *In* Proceedings of the Annual Canadian Mineral Processors Meeting, January 23-26, 1973, Ottawa, Ont.

Perroud, P. (2006). Athena Mineralogy, Mineral Search Form. <http://un2sg4.unige.ch/athena/mineral/search.html> accessed August 4, 2006.

Peterson, R.C. (2005). Personal communication.

Pierce, M.L. & Moore, C.B. (1982): Adsorption of arsenite and arsenate on amorphous iron hydroxide. *Water Res.*, **16**, 1247-1253.

Pitcher, P.N. (1953). The Giant Yellowknife Operation. *Can. Inst. Mining Metall., Trans.* **56**, 55-58.

Pokrovski, G.S., Zakirov, I.V., Roux, J., Testemale, D., Hazemann, J-L, Bychkov, A.Y. & Golikova, G.V. (2002): Experimental study of arsenic speciation in vapor phase at 500°C: Implications for As transport and fractionation in low-density crustal fluids and volcanic gases. *Geochim. Cosmochim. Acta,* **66**, 3453-3480.

Ragaini, R.C., Ralston, H.R. & Roberts, N. (1977): Environmental trace metal contamination in Kellogg, Idaho, near a lead smelting complex. *Environ. Sci.Technol.* **11**, 773-781.

Raposo, J.C., Zuloaga, O., Olazabal, M.A. & Madariaga, J.M. (2004): Study of the precipitation equilibria of arsenate anion with calcium and magnesium in sodium perchlorate at 25 °C. *Appl. Geochem.* **19**, 855-862.

Reimann, C., Banks, D. & de Caritat, P. (2000): Impacts of airborne contamination on regional soil and water quality: The Kola Peninsula, Russia. *Environ. Sci. Technol.* **34**, 2727-2732.

Reimer, K.J., Ollson, C.A. & Koch, I. (2003): An approach for characterizing arsenic sources and risk at contaminated sites: Application to gold mining sites in Yellowknife, NWT, Canada. *In* Biogeochemistry of environmentally important trace elements (Y. Cai & O.C. Braids eds.). *ACS Symposium Series,* **835,** 166-180.

Ressler, T., Wong, J., Roos, J. & Smith, I.L. (2000): Quantitative speciation of Mn-bearing particulates emitted from autos burning (methylcyclopentadienyl) manganese tricarbonyl-added gasolines using XANES Spectroscopy. *Environ. Sci. Technol.* **34**, 950-958.

Risklogic Scientific Services Inc. (2002). Assessment of Human Health Risks Posed by Arsenic contamination in Yellowknife, NWT. Report to Yellowknife Arsenic Soils Remediation Committee (YSARC), c/o Environment Canada, Yellowknife, April 2002, 50 pages plus Appendices.

Robinson, J.J. (1988): The extraction of gold from sulphidic concentrates by roasting and cyanidation. *J. S. Afr. Inst. Min. Metall.* **88**(4), 117-130.

Rodriguez, R.R., Basta, N.T., Casteel, S.W. & Pace, L.W. (1999): An in vitro gastrointestinal method to estimate bioavailable arsenic in contaminated soils and solid media. *Environ. Sci. Technol.* **33**, 642-649.

Rollo, H.A. (2003). Processed kimberlite-water interactions in diamond mine waste, Ekati Diamond Mine, N.W.T., Canada, M.Sc. Thesis, Queen's University.

Royal Oak Mines (1992): Royal Oak Mines Inc. – Yellowknife Division, The Giant Mine, Water License N1L3-0043, Submission in support of water licence renewal, September 1992. Unpublished report.

Ruby, M.V., Schoof, R., Brattin, W., Goldade, M., Post, G., Harnois, M., Mosby, D.E., Casteel, S.W., Berti, W., Carpenter, M., Edwards, D., Cragin, D. & Chappell, W. (1999):

Advances in evaluating the oral bioavailability of inorganics in soil for use in human health risk assessment. *Environ. Sci. Technol.* **33**, 3697-3705.

Ruby, M.V., Davis, A., Schoof, R., Eberle, S. & Sellstone, C.M. (1996): Estimation of lead and arsenic bioavailability using a physiologically based extraction test. *Environ. Sci. Technol.* **30**, 422-430.

Saha, J.C., Dikshit, A.K., Bandyopadhyay, M. & Saha, K.C. (1999): A review of arsenic poisoning and its effects on human health. *Crit. Rev. Anal. Chem.* **29**(3), 281-313.

Savage, K.S., Bird, D.K. & O'Day, P.A. (2005): Arsenic speciation in synthetic jarosite. *Chem. Geol.* **215**, 473-498.

Savage, K.S., Bird, D.K. & Ashley, R.P. (2000): Legacy of the California gold rush: environmental geochemistry of arsenic in the southern mother lode gold district. *International Geology Review.* **42**, 385-415.

Savage, K.S., Tingle, T.N., O'Day, P.A., Waychunas, G.A. & Bird, D.K. (2000): Arsenic speciation in pyrite and secondary weathering phases, Mother Lode Gold District, Tuolumne County, California. *Appl. Geochem.* **15**, 1219-1244.

Schaufuss, A.G., Nesbitt, H.W., Scaini, M.J., Hoechst, H., Bancroft, M.G. & Szargan, R. (2000): Reactivity of surface sites on fractured arsenopyrite (FeAsS) toward oxygen. *Am. Mineral.* **85**, 1754-1766.

Siddorn, J.P., Cruden, A.R., Hauser, R.L., Armstrong, J.P. & Kirkham, G. (2005): The Giant-Con gold deposits: Preliminary integrated structural and mineralization history, Chapter 18. *In* Gold in the Yellowknife Greenstone Belt, Northwest Territories: Results of the EXTECH III Multidisciplinary Research Project (C.D. Anglin, H. Falck, D.F. Wright & E.J. Ambrose, eds.). *Geol. Assoc. Can. Spec. Pub.* **3**.

Silke, R. (1999): Report on Minesites in the Yellowknife Region, Open Report #1999-001, Indian and Northern Affairs Canada, NWT Geology Division.

Simon G., Huang H., Penner-Hahn J.E., Kesler S.E., and Kao L. (1999): Oxidation state of gold and arsenic in gold-bearing arsenian pyrite. *Am. Min.* **84**, 1071-1079.

Smedley, P.L. & Kinniburgh, D.G. (2002): A review of the source, behaviour and distribution of arsenic in natural waters. *App. Geochem.* **17**, 517-568.

Smedley, P.L., Kinniburgh, D.G., Macdonald, D.M.J., Nicolli, H.B., Barros, A.J., Tullio, J.O., Pearce, J.M. & Alonso, M.S. (2005): Arsenic associations in sediments from the loess aquifer of La Pampa, Argentina. *Appl. Geochem.* **20**,989-1016.

Smith, K.S. & Huyck, H.L.O. (1998): An overview of the abundance, relative mobility, bioavailability, and human toxicity of metals. *In* Reviews in Economic Geology, The Environmental Geochemistry of Mineral Deposits, Part A: Processes, Techniques, and Health Issues. (G.S. Plumlee, & M.J. Logson, eds.). **6A**, 29-70.

SRK Consulting Engineers and Scientists (2002): Giant Mine, arsenic trioxide management alternatives, final report, December 2002. Prepared for Canadian Department of Indian Affairs & Northern Development, Yellowknife, NWT.

Stefanski, M.J. & Halverson, G.B. (1992): Gold Recovery Improvement Investigations at Giant Yellowknife Mine. In Geological Survey of Canada Open File 2484, Project Summaries, Canada-Northwest Territories Mineral Development Subsidiary Agreement. (D.G. Richardson, & M. Irving, eds.). 1987-1991, 217-219.

Stichbury, M-L.K., Bain, J.G., Blowes, D.W. & Gould, W.D. (2000): Microbially-mediated dissolution of arsenic-bearing minerals in a gold mine tailings impoundment. *In* ICARD 2000, Proc. Fifth Int. Conf. Acid Rock Drainage 1. Society for Mining, Metallurgy, and Exploration, Inc., Littleton, Colorado (97-103)..

Stoffegren, R.E. & Alpers, C.N. (1987): Woodhousite and svanbergite in hydrothermal ore deposits: products of apatite destruction during advanced argillic alteration. *Can. Mineral.* **25,** 201-211.

Strawn, D., Doner, H., Zavarin, M. & McHugo, S. (2002): Microscale investigation into the geochemistry of arsenic, selenium, and iron in soil developed in pyritic shale materials. *Geoderma* **108**, 237-257.

Swash, P.M. & Ellis, P. (1986). The roasting of arsenical gold ores: A mineralogical perspective. *In* Gold 100. Proceedings of the International Conference on Gold. Volume 2: *Extractive Metallurgy of Gold.* SAIMM, Johannesburg.

Swash, P.M. & Monhemius, A.J. (1995): Synthesis, characterization and solubility testing of solids in the Ca-Fe-AsO4 system. *In* Proceedings, Sudbury '95 - Mining and the Environment. (T.P. Hynes, & M.C. Blanchette, eds.). **1**, 17-28.

Tait, R.J.C. (1961): Recent progress in milling and gold extraction at Giant Yellowknife Gold Mines Limited. *Can. Inst. Mining Metall., Trans.* **64**, 204-216.

Tessier, A., Campbell, P.G.C. & Bisson, M. (1979): Sequential extraction procedure for the speciation of particulate trace metals analytical chemistry. **51**(7), 844-851.

Thornton, I. (1996): Sources and pathways of arsenic in the geochemical environment. *In* Environ. Geochem. Health., GSA Publication No. 113 (J.D. Appleton, R. Fuge, & G.J.H. McCall, eds.). 153-161.

Tossell, J.A. (2000): Metal-thiometalate transport of biologically active trace elements in sulfidic environments: theoretical evidence for copper thioarsenite complexing. *Environ. Sci. Technol.* **34**(8), 1483-1488.

US EPA (2003). Response to Requests to Cancel Certain Chromated Copper Arsenate (CCA) Wood Preservative Products and Amendments to Terminate Certain Uses of other CCA Products. US Federal Register, April 9, 2003, Volume 68, Number 68.

Valberg, P.A., Beck, B.D., Bowers, T.S., Keating, J.L., Bergstrom, P.D. & Boardman, P.D. (1997): Issues in setting health-based cleanup levels for arsenic in soil. *Reg. Tox. Pharm.*, **26**, 219-229.

van Elteren, J.T., Slejkovec, Z., Arcon, I. & Glass, H-J. (2006): An interdisciplinary physical-chemical approach for characterization of arsenic in a calciner residue dump in Cornwall (UK). *Environ. Pollut.* **139**, 477-488.

Vian, A., Iriarte, C. & Romero, A. (1963). Fluidized roasting of arsenopyrites. *I&EC Process Design and Development* **2**(3), 214-223.

Vink, B.W. (1996): Stability relations of antimony and arsenic compounds in the light of revised and extended Eh-pH diagrams. *Chem. Geol.* **130**, 21-30.

Walker, S.R. & Jamieson H.E. (2002): Mineralogical characterization of arsenic-bearing phases, Giant Mine Yellowknife Bay Tailings, Yellowknife, NWT. Unpublished report to Indian and Northern Affairs Canada, Yellowknife and Golder Associates Ltd., Vancouver, BC.

Walker, S.R., Jamieson, H.E., Lanzirotti, A., Andrade, C.F. & Hall, G.E.M. (2005): The speciation of arsenic in iron oxides in minew wastes from the Giant gold mine, NWT: Application of synchrotron micro-XRD and micro-XANES at the grain scale. *Can. Min.*, **43**, 1205-1244.

Waychunas, G.A. (2001): Structure, aggregation and characterization of nanoparticles. *In* Nanoparticles and the Environment (J.F.Banfield,& A. Navrotsky, eds.). *Rev. Mineral. Geochem.* **44**, 105-166.

Waychunas, G.A., Rea, B.A., Fuller, C.C.& Davis, J.A. (1993): Surface chemistry of ferrihydrite: Part 1. EXAFS studies of the geometry of coprecipitated and adsorbed arsenate. *Geochim. Cosmochim. Acta,* **57** (10), 2251-2269.

Webmineral (2006): Webmineral, Search Page. <http://www.webmineral.com/cgi-bin/search/search.pl> accessed on August 4, 2006.

Wedepohl, K.H. (1995): The composition of the continental crust. *Geochim. Cosmochim. Acta.* **59**, 1217-1232.

Wertime, T.A. (1973): The Beginnings of Metallurgy: A New Look. *Science.* **182**(4115), 875-887.

Wilkin, R.T. (2001): USGS Workshop on Arsenic in the Environment - Final Abstracts. <http://wwwbrr.cr.usgs.gov/Arsenic/FinalAbsPDF/wilkin.pdf> accessed on May 4, 2004.

Williams, M., Fordyce, F., Paijitprapapon, A. & Charoenchaisri, P. (1996): Arsenic contamination in surface drainage and groundwater in part of the Southeast Asian tin belt, Nakhon Si Thammarat Province, Southern Thailand. *Environ. Geol.* **27**, 16-33.

Williams, T.M., Rawlins, B.G., Smith, B. & Breward, N. (1998): In-vitro determination of arsenic bioavailability in contaminated soil and mineral beneficiation waste from Ron Phibun, Southern Thailand: a basis for improved human risk assessment. *Environ. Geolchem. Health.* **20**, 169-177.

Winship, K.A. (1984): Toxicity of inorganic arsenic salts. *Adv. Drug React. Ac. Pois. Rev.* **3**, 129-160.

Wolska, E. (1990): Studies on the ordered and disordered Al substituted maghemites. *Solid State Ionics.* **44**, 119-123.

Appendix A – Yellowknife Bay Tailings

Direct Tailings Discharge to Yellowknife Bay

Mining and milling operations commenced at the Giant mine in May 1948. At that time mill tailings were directed to a small inlet on Yellowknife Bay (Figure 1-2). A 1950 aerial photograph (A12855-284) obtained from the National Airphoto Library (NAPL) seems to shows active development of a "tailings beach" at this inlet. A high suspended sediment load is apparent in the photo extending some 1.5 km to the north west along the Yellowknife Bay shoreline. Eddy currents containing sediment (i.e. tailings) can also be observed rotating eastward and southward out into Yellowknife Bay. Sometime around 1951 (EBA, 2001), tailings discharge was directed to a low lying region occupied by a small lake (Bow Lake) some 800 m to the north. A 1964 aerial photograph shows a drier looking tailings beach at the Yellowknife Bay inlet with an erosional scarp now formed along the new shoreline. Suspended sediment is again observed in Yellowknife Bay adjacent to the tailings beach extending northward some 400m where it seems to end fairly abruptly at an eddy current. Later air photos show the continued erosion of the bank at the former tailings beach area. Any variation in erosion over time probably correlates to fluctuating lake levels.

In the mid to late 1980s Giant Yellowknife mines undertook a tailings retreatment program (TRP) to reclaim gold from historic tailings. A number of initiatives to characterize historic tailings were undertaken at that time. Although very little of this information apparently survived, a few reports and memos have surfaced that are pertinent to the historic tailings at the site. A memo (Halverson, 1984) documenting results of a tailings drilling program summarizes historic tonnages of tailings produced at Giant in each fiscal year up to that time. The memo indicates that the flotation portion of the tailings produced between 1948 and 1951 (ie. to the end of fiscal year 1950) are probably the Yellowknife Bay tailings. The tailings tonnages reported in this

memo for the fiscal years 1948 to 1950 are presented and highlighted in Table A-1. All tonnages are assumed to be dry short tons.

An additional internal Giant Yellowknife Mines memo (Bartlett, 1989) identifies 235,000 tons as the "very approximate tonnage" available at Yellowknife Bay for the TRP (presumably referring to the Yellowknife Bay tailings). This number may be based on availability for hydraulic mining as opposed to actual quantities discharged.

Table A-1 - Recorded Tonnages of Early Mine Tailings Produced at Giant Mine

	Estimated Tonnage† to Tailings (Goodfellow, 1987)		
Year	Flotation Tailings	Calcine Residue‡	Tons to Tailings
1948/49	77,115	4,224	81,339
1949/50	114,185	11,146	125,331
1950/51	134,155	13,246	147,401
Total 1948 to 1951	325,455	28,626	354,071

† All tonnages assumed to be dry short tons.
‡ Similar tabulation from 1984 (Halverson, 1984) indicates "beach on Y.K.Bay" may be floatation portion of tailings up to 1950/51.
* Memo notes that calcine residue was used to fill "B shaft. (Pit)" for the years 52/53 through 54/55).

Though not considered in detail here, the fact that tailings were presumably disposed of in both summer and winter environments may have lead to different dispersal characteristics depending on whether the tailings froze during deposition or not. In addition, on-going erosion of the tailings beach material has likely led to the mixing of tailings materials from different original depositional environments (eg. weathered sulfides from the beach tailings areas could be redeposited with submerged anoxic tailings containing unweathered sulfides). This is further complicated by the fact that relatively large volumes of tailings were emplaced in a relatively short period of time. This may have resulted in the base of the submerged tailings containing

relatively undisturbed deposits that were protected from erosional activity by their own bulk or by other later deposits.

The following is a summary of information extracted from Grogan (1953), Tait (1961), and Foster (1963) that highlight the potential influences on tailings character of early tailings at the mine with a specific emphasis on the Tailings deposited at Yellowknife Bay.

- Ore mined until 1958 contained significant free milling gold that may suggest a different ore character at that time compared to recent ore,
- milling and stockpiling of the flotation concentrate commenced in May 1948,
- roasting of flotation concentrate began in January 1949 and utilized an Edwards (hearth type) roaster which was supplemented in mid-1952 (and later completely replaced) by two stage fluosolids roasting,
- tonnages processed were gradually increased from 225 tons per day in 1948 to 425 tons per day by 1950 and 700 tons per day by 1952,
- indirect references suggest stockpiling of calcine residue was routinely carried out but may have been limited to the summer months only,
- primary grinding was fine, resulting in flotation tailings 70 to 80 % finer than 200 mesh (<0.075 mm),
- calcine was reground before cyanidation resulting in material >90% finer than 325 mesh (< 0.045 mm),
- until October 1951 there was no dust collection or off-gas treatment,
- after October 1951, dust and gas was collected by a cold Cottrell (electrostatic precipitator operating at ambient temperature) and pneumatically disposed of to underground vaults (thus

no Cottrell dust would have been discharged to the tailings ponds until hot Cottrell electrostatic precipitation was on-line),

- hot Cottrell trials began in 1955, but were not successfully operated until late 1958 or 1959 (routine discharge of Cottrell dust with the tailings did not start until late 1958 and then continued until closure of the mine in 1999),
- cyclone separation of the coarse (sand) fraction of the calcine residue and flotation tailings for use as mine backfill began in 1957 (decrease in tailings discharge tonnage by about 45% and resulting in discharge of finer tailings "slimes" with much of the sand removed. (Halverson & Raponi 1987)

Potential Distribution and Reworking of Tailings Fines in Yellowknife Bay

In addition to direct tailings discharge to Yellowknife Bay between 1948 and 1951, tailings decant water was discharged further to the south in Yellowknife Bay (ie. Back Bay via. Baker Creek) beginning sometime in the 1950s. The exact date would have been when the natural containment capacity of the Bow Lake basin was exceeded. Historically, tailings decant (and subsequently treated water) has been directed eastward from the Bow Lake tailings management area into Baker Creek which flows generally southward and enters Back Bay some 1.5 km south west of the Yellowknife Bay tailings beach. It is also important to note that tailings decant water was redirected for a short period of time (mid-1960s) to the north east of North Pond, entering Yellowknife Bay just below the Yellowknife River (approximately 2.2 km north of the Yellowknife Bay tailings beach) (Grainge, 1963 and Giant Yellowknife Mines, 1981). Therefore, for many years prior to 1981 and (especially before 1970), tailings decant water is likely to have carried fine suspended tailings to Back Bay via the routes described above. Pulses of heavier loads (eg. during spring runoff and other upset conditions such as spills) are also likely to have occurred.

The tailings decant process has the potential to mobilize fine tailings as suspended sediment into the receiving waters. This was apparently a problem in early years of mine operations (Berube *et al.*, 1974) and attempts were made to address this by dam building to provide additional sedimentation time and to maximize tailings storage capacity for the winter months (Berube *et al.* 1974). From an early date, the original tailings containment area was partitioned into a series of settling basins (approximately present day North Pond and the area of the Settling and Polishing Ponds) (Figure 1-2) to maximize settling time for the fine tailings materials.

The tailings decant practice has continued throughout the life of the mine, although over the years additional effluent treatment methods were gradually put in place to reduce As discharge to Back Bay. The measures ranged from i) early on (date unknown at present) gravity settling as described above, ii) from before 1965 to 1981 liming of high As tailings streams (eg. calcine residue and Cottrell tailings) before discharge to the tailings impoundment (Cross 1987, Berube *et al.* 1974), and iii) in 1981 commissioning of a tailings pond effluent treatment system (Halverson and Raponi, 1987). The mill is now shut down, however, effluent treatment presently continues in order to treat excess water in the tailings impounds due to continuing mine sewage discharge, mine dewatering and surface runoff.

The amount and grain size of fine tailings dispersed from tailings decant operations to Back Bay in this manner would depend on the operational characteristics of the decanting process at a given time and downstream flow patterns in the discharge route. It is expected such tailings would be fine (e.g. silt) and tend to disperse throughout the Yellowknife Bay area. Therefore in the vicinity of the Yellowknife Bay tailings overprinting and mixing of these fine tailings (if present) is volumetrically expected to be very small relative to the direct discharge material.

Also, while the Cottrell tailings (cyanided electrostatic precipitator dust) is not a component of the original Yellowknife Bay tailings, after 1958 it was collected as part of the off-gas treatment and discharged with the main tailings stream. This material is very fine grained (fine silt, >90% less than 14 μm according to Foster, 1963) and probably constituted only 1% w/w or so of the total tailings stream (up to 2% during operation of the sand plant which redirected almost half of the other tailings streams to mine backfill). However, of the three main solids discharge streams (Cottrell tailings, calcine residue and flotation tailings) the Cottrell tailings carried the highest concentrations of total As (Table 1-4) resulting in significant potential As loadings from the relatively small volumes discharged. The fine grained nature of this material and similarity to fine calcine may make it difficult to identify conclusively in historic tailings deposits.

If tailings water decant methods led to dispersal of fine grained material to Yellowknife Bay, this fine material would tend to be concentrated around the exit from Baker Creek into Back Bay and to a lesser extent near the Narrows at the north end of Yellowknife Bay. Depending on prevailing currents in Back Bay and Yellowknife Bay, some of this material could also have been deposited in the vicinity of the direct discharged Yellowknife Bay tailings. The 1964 airphoto (NAPL A18310-29) shows an apparent sediment plume extending from the Baker Creek outlet north-eastward almost as far as the Yellowknife Bay tailings.

Appendix B – Tailings Sample Locations

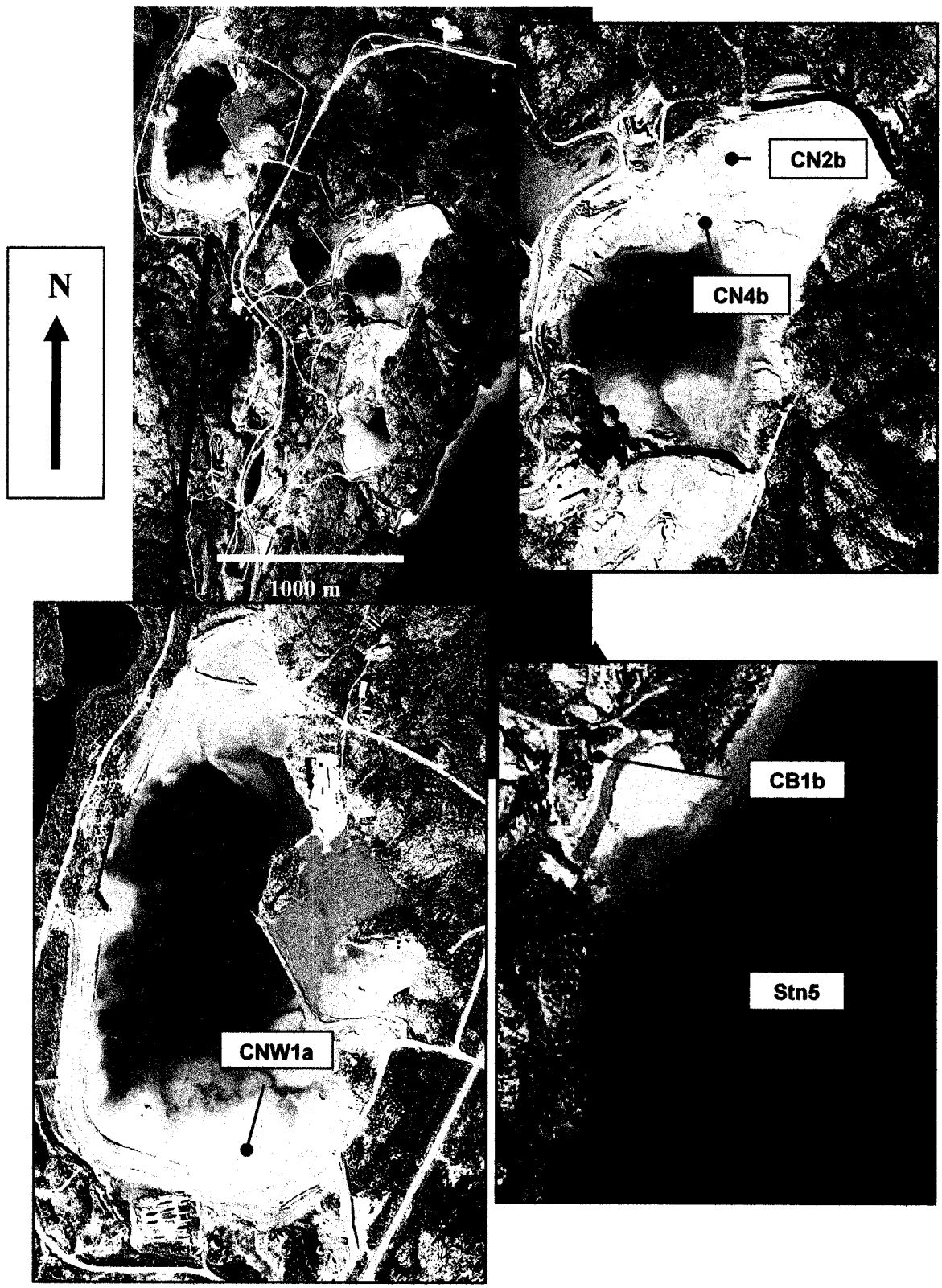

Figure B-1. Sample locations. Upper left image is Giant mine site. The other three airphoto images are magnified areas showing sample sites.

Appendix C – List of Thin Sections and Analyses

Table C-1 Thin Section List with Type of Analysis

	Section ID[1]	Type[2]			Analyses[3]
		Std	Si	XRD	
Mill	M1M(si)	X	X		Petr., EPMA, μXANES
	M2M(r)		X	X	Petr., EPMA(q), μXANES, μXRD
	M4M		X		Petr., EPMA, μXANES
	CM1a		X		Petr., μXANES
Tailings	CNW1a S2		X	X	Petr., EPMA(q), μXANES, μXRD
	CN2b S1	X			
	CN2b S2	X			
	CN2b S3			X	Petr, μXANES, μXRD
	CN4b S1b		X		Petr, μXANES
	CN4b S2		X		Petr., μXANES
	CHC1b S1(si)	X	X		Petr., μXANES
Yellowknife Bay	CB1bS3(r)		X	X	Petr., EPMA, μXANES
	CB1bS4		X		Petr., μXANES
	P1Stn1		X		Petr., μXANES
	P2Stn1		X		Petr.
	P3Stn1		X		Petr.
	P4Stn1		X		Petr.
	P5Stn2		X		Petr.
	P6Stn2		X		Petr.
	P7Stn5(r)		X	X	Petr., μXANES, μXRD
	P8Stn5(r)		X	X	Petr., μXANES, μXRD
Giant Townsite	29053		X		Petr. EPMA(q), μXANES
	29057	*			Petr.
	29064(r)†		X	X	Petr.
	29066		X		Petr., EPMA(q), μXANES
	29072(r)†		X	X	Petr., EPMA(q), μXANES,

[1] Identifying name of thin section. "si" – denotes silica glass "r" denotes removable section for μXRD.

[2] Std.=standard glass thin section, Si=silica glass (As-free), XRD=removable thin section for μXRD.

[3] Petr. – petrography, EPMA(q) – quantitative, all other EMPA is qualitative.

* Polished section – organic rich – polished thin-section not possible for this material.

† Note: Two removable sections made from a single off-cut ("b" designates second or "bottom" section).